Structure and function analysis of sulfate reducing communities in wastewater treatment systems

- A combined molecular and microsensor study -

Dissertation
zur Erlangung des Grades eines
Doktors der Naturwissenschaften
-Dr. rer. nat.-

dem Fachbereich Biologie/Chemie der
Universität Bremen
vorgelegt von

Cecilia Maria Santegoeds
aus Eindhoven, Niederlande

Bremen
Februar 1999

Die vorliegende Arbeit wurde in der Zeit von November 1995 bis Februar 1999 am Max Planck Institut für Marine Mikrobiologie in Bremen angefertigt.

1. Gutachter: Prof. Dr. Friedrich Widdel
2. Gutachter: Dr. Dirk de Beer

Tag des Promotionskolloquiums: 1. April 1999

Δια το θαυμαζειν οι ανθρωποι ηρξαντο φιλοσοφειν

Aristoteles Metaphysik $982^{b}12$

voor PaMa

Preface

This thesis deals with the dynamics of biofilm systems from wastewater treatment basins and reactors. Aerobic-anaerobic interactions within these biofilms were investigated, in particular the interactions of sulfate reducing populations with other populations (like methanogens, denitrifyers and nitrifyers) and their response to different environmental parameters (oxygen and nitrate gradients).

In the following chapters a short introduction of the techniques is given (chapter 1) and the experimental data are presented and discussed (chapter 2-6). At the end of the thesis the Ph.D. project is summarized.

This thesis would not have been accomplished without the help of several people, which I would like to thank all. My supervisors, Dirk de Beer and Gerard Muyzer were always present with good advice and help whenever I needed it. I am grateful for all your help and support I received during these last three years. I thank Prof. Widdel for his suggestions on this thesis and am most grateful for all the support I received from him and from Bo Barker Jørgensen, as Körber price recipient, during my Ph.D. study at the Max Planck Institute in Bremen. The Körber Foundation is acknowledged for the financial support I received during my Ph.D. study. I am grateful to Rudi Amann and Karl-Heinz Schleifer for their invaluable support over the course of this Körber project.

At the Delft University of Technology I would like to thank Piet Bos and Lex Scheffers, who stimulated my interest in microbiology through their lectures. In particular, I am grateful to Gijs Kuenen, who guided me through my Master thesis and encouraged me to spend one year at the laboratory of Dave Ward at the Montana State University in Bozeman, USA.

I am most thankful to Dave Ward and his people in the lab, Mary Bateson, Mike Ferris and Stephen Nold for introducing me to the field of molecular ecology and molecular techniques. Thanks a lot for all your help, and also for all the fun and the wonderful time I had in Bozeman.

I would like to thank the former head of the microsensor department at the Max Planck Institute in Bremen, Michael Kühl, for his kind support. I had a great time in the microsensor group. The technical assistants, Anja, Gaby and Vera are thanked for all the microsensors they built for me. Andi Schramm introduced me to the FISH techniques and CLSM and helped me on a variety of other topics. The rest of the 'Bayern-Gang', Bernard, Frank-Oliver and Willi were always helpful with the ARB program and with PC problems. "So long, and thanks for all the FISH!" My office 'mates' Ferran, Roland and Stefan were always there for nice conversations and good office atmosphere. Volker and Armin are thanked for correcting parts of this thesis. And last but not least I am grateful to Andrea and Anne for all the discussions and diversions we had, especially during these last months. It was good to have you around. All the other colleagues at the Max Planck Institute in Bremen that I forgot to mention, thanks a lot for the great team work and the good times we had.

I would like to thank the people at the Prague Institute of Chemical Technology, Jiri Wanner and his coworkers, and at the University of Aarhus, Niels Peter Revsbech and Lars Riis Damgaard for the fruitful collaborations and experimental excursions abroad. Working with you was a great

experience. My co-authors of the manuscripts in this thesis are thanked for their support and cooperation.

Finally I would like to thank my family and friends in the Netherlands and England for their support and friendship. You were so close to me although we were often so far apart. I am especially grateful to my parents, who are always willing to listen and help, even with the editing and correcting of the last parts of this thesis. Ik dank jullie van harte, mama en papa!

Bremen, January 1999

Sjila Santegoeds

Contents

Chapter 1

General Introduction

Microsensors and molecular techniques: Tools to determine chemical microgradients and the distribution and activity of bacterial populations in wastewater treatment systems

Parts of this chapter have been published in: "Microsensor as a tool to determine chemical microgradients and bacterial activity in wastewater biofilms and flocs", Biodegradation **9**: 159-167 (1998), by Cecilia M. Santegoeds, Andreas Schramm, and Dirk de Beer.

INTRODUCTION

Isolation and cultivation of bacterial strains are the classical microbiological techniques to characterize microorganisms and their activities. These methods have, however, two major drawbacks: first, most microorganisms cannot be cultivated (5, 69, 73), second, microorganisms in pure or defined cultures do not necessarily reflect the same behavior as in natural environments (25). Especially growth conditions in complex ecosystems, like biofilms or aggregates, are difficult to simulate in defined cultures.

Biofilms, flocs and aggregates are microbial consortia, which are present among others in wastewater treatment plants and bioreactors. In these systems they are responsible for the degradation of organic waste and the removal of nutrients. Biofilms can be defined as surface associated microbial layers, ranging from a few cell layers to some millimeters in thickness. Aggregates are dense, suspended microbial agglomerates, whereas flocs are more loose microbial consortia. Flocs disassociate and re-associate rapidly depending on the hydrodynamics of the system and thus have, unlike biofilms and aggregates, a non-stratified structure. The microbial cells in biofilms, aggregates and flocs are embedded in extra-cellular polymeric substance (EPS). Free convection is hindered, resulting in mass transfer resistance and, consequently, steep chemical gradients and limitation of conversion rates within the structures (24, 33, 44). Thus the conditions within these immobilized systems with their various microenvironments and microbial populations differ from the bulk water conditions. Extrapolation of the system behavior to that of cells is impossible without knowing their microenvironment. Therefore, techniques with high spatial resolution are needed, such as molecular techniques and microsensors, for structure and function analysis of biofilms, flocs and aggregates.

Molecular methods were developed during the last years to identify the bacteria present in environmental samples, by sequence comparison and phylogenetic analysis, and to reveal their spatial distribution, i.e. by genetic fingerprinting (49) and *in situ* hybridization techniques (5). As techniques based on nucleic acid analysis do not include cultivation, they circumvent the biases created by culture dependent techniques. Most of these molecular tools, however, do not provide information about the *in situ* activity of the bacteria. Both the *in situ* bacterial activity and the microenvironmental conditions can be determined with microsensors.

Microsensors can measure chemical and physical variables with high spatial resolution (< 50 µm) due to their small tip-diameter (1 - 20 µm). Microsensors are powerful tools, especially for measurements of environmental conditions in complex microbial communities, such as microbial mats, biofilms and aggregates. In these systems high metabolic rates of the dense microbial populations and molecular diffusion cause steep chemical gradients and narrow zones of microbial activity. Due to the small dimensions and low analyte consumption of microsensors, microgradients can be measured without significant disturbance of the sample structure and the gradients themselves. Furthermore, such measurements allow studies of internal cycling processes, such as coupled sulfate reduction and sulfide oxidation measurements (38, 41). Microsensors have been developed during the last years for measuring important metabolites like O_2 (36, 59), H_2S (30), S^{2-}(59), pH (29, 37), H_2 (26), NO_3^- (22, 42), NO_2^- (19), N_2O (61), NH_4^+ (23), CO_2 (18), and CH_4 (17). The microsensors used in environmental studies can be divided in two groups: electrochemical microsensors and fiber-

optical microsensors. More detailed reviews of microsensors and their application in environmental analysis can be found elsewhere (40, 59). A recent review of Amann and Kühl (2) addresses the combined use of molecular techniques and microsensors in microbial ecology.

Here, a short introduction of some molecular techniques is given and a brief review of microsensors.

MOLECULAR TECHNIQUES

The molecular techniques allow us to study the diversity, distribution and abundance of microorganisms in nature without the need of isolation. Most methods use the rRNA molecule as a molecular marker because, i) it is present in all organisms; ii) it contains conserved and variable sequence regions, which is a prerequisite for probing and phylogenetic analysis; iii) a 16S rRNA database is available with over 16,000 sequences, which is necessary for sequence comparison and probe designing; and iv) one bacterial cell contains over 10,000 copies of the rRNA molecule, which makes probing easier and sensitive. But also other genes can be used as molecular markers, such as protein encoding genes. Recently primers for the [NiFe] hydrogenase gene present in *Desulfovibrio* species (72) and primers for the dissimilatory sulfite reductase gene, present in all sulfate reducing bacteria (71), were developed. However, only a short review will be given here on the 16S rRNA based techniques. Two groups of molecular methods are discussed, genetic fingerprinting techniques for diversity studies of microbial communities and hybridization methods for abundance and distribution analysis of populations. An overview of a microbial community study with molecular techniques is given in Figure 1.

Genetic fingerprinting techniques

Different fingerprinting techniques are available to study the diversity of microbial communities and population changes in time or after disturbances, like randomly amplified polymorphic DNA (RAPD, also called DNA amplification fingerprinting or DAF (74)), amplified ribosomal DNA restriction analysis (ARDRA (47)), terminal restriction fragment length polymorphisms (T-RFLP (45)), and denaturing gradient gel electrophoresis (DGGE (52)). These techniques rely on the nucleic acid (DNA and RNA) extraction of the environmental samples for which different methods are available (1). The extracted nucleic acids are (specifically) amplified in the polymerase chain reaction (PCR) using a diverse set of primers and are separated on an agarose or polyacrylamide gel by electrophoresis. The separation is either based on the different sized PCR products (DAF, ARDRA and T-RFLP) or on sequence differences (DGGE). The resulting pattern reflects the microbial diversity of the environmental sample and will show the dynamics of the system when successional samples are taken. More details about the identity of single bands in the pattern can be retrieved by blotting and hybridizing the gel with specific probes (see below) or by re-amplification and sequencing of gel bands (50). The retrieved sequences can be phylogenetically analyzed and used for probe designing.

Fingerprinting techniques have been successfully used to monitor community changes in wastewater treatment systems. Population differences between various bioreactors (10) and microbial community changes in a bioreactor over time (75) were studied with RAPD. ARDRA was used in a biofilm community study of fluidized bed reactors (48). The microbial diversity was analyzed in different sludges with T-RFLP (45) and a biofilm development study in an activated sludge basin was performed with DGGE (63).

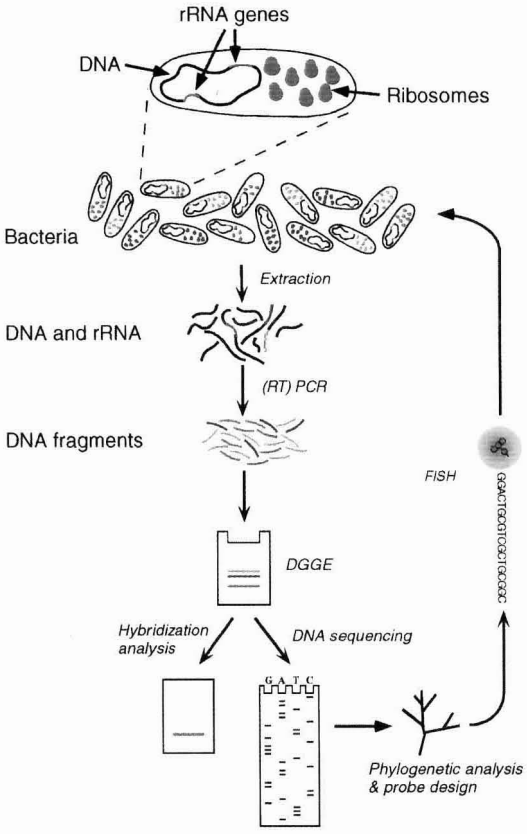

Fig. 1. An overview of a microbial community study using molecular techniques. Nucleic acids from an environmental sample are extracted, amplified and analyzed by denaturing gradient gel electrophoresis (DGGE). Sequences are retrieved and probes are designed for detection and quanti-fication of specific bacteria with fluorescence in situ hybridization (FISH). This figure was modified from Muyzer et al. (51).

Hybridization techniques

Different hybridization analyses are known and some will be discussed here. The dot-blot hybridization of rRNA is a method to quantify and identify the RNA of different populations by extracting the environmental RNA, spotting it on a membrane and hybridizing the RNA with radioactive 16S rRNA targeted oligonucleotide probes. The relative RNA abundance of a specific population is determined by the amount of the specific probe for this population bound to the sample relative to the amount of an universal probe hybridizing with the same sample. The method has been used to quantify proteobacteria in activated sludge (70), and methanogens and sulfate reducing bacteria in anaerobic bioreactors (28, 53, 56, 57). This technique can also be applied on blots of

fingerprinting gels, like for instance DGGE gels. Then, instead of RNA denatured DNA is hybridized with taxon specific probes to determine the presence of specific populations.

Whole cell hybridization is used for identification and quantification of microbial species and to observe the spatial distribution of populations in environmental samples. For this purpose probes are labeled either with a fluorescent dye, a radioactive label, an enzyme or a marker molecule like digoxigenin (67). The labeled oligonucleotide probes will hybridize with the rRNA molecules inside intact target cells. The hybridized cells in the fluorescence *in situ* hybridization (FISH) can be visualized under an epifluorescence microscope. A more detailed protocol for FISH is described by Amann et al. (4). The FISH analysis is frequently used in microbial community studies of wastewater treatment systems, like the detection of proteobacteria (70), sulfate-reducing bacteria (46) and several other populations (34) in activated sludge, and the identification of sulfate reducing bacteria (3, 55) and nitrifiers (64, 65) in biofilms from wastewater treatment plants and bioreactors.

MICROSENSORS

Electrochemical microsensors

Three types of electrochemical microsensors are most often used in environmental applications: potentiometric microsensors, amperometric microsensors and micro-biosensors; the latter are actually amperometric microsensors including a biological reaction in the sensor tip. The principles and some examples of each type will be described below. Environmental application of voltametric microelectrode methods have also been reported recently (11), but will not be discussed here.

Potentiometric microsensors. Potentiometric microsensors are based on charge separation of ions across a membrane. An electrical potential difference is hereby generated according to the Nernst equation:

$$\Delta E = \frac{RT}{zF} \ln\left(\frac{a_i}{a_e}\right) = E_0 + k \cdot \log(a_i) \qquad (1)$$

with R is the gas constant, T the absolute temperature, z the charge of the ion, F the Faraday constant, a_i and a_e the ion activities, in the sample and in the electrolyte solution, respectively. As the activity in the electrolyte solution (a_e) may be considered constant, the electrical potential difference across the membrane becomes proportional to the logarithm of the ion activity in the sample. The formula can then be simplified as shown above introducing a constant, k, and an offset potential, E_0. The potential is measured with a high-impedance ($10^{15}\ \Omega$) voltmeter.

There are three major types of potentiometric microsensors: (a) full glass, (b) Ag/Ag^+ half cell and (c) liquid ion-exchange (LIX) based microsensors.

(a) Full glass microsensor. The only full glass microsensor relevant for microbial ecology is the pH glass electrode described by Hinke (29) and Thomas (68). This microelectrode is a small version of the commercially available pH electrodes, in which the H^+ selective membrane is made of a special glass. The sensors have a long lifetime, but have a sensing length of approximately 20 µm,

which might be a disadvantage if high spatial resolution is demanded. In that case LIX pH microsensors are recommended (see below).

(b) Ag/Ag$^+$ half cell microsensor. The sulfide microsensor described by Revsbech et al. (60) and Kühl et al. (38) works as an Ag/Ag$^+$ half cell. A platinum wire coated at the tip with silver and a silver salt of the ion to be analyzed (in this case Ag_2S) functions as a sensor in combination with an external reference electrode. The Ag$^+$ activity determines the potential of the sensor and is depending on the solubility of the silver salt and therefore on the S^{2-} activity in the analyzed medium. Dissolved S^{2-} is in equilibrium with H_2S, HS^- and H^+, according to the following equation:

$$H_2S \overset{K_1}{\rightleftharpoons} H^+ + HS^- \overset{K_2}{\rightleftharpoons} 2H^+ + S^{2-} \qquad (2)$$

K_1 and K_2 are dissociation constants. Since the sensor measures only S^{2-}, also the pH has to be measured for determination of the total dissolved sulfide concentration. A disadvantage of the microsensor is the slow response time, especially at low concentrations. Furthermore, it can only be used under anoxic conditions, since the high negative potential of the microsensor can reduce oxygen.

(c) Liquid ion-exchange (LIX) based microsensor. The principle of the LIX microsensor is the same as of the other potentiometric microsensors. The ion-selective membrane is in this case a liquid ion exchanger (Figure 2.). Liquid ion exchangers are commercially available (e.g. from Fluka). To seal the capillary tip of the microsensor with the hydrophobic membrane, the glass has to be silanized (6, 68). The LIX membrane can be solidified in the tip with PVC. A protein coating (BSA) of the tip prevents interaction of hydrophobic substances from the sample with the LIX (19). The microsensor is shielded with an outer casing containing 1 M KCl to reduce electrical noise (40).

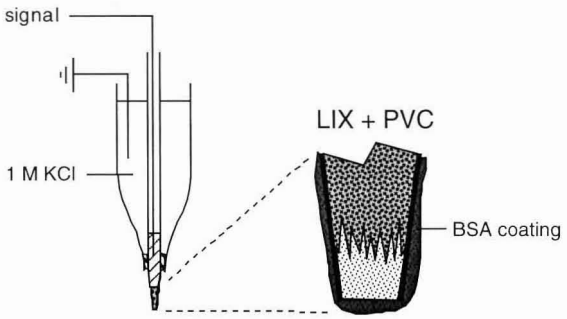

Fig. 2. Schematic drawing of a LIX microsensor.

The LIX microsensors currently used in environmental applications are H^+ (8, 66), NO_3^- (22), NO_2^- (19), NH_4^+ (23), and Ca^{2+} (7). The CO_2 microsensor contains a pH-LIX sensor (18). The LIX microsensors can be made very small (approximately 1 µm tip diameter) and allow, therefore, an extremely high spatial resolution (~ 5 µm). However, the short lifetime of LIX microsensors (usually a few days) is a disadvantage, as well as the low selectivity of the NH_4^+ sensor for Na^+ and K^+, and the NO_3^- and NO_2^- sensors for Cl^-, which prohibits their use in seawater. For measurements in marine environments a recently developed NO_3^- biosensor (42) can be recommended.

Amperometric microsensors. Amperometric microsensors for O_2 (58, 59), H_2S (30), H_2 (26), N_2O (61) and HClO (20), measure the current caused by electrochemical reactions of the analyte at the tip of the microsensor. The current, measured by a sensitive pico-ampere meter, is proportional to the concentration of the substrate. The electrochemical reaction is driven by a potential difference between the working electrode and the reference.

The oxygen microelectrode is a well known and often described sensor, which has improved drastically over the years. From a simple cathode-type oxygen microelectrode (9, 60), it developed to a Clark-type microsensor (62) with a cathode situated behind a silicone membrane and immersed in an electrolyte solution. This sensor has a more stable signal, is insensitive for calcium and magnesium ions and is pH independent. Later a guard cathode was added to prevent diffusion of oxygen to the cathode from behind and thus reduce the background signal (58).

The use of the combined O_2/N_2O microsensor for denitrification studies (61) is limited by its complex construction. Other microsensors may be preferred (e.g. the NO_3^- biosensor or the LIX sensors for NH_4^+, NO_3^- and NO_2^-).

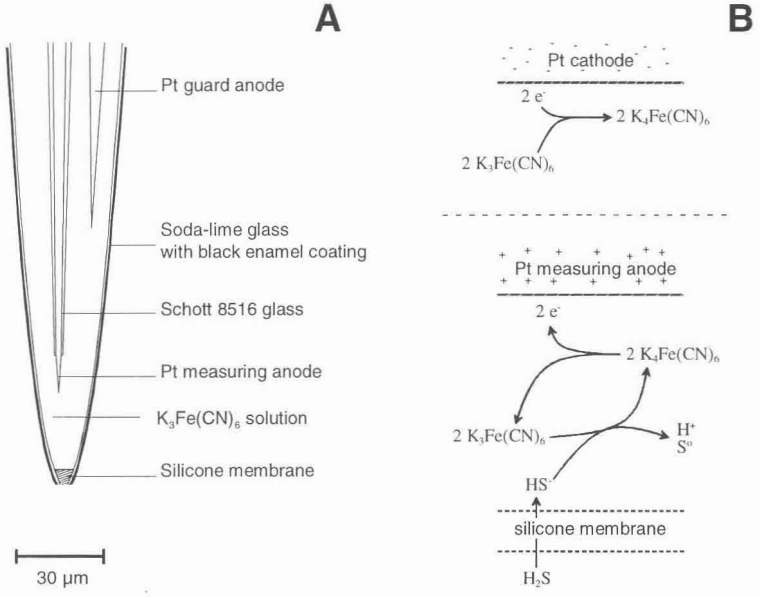

Fig. 3. Scheme of a H_2S microsensor from Kühl et al. (41), with kind permission from Inter-Research Science Publisher. (A) View of the sensor tip. (B) Chemical reactions at the counter electrode (upper part, not shown in A) and at the measuring anode (lower part).

The H_2S microelectrode is a new Clark-type sensor (30, 41). H_2S penetrates through a silicone membrane and is oxidized to sulfur by ferricyanide in the electrolyte solution behind the membrane (Figure 3.). The formed ferrocyanide is then re-oxidized to ferricyanide at the platinum working electrode. The sensor detects only H_2S; therefore, the local pH must be known to determine the total

dissolved sulfide concentration. In acidic and moderate alkaline environments (pH < 9) the following formula can then be used to calculate the total dissolved sulfide concentration (30):

$$\left[S_{tot}^{2-}\right] = \left[H_2S\right]\left(1 + \frac{K_1}{\left[H_3O^+\right]}\right) \qquad (3)$$

K_1 is the dissociation constant from equation 2 (K_2 can be neglected at this pH range).

The microsensor can be calibrated in dilution series of sulfide. The dilution series, consisting of the same medium as used for the microsensor measurements, are kept at constant pH (phosphate buffered) and are flushed with nitrogen to avoid chemical oxidation of the sulfide. The signal in the dilution series is proportional to the total dissolved sulfide, determined by chemical analysis (14). An example of a calibration curve can be seen in Figure 4. The detection limit of the sensor is 1-2 µM H_2S. Contrary to the (old) Ag/Ag_2S sensor the H_2S microsensor is insensitive to oxygen, which is highly advantageous for studies at oxic-anoxic interfaces, which are often encountered in environmental applications. This, together with its fast response time (< 0.5 s) and low stirring sensitivity, makes it a much more preferable tool than the Ag/Ag_2S microsensor (40).

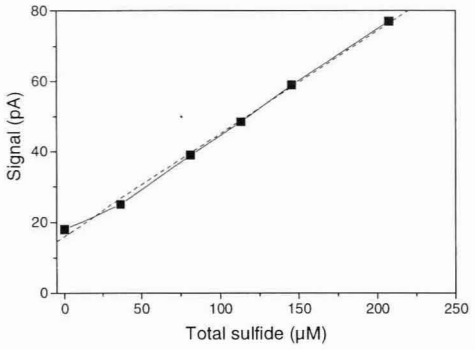

Fig. 4. A calibration curve of the H_2S microsensor obtained in buffered, anaerobic artificial wastewater at pH 7.5. The dashed line indicates the linear regression of the data points.

Micro-biosensors. A glucose microsensor, based on a glucose oxidase reaction, was the first micro-biosensor developed (15). Two new types of micro-biosensors, that are more relevant for environmental studies, are based on the specific activity of bacteria in the tip of the sensor (Figure 5.); a nitrate (42, 43) and a methane biosensor (16, 17). In the nitrate biosensor a *Agrobacterium radiobacter* strain converts nitrate to N_2O by incomplete denitrification; N_2O is then measured by an internal N_2O microsensor. The methane sensor contains methane oxidizing bacteria, that oxidize the methane diffusing into the tip with O_2 from a reservoir in the microsensor. The O_2 consumption is proportional to the methane concentration and is measured by an internal oxygen microelectrode. The biosensors have a tip diameter of 20 - 50 µm, a detection limit of ca. 0.1 µM for nitrate and ca. 2-10 µM for methane with lifetimes of a few days for the nitrate biosensor and several months for the methane biosensor.

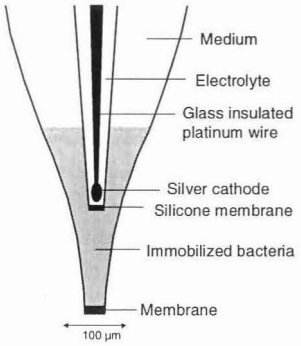

Fig. 5. Scheme of a nitrate micro-biosensor. Redrawn from Larsen et al. (42).

Optical microsensors

Fiber-optical microsensors (micro-optodes) are made of tapered fibers that collect and direct light from the sensor tip to the opto-electronic measuring equipment. The measuring system is sophisticated, containing bright light emitting diodes (LED) for fluorescence excitation, excitation and emission filters, a fiber coupler (beam splitter) and a photomultiplier as detector (35, 36, 40).

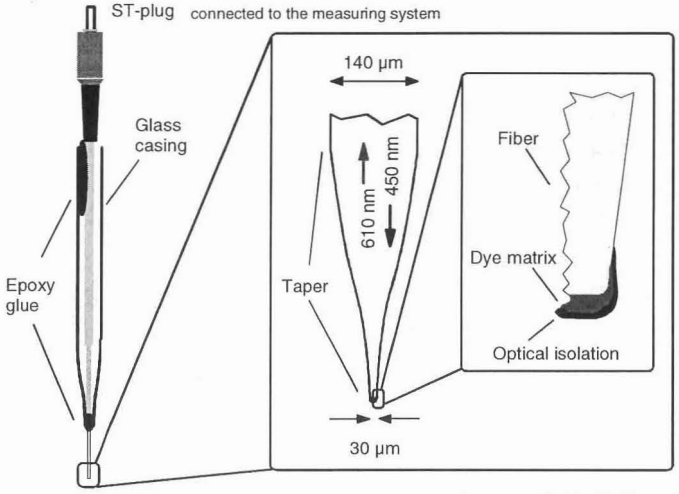

Fig. 6. Schematic drawing of an optical microsensor, a micro-optode (O. Kohls, unpublished).

Micro-optodes have recently been developed as an alternative to existing electrochemical microsensors. They have the advantage of easy manufacturing, long term stability and mechanical strength. The optical fiber microsensors are based on analyte dependent changes in luminescence or absorption of an indicator chemistry fixed at the micro-fiber tip. A general scheme of a micro-optode can be found in Figure 6. Three types of optical microsensors have been developed for environmental studies, the oxygen (36), the temperature (35) and the pH micro-optode (37). The fiber optical

sensors have tips of 20-30 µm diameter and have response times of a few seconds. As there is no analyte consumption, the micro-optodes are insensitive to stirring.

Microsensor applications

Microsensors can be applied in many different environmental studies. They have been used for instance in microbial mats for photosynthesis studies (32, 39), in sediments (marine and freshwater) to study the boundary layer and microbial conversions (31, 33), in biofilms and marine snow aggregates for structure and function analysis (19, 21, 38, 54), but also in more exotic environments like the termite gut (13, 26).

COMBINED USE OF MICROSENSORS AND MOLECULAR TECHNIQUES

The combination of microsensor and molecular techniques opens new possibilities in microbial ecology. It is now possible to study the microorganisms in their natural habitat, to localize the organisms, to quantify them, determine their activity and study their *in situ* microenvironment (2). The strength of this approach was shown by pioneering studies of Ramsing et al. (55) on sulfate reducing populations in biofilms and by Schramm et al. (65) describing the nitrifying population in a trickling-filter biofilm. But also cyanobacterial microbial mats from a hot spring (27), and sulfide-oxidizing populations in sediments from the Wadden sea (12) have been studied in this way. In other microbial systems the combined use of microsensors and molecular techniques will improve our understanding of the functioning of the microbial communities too. The next chapters in this thesis show more examples of combined microsensor and molecular techniques to study sulfate reducing biofilms and aggregates from wastewater treatment systems.

OUTLINE OF THIS THESIS

The aim of this thesis was to study the interactions of anaerobic and aerobic processes in wastewater treatment systems, such as biofilms, activated sludge flocs and aggregates and determine the microorganisms involved in the sulfur cycle, like the sulfate reducing and sulfur oxidizing bacteria. The combined use of microsensors and molecular techniques enabled us to study the function as well as structure of the microbial communities in these different systems.

The research started with a model system, a biofilm grown in a flow cell in the laboratory. This system allowed us to determine the environmental conditions and alter them to study the effects on biofilm growth. A planar optode was developed and used to study the oxygen distribution at the substratum of the biofilm in two dimensions and the effect of different parameters, like flow velocity and substrate addition (Chapter 2). However, sulfate reduction could not be studied in the biofilm, because of sloughing. Therefore, the development of a biofilm was studied in a different system, under more natural conditions. An oxygen impermeable plastic foil was submerged in an activated sludge basin of a municipal wastewater treatment plant and samples were taken weekly and brought to the laboratory for further microsensor and molecular analysis (Chapter 3 and 4). It was found that sulfate reducing bacteria were always present but were not sulfidogenically active in the first 6 weeks of biofilm development. This change in activity after 6 weeks could not be explained with the molecular techniques used and therefore the presence and importance of a yet undetectable group of sulfate reducing bacteria, the Gram positive *Desulfotomaculum* species, was suspected. From the oxygen and sulfide microsensor profiles it was further calculated that the sulfate reducing process within the biofilm was as important as the aerobic mineralization.

In wastewater treatment systems the mineralization process is performed mainly by the activated sludge flocs present in the activated sludge basin, as they contain the mayor part of the microbial biomass. Therefore the activated sludge flocs were studied for their nitrifying, denitrifying and sulfate reducing capabilities with microsensors and radiotracer techniques (Chapter 5). The presence of sulfate reducing bacteria was inferred from the molecular analysis, but no activity could be measured. An explanation for the absence of sulfate reduction could be the aerobic environment outside and inside the activated sludge flocs.

The final study was performed in a completely anaerobic environment. Methanogenic and sulfidogenic interactions were studied with H_2S and methane microsensors and molecular techniques in aggregates from an upflow anaerobic sludge bed (UASB) reactor (Chapter 6). A layered structure of methanogenic and sulfidogenic aggregates was revealed by FISH, with sulfate reducing bacteria at the outside of the aggregates, methanogens in the inner parts and syntrophic bacteria occupying the space in between. Microsensor analysis of the aggregates revealed the same spatial distribution of SRB and methanogens.

REFERENCES

1. **Akkermans, A. D. L., J. D. van Elsas, and F. J. de Bruijn.** 1995. Molecular Microbial Ecology Manual. Kluwer Academics Publishers, Dordrecht, The Netherlands.
2. **Amann, R., and M. Kühl.** 1998. *In situ* methods for assessment of microorganisms and their activities. Curr. Opinion Microbiol. **1:**352-358.
3. **Amann, R., J. Stromley, R. Devereux, R. Key, and D. A. Stahl.** 1992. Molecular and microscopic identification of sulfate-reducing bacteria in multispecies biofilms. Appl. Environ. Microbiol. **58:**614-623.
4. **Amann, R. I.** 1995. In situ identification of micro-organisms by whole cell hybridization with rRNA-targeted nucleic acid probes, p. 1-15. *In* A. D. L. Akkermans, J. D. Van Elsas, and F. J. De Bruijn (eds.), Molecular Microbial Ecology Manual, vol. 3.3.6. Kluwer, Dordrecht, The Netherlands.
5. **Amann, R. I., W. Ludwig, and K.-H. Schleifer.** 1995. Phylogenetic identification and in situ detection of individual microbial cells without cultivation. Microbiol. Rev. **59:**143-169.
6. **Ammann, D.** 1986. Ion-selective microelectrodes: principles, design and applications. Springer, Berlin.
7. **Ammann, D., T. Bührer, U. Schefer, M. Müller, and W. Simon.** 1987. Intracellular neutral carrier based Ca^{2+} microelectrode with sub-nanomolar detection limit. Pflügers Arch. **409:**223-228.
8. **Ammann, D., F. Lanter, R. A. Steiner, P. Schulthess, Y. Shio, and W. Simon.** 1981. Neutral carrier based hydrogen-ion selective microsensor for extra- and intracellular studies. Anal. Chem. **53:**2267-2269.
9. **Baumgärtl, H., and D. W. Lübbers.** 1983. Platinum needle electrodes for polarographic measurement of local O_2 pressure in cellular range of living tissue. Its construction and properties, p. 37-65. *In* E. Gnaiger and H. Forstner (eds.), Polarographic oxygen sensors: Aquatic and physiological applications. Springer-Verlag, Heidelberg.
10. **Breen, A., A. F. Rope, D. Taylor, J. C. Loper, and P. R. Sferra.** 1995. Application of DNA amplification fingerprinting (DAF) to mixed culture bioreactors. J. Ind. Microbiol. **14:**10-16.
11. **Brendel, P. J., and G. W. Luther III.** 1995. Development of a gold amalgam voltametric microelectrode for determination of dissolved Fe, Mn, O_2, and S(II-) in porewaters of marine and freshwater sediments. Environ. Sci. Technol. **29:**751-761.
12. **Brinkhoff, T., C. M. Santegoeds, K. Sahm, J. Kuever, and G. Muyzer.** 1998. A polyphasic approach to study the diversity and vertical distribution of sulfur-oxidizing *Thiomicrospira* species in coastal sediments of the German Wadden sea. Appl. Environ. Microbiol. **64:**4650-4657.
13. **Brune, A., D. Emerson, and J. A. Breznak.** 1995. The termite gut microflora as an oxygen sink: Microelectrode determination of oxygen and pH gradients in guts of lower and higher termites. Appl. Environ. Microbiol. **61:**2681-2687.
14. **Cline, J. D.** 1969. Spectrophotometric determination of hydrogen sulfide in natural waters. Limnol. Oceanogr. **14:**454-458.
15. **Cronenberg, C. C. H., H. van Groen, D. de Beer, and J. C. van den Heuvel.** 1991. Oxygen-independent glucose microsensor based on glucose oxidase. Anal. Chim. Acta. **242:**275-278.
16. **Damgaard, L. R., L. H. Larsen, and N. P. Revsbech.** 1995. Microscale biosensors for environmental monitoring. Trends Anal. Chem. **14:**300-303.
17. **Damgaard, L. R., and N. P. Revsbech.** 1997. A microscale biosensor for methane containing methanotrophic bacteria and an internal oxygen reservoir. Anal. Chem. **69:**2262-2267.
18. **De Beer, D., A. Glud, E. Epping, and M. Kühl.** 1997. A fast responding CO_2 micro-electrode for profiling sediments, microbial mats, and biofilms. Limnol. Oceanogr. **42:**1590-1600.
19. **De Beer, D., A. Schramm, C. M. Santegoeds, and M. Kühl.** 1997. A nitrite microsensor for profiling environmental biofilms. Appl. Environ. Microbiol. **63:**973-977.
20. **De Beer, D., R. Srinivasan, and P. S. Stewart.** 1994. Direct measurements of chlorine penetration into biofilms during disinfection. Appl. Environ. Microbiol. **60:**4339-4344.

21. **De Beer, D., P. Stoodley, F. Roe, and Z. Lewandowski.** 1994. Effect of biofilm structures on oxygen distribution and mass transfer. Biotechnol. Bioeng. **43:**1131-1138.
22. **De Beer, D., and J. P. R. A. Sweerts.** 1989. Measurements of nitrate gradients with an ion-selective microelectrode. Anal. Chim. Acta. **219:**351-356.
23. **De Beer, D., and J. C. van den Heuvel.** 1988. Response of ammonium-selective microelectrodes based on the neutral carrier nonactin. Talanta. **35:**728-730.
24. **De Beer, D., J. C. van den Heuvel, and S. P. P. Ottengraaf.** 1993. Microelectrode measurements of the activity distribution in nitrifying bacterial aggregates. Appl. Environ. Microbiol. **59:**573-579.
25. **Dunbar, J., S. White, and L. J. Forney.** 1997. Genetic diversity through the looking glass: effect of enrichment bias. Appl. Environ. Microbiol. **63:**1326-1331.
26. **Ebert, A., and A. Brune.** 1997. Hydrogen concentration profiles at the oxic-anoxic interface: A microsensor study of the hindgut of the wood-feeding lower termite *Reticulitermes flavipes* (Kollar). Appl. Environ. Microbiol. **63:**4039-4046.
27. **Ferris, M. J., S. C. Nold, N. P. Revsbech, and D. M. Ward.** 1997. Population structure and physiological changes within a hot spring microbial mat community following disturbance. Appl. Environ. Microbiol. **63:**1367-1374.
28. **Harmsen, H. J. M., A. D. L. Akkermans, A. J. M. Stams, and W. M. de Vos.** 1996. Population dynamics of propionate-oxidizing bacteria under methanogenic and sulfidogenic conditions in anaerobic granular sludge. Appl. Environ. Microbiol. **62:**2163-2168.
29. **Hinke, J.** 1969. Glass microelectrodes for the study of binding and compartmentalisation of intracellular ions, p. 349-375. *In* M. Lavallee, O. F. Schanne, and N. C. Herbert (eds.), Glass microelectrodes, Wiley.
30. **Jeroschewski, P., C. Steuckart, and M. Kühl.** 1996. An amperometric microsensor for the determination of H_2S in aquatic environments. Anal. Chem. **68:**4351-4357.
31. **Jørgensen, B. B., and D. J. Des Marais.** 1990. The diffusive boundary layer of sediments: Oxygen microgradients over a microbial mat. Limnol. Oceanogr. **35:**1343-1355.
32. **Jørgensen, B. B., and D. J. Des Marais.** 1988. Optical properties of benthic photosynthetic communities: Fiber-optic studies of cyanobacterial mats. Limnol. Oceanogr. **33:**99-113.
33. **Jørgensen, B. B., and N. P. Revsbech.** 1985. Diffusive boundary layers and the oxygen uptake of sediments and detritus. Limnol. Oceanogr. **30:**11-21.
34. **Kämpfer, P., R. Erhart, C. Beimfohr, J. Böhringer, M. Wagner, and R. Amann.** 1996. Characterization of bacterial communities from activated sludge: culture-dependent numerical identification versus *in situ* identification using group- and genus-specific rRNA-targeted oligonucleotide probes. Microbiol. Ecol. **32:**101-121.
35. **Klimant, I., M. Kühl, R. N. Glud, and G. Holst.** 1997. Optical measurements of oxygen and temperature in microscale: strategies and biological applications. Sensors and Actuators B. **38-39:**29-37.
36. **Klimant, I., V. Meyer, and M. Kühl.** 1995. Fiber-optic oxygen microsensors, a new tool in aquatic biology. Limnol. Oceanogr. **40:**1159-1165.
37. **Kohls, O., I. Klimant, G. Holst, and M. Kühl.** 1997. Development and comparison of pH microoptodes for use in marine systems. Proc. SPIE. **2978:**82-94.
38. **Kühl, M., and B. B. Jørgensen.** 1992. Microsensor measurements of sulfate reduction and sulfide oxidation in compact microbial communities of aerobic biofilms. Appl. Environ. Microbiol. **58:**1164-1174.
39. **Kühl, M., C. Lassen, and B. B. Jørgensen.** 1994. Optical properties of microbial mats: Light measurements with fiber optic microprobes, p. 149-167. *In* L. J. Stal and P. Caumette (eds.), Microbial mats: Structure, development, and environmental significance. Springer-Verlag, Berlin.
40. **Kühl, M., and N. P. Revsbech.** 1998. Microsensors for the study of interfacial biogeochemical processes. *In* B. P. Boudreau and B. B. Jørgensen (eds.), The bentic boundary layer, vol. in press. Oxford University Press, Oxford.
41. **Kühl, M., C. Steuckart, G. Eickert, and P. Jeroschewski.** 1998. A H_2S microsensor for profiling biofilms and sediments: application in an acidic lake sediment. Aquat. Microb. Ecol. **15:**201-209.

42. **Larsen, L. H., T. Kjaer, and N. P. Revsbech.** 1997. A microscale NO_3^- biosensor for environmental applications. Anal. Chem. **69:**3527-3531.

43. **Larsen, L. H., N. P. Revsbech, and S. J. Binnerup.** 1996. A microsensor for nitrate based on immobilized denitrifying bacteria. Appl. Environ. Microbiol. **62:**1248-1251.

44. **Lens, P., D. De Beer, C. Cronenberg, S. Ottengraf, and W. Verstraete.** 1995. The use of microsensors to determine population distribution in UASB aggregates. Water Sci. Technol. **31:**273-280.

45. **Liu, W. T., T. L. Marsh, H. Cheng, and L. J. Forney.** 1997. Characterization of microbial diversity by determining terminal restriction fragment length polymorphesms of genes encoding 16S rRNA. Appl. Environ. Microbiol. **63:**4516-4522.

46. **Manz, W., M. Eisenbrecher, T. R. Neu, and U. Szewzyk.** 1998. Abundance and spatial organization of Gram-negative sulfate-reducing bacteria in activated sludge investigated by in situ probing with specific 16S rRNA targeted oligonucleotides. FEMS Microbiol. Ecol. **25:**43-61.

47. **Massol-Deyá, A., D. A. Odelson, R. F. Hickey, and J. M. Tiedje.** 1995. Bacterial community fingerprinting of amplified 16S and 16-23S ribosomal DNA gene sequences and restriction endonuclease analysis (ADRA), p. 1-8. *In* A. D. L. Akkermans, J. D. van Elsas, and F. J. de Bruijn (eds.), Molecular Microbial Ecology Manual, vol. 3.3.2. Kluwer Academic Publishers, Dordrecht, The Netherlands.

48. **Massol-Deyá, A., R. Weller, L. Ríos-Hernández, J.-Z. Zhou, R. F. Hickey, and J. M. Tiedje.** 1997. Succession and convergence of biofilm communities in fixed-film reactors treating aromatic hydrocarbons in groundwater. Appl. Environ. Microbiol. **63:**270-276.

49. **Muyzer, G.** 1999. Genetic fingerprinting of microbial communities - present status and future perspectives. *In* C. Bell (ed.), Proceedings of the Eighth International Symposium on Microbial Ecology, Halifax, Canada. In press.

50. **Muyzer, G., T. Brinkhoff, U. Nübel, C. Santegoeds, H. Schäfer, and C. Wawer.** 1998. Denaturing gradient gel electrophoresis (DGGE) in microbial ecology, p. 1-27. *In* A. D. L. Akkermans, J. D. van Elsas, and F. J. de Bruijn (eds.), Molecular Microbial Ecology Manual, vol. 3.4.4. Kluwer, Dordrecht, The Netherlands.

51. **Muyzer, G., and N. B. Ramsing.** 1995. Molecular methods to study the organization of microbial communities. Water Sci. Technol. **32:**1-9.

52. **Muyzer, G., and K. Smalla.** 1998. Application of denaturing gradient gel electrophoresis (DGGE) and temperature gradient gel electrophoresis (TGGE) in microbial ecology. Antonie van Leeuwenhoek. **73:**127-141.

53. **Oude Elferink, S. J. W. H., W. J. C. Vorstman, A. Sopjes, and A. J. M. Stams.** 1998. Characterization of the sulfate-reducing and syntrophic population in granular sludge from a full-scale anaerobic reactor treating papermill wastewater. FEMS Microbiol. Ecol. **27:**185-194.

54. **Ploug, H., M. Kühl, B. Buchholz-Cleven, and B. B. Jørgensen.** 1997. Anoxic aggregates - an ephemeral phenomenon in the pelagic environment? Aquat. Microb. Ecol. **13:**285-294.

55. **Ramsing, N. B., M. Kühl, and B. B. Jørgensen.** 1993. Distribution of sulfate-reducing bacteria, O_2, and H_2S in photosynthetic biofilms determined by oligonucleotide probes and microelectrodes. Appl. Environ. Microbiol. **59:**3840-3849.

56. **Raskin, L., L. K. Poulsen, D. R. Noguera, and B. E. Rittmann.** 1994. Quantification of methanogenic groups in anaerobic biological reactors by oligonucleotide probe hybridization. Appl. Environ. Microbiol. **60:**1241-1248.

57. **Raskin, L., B. E. Rittmann, and D. A. Stahl.** 1996. Competition and coexistance of sulfate-reducing and methanogenic populations in anaerobic biofilms. Appl. Environ. Microbiol. **62:**3847-3857.

58. **Revsbech, N. P.** 1989. An oxygen microelectrode with a guard cathode. Limnol. Oceanogr. **55:**1907-1910.

59. **Revsbech, N. P., and B. B. Jørgensen.** 1986. Microelectrodes: their use in microbial ecology. Adv. Microb. Ecol. **9:**293-352.

60. **Revsbech, N. P., B. B. Jørgensen, T. H. Blackburn, and Y. Cohen.** 1983. Microelectrode studies of the photosynthesis and O_2, H_2S and pH profiles of a microbial mat. Limnol. Oceanogr. **28:**1062-1074.

61. **Revsbech, N. P., L. P. Nielsen, P. B. Christensen, and J. Sørensen.** 1988. A combined oxygen and nitrous oxide microsensor for denitrification studies. Appl. Environ. Microbiol. **45:**2245-2249.

62. **Revsbech, N. P., and D. M. Ward.** 1983. Oxygen microelectrode that is insensitive to medium chemical composition: Use in an acid microbial mat dominated by *Cyanidium caldarum*. Appl. Environ. Microbiol. **45:**755-759.

63. **Santegoeds, C. M., T. G. Ferdelman, G. Muyzer, and D. de Beer.** 1998. Structural and functional dynamics of sulfate-reducing populations in bacterial biofilms. Appl. Environ. Microbiol. **64:**3731-3739.

64. **Schramm, A., D. de Beer, M. Wagner, and R. Amann.** 1998. Identification and activities in situ of *Nitrosospira* and *Nitrospira* spp. as dominant populations in a nitrifying fluidized bed reactor. Appl. Environ. Microbiol. **64:**3480-3485.

65. **Schramm, A., L. H. Larsen, N. P. Revsbech, N. B. Ramsing, R. Amann, and K.-H. Schleifer.** 1996. Structure and function of a nitrifying biofilm as determined by in situ hybridization and the use of microelectrodes. Appl. Environ. Microbiol. **62:**4641-4647.

66. **Schulthess, P., Y. Shijo, H. V. Pham, E. Pretsch, D. Ammann, and W. Simon.** 1981. A hydrogen ion-selective liquid-membrane electrode based on tri-n-dodecylamine as neutral carrier. Anal. Chim. Acta. **131:**111-116.

67. **Stahl, D. A., and R. Amann.** 1991. Development and application of nucleic acid probes, p. 207-248. *In* E. Stackebrandt and M. Goodfellow (eds.), Nucleic Acid Techniques in Bacterial Systematics, vol. 8. John Wiley & Sons Ltd.

68. **Thomas, R. C.** 1978. Ion-sensitive intracellular microelectrodes, how to make and use them. Academic Press, London.

69. **Torsvik, V., J. Goksoyr, and F. L. Daae.** 1990. High diversity in DNA of soil bacteria. Appl. Environ. Microbiol. **56:**782-787.

70. **Wagner, M., R. Amann, H. Lemmer, and K.-H. Schleifer.** 1993. Probing activated sludge with oligonucleotides specific for proteobacteria: inadequacy of culture-dependent methods for describing microbial community structure. Appl. Environ. Microbiol. **59:**1520-1525.

71. **Wagner, M., A. J. Roger, J. L. Flax, G. A. Brusseau, and D. A. Stahl.** 1998. Phylogeny of dissimilatory sulfite reductases supports an early origin of sulfate respiration. J. Bacteriol. **180:**2975-2982.

72. **Wawer, C., and G. Muyzer.** 1995. Genetic diversity of *Desulfovibrio* spp. in environmental samples analyzed by denaturing gradient gel electrophoresis of [NiFe] hydrogenase gene fragments. Appl. Environ. Microbiol. **61:**2203-2210.

73. **Wayne, L. G., D. J. Brenner, R. R. Colwell, P. A. D. Grimont, O. Kandler, M. I. Krichevsky, C. Moore, W. E. C. Moore, R. G. E. Murray, E. Stackebrandt, M. P. Starr, and H. G. Trüper.** 1987. Report of the ad hoc committee on reconciliation of approaches to bacterial systematics. Int. J. Syst. Bacteriol. **37:**463-464.

74. **Welsh, J., and M. McClelland.** 1990. Fingerprinting genomes using PCR with arbitrary primers. Nucl. Acids Res. **18:**7213-7218.

75. **Wikström, P., A.-C. Andersoon, and M. Forsman.** 1999. Biomonitoring complex communities using random amplfied polymorphic DNA and principal component analysis. FEMS Microbiol. Ecol. **28:**131-139.

Chapter 2

Oxygen dynamics at the base of a biofilm studied with planar optodes

Ronnie Nøhr Glud[1,2], Cecilia Maria Santegoeds[1], Dirk de Beer[1], Oliver Kohls[1], Niels Birger Ramsing[3]

[1]Max Planck Institute for Marine Microbiology, Celsiusstr. 1, 28359 Bremen, Germany.
[2]University of Copenhagen, Marine Biological Laboratory, Strandpromenaden 5, 3000 Helsingør, Denmark.
[3]University of Aarhus, Institute of Biology, Dept. of Microbial Ecology, 8000 Aarhus C., Denmark.

This chapter has been published in Aquatic Microbial Ecology 14:223-233 (1998).

ABSTRACT

The O_2 dynamics at the base of biofilms was studied using planar optodes. Biofilms were grown directly on the optodes and the two dimensional distribution of O_2 at the base of biofilms was resolved at a spatial resolution of 30 x 30 µm, using a CCD camera. The average O_2 saturation at the base decreased and the heterogeneity increased as biofilms developed. In mature biofilms heterogeneous O_2 distributions were caused by clusters of high biomass which had low O_2 saturations surrounded by O_2-rich voids and channels. The O_2 distribution at the base of biofilms was highly dependent on the free flow velocity above the biofilm e.g. in a 400 µm thick biofilm the average O_2 saturation increased from 0 to 23.1% air saturation as the free flow velocity increased from 6.2 to 35.1 cm s^{-1}. Addition of glucose to a concentration of 2 mM in the water phase at maximum flow velocity caused the O_2 consumption rate to increase and the base of the biofilm to go anoxic. The insertion of an O_2 microelectrode into a biofilm caused the O_2 saturation at the base of the biofilm to increase by approximately 25 µM. This effect, presumably caused by hydrodynamic disturbances, typically extended several mm away from the position of the microsensor tip. The presented data, show for the first time the true distribution of O_2 at the basis of heterogeneous biofilms and demonstrate the great potential of planar optodes to study solute dynamics within biofilms at a very high spatial and temporal resolution.

INTRODUCTION

Under physiological conditions most submerged surfaces will become colonized by bacteria that gradually form denser biofilms. During the initial development, the base of a biofilm will be all oxic; however, as the thickness increases anoxic areas are expected to occur. The metabolism and function of such communities are largely controlled by the electron acceptors available above and within the biofilm. Oxygen is energetically the most favorable electron acceptor and it therefore plays an important role for the turnover of organic matter within a biofilm. Further, O_2 act as a reoxidizer of reduced compounds diffusing up to the oxic zone from deeper layers. The oxic conditions within a biofilm also determine the extent to which denitrification is coupled to nitrification, and consequently regulate how well a biofilm act as a NO_3^- scavenger (4).

Biofilms may not be homogenous layers of cells, as conventionally thought, but often they have a complex heterogeneous structure, that is dependent on growth conditions and the microbial composition (e.g. 1, 15). Recent investigations with confocal microscopy have shown that they typically contain dense cell clusters, surrounded by voids (3, 5). Liquid may flow through the voids, insuring an efficient exchange of solutes between the biofilm and the water phase, and probably enable cells to maintain a high growth rate. The patchy distribution of reduced and oxidized zones in well-developed biofilms may initiate pit corrosion on metal surfaces, and the O_2 distribution is of importance for metal deterioration in aquatic environments (8). To resolve the heterogeneous distribution and dynamics of solutes like O_2 within such a community, techniques with a high spatial and temporal resolution are required (6).

Due to their small size, high spatial resolution, fast response time and low stirring sensitivity, microelectrodes are ideal tools for studying O_2 dynamic in compact, laminated benthic communities (2, 11, 19). Recently, a new fiber optic microsensor (microoptode), which complements the microelectrode, has been developed and applied in the field of aquatic biology (13). The main advantages of optodes include a better long-term stability and simpler manufacturing procedures as compared to O_2 microelectrodes. The measuring principle in this sensor is based on the dynamic quenching of an immobilized fluorophore by O_2, which decreases the fluorescence quantum yield (12). In microoptodes, the fluorophore is fixed to the tip of a beveled glass fiber and the excitation light is guided through the fiber to the tip of the sensor. The fiber also guides the fluorescent light emitted by the fluorophore after excitation back to the measuring circuit (13).

Both types of microsensors measure the O_2 tension at a single point and microprofiles are obtained by moving the sensor stepwise within the medium. However, in the spatially heterogeneous biofilms described above a large numbers of profiles are required in order to describe the solute dynamics. Further, it has been shown that the presence of a microsensor can change the distribution of O_2 within sediments due to a hydrodynamic disturbance of the diffusive boundary layer (DBL); such effects must be expected to be more pronounced in biofilms with steep concentration gradients (9). In other words, to quantify and describe the O_2 dynamics within a heterogeneous biofilm, non-conventional techniques are required. Techniques combining color indicators for specific solutes with microscopy and digital imaging, have been attempted; however, calibration problems related to determination of the indicator concentration have often hampered the use of these techniques (1).

Recently an alternative approach based on the principle of dynamic quenching, planar optodes, has allowed 2-dimensional determination of O_2 dynamics within marine sediments (10). Instead of fixing an immobilized fluorophore to the tip of a microoptodes, the sensing agent was immobilized in thin sheets, 'planar optodes'. Images of the O_2-sensitive fluorescent light emitted by the planar optode were acquired with a CCD camera, allowing quantification of the O_2 saturation in front of the planar optode (10). The optodes are simple to construct and a robust calibration routine ensures high quality data. By growing biofilms directly on planar optodes we were able to quantify the 2-dimensional O_2 dynamics at the base of a biofilm without disturbance. We hereby present data that quantify O_2 saturations and dynamics at the base of biofilms as a function of the biofilm development (thickness), flow velocity of the overlying water, and addition of organic substrates.

MATERIALS AND METHODS

Planar oxygen optode. The planar optodes consisted of three layers: A transparent polyester support foil 175 µm thick, a 10 µm sensing layer and a 20 µm black silicone layer (10). The polyester support foil was included in order to handle and to fix the sensing agent in the experimental set up described below. The sensing layer consisted of an immobilized O_2 quenchable ruthenium complex, which had maximum light absorbance in the blue range and emitted red fluorescent light (14). In order to increase the scatter intensity, titanium dioxide grains (diameter approximately 1 µm) were added (14). The black silicone acted as an optical isolation, which insured that the excitation light never reached the internal parts of the experimental setup and that scatter in the biofilms did not

affect the CCD images, for more details see Glud et al. (10). The size of the employed planar optodes was 25 x 55 mm.

Experimental set up. All experiments were performed in a 100 cm long and 4 cm wide transparent flow-cell. An adjustable circulation micropump (Ismatec, MC-Z) ensured a stable but adjustable flow rate above the biofilm (Fig. 1A). Medium was added to the flow-cell through a peristaltic pump (Gilson M312), and a constant overflow maintained the water level and nutrient concentration for a given flow velocity (Fig. 1A). The minimal medium was added at a rate of 50 ml min^{-1} and consisted of KH_2PO_4 (220 µM), K_2HPO_4 (400 µM), $(NH_4)_2SO_4$ (760 µM), Na-Acetate (200 µM) and $MgSO_4$ (41 µM). A Clark type O_2 microelectrode (tip size < 5 µm) was used to continuously monitor the O_2 saturation in the free flowing water phase (18, 19).

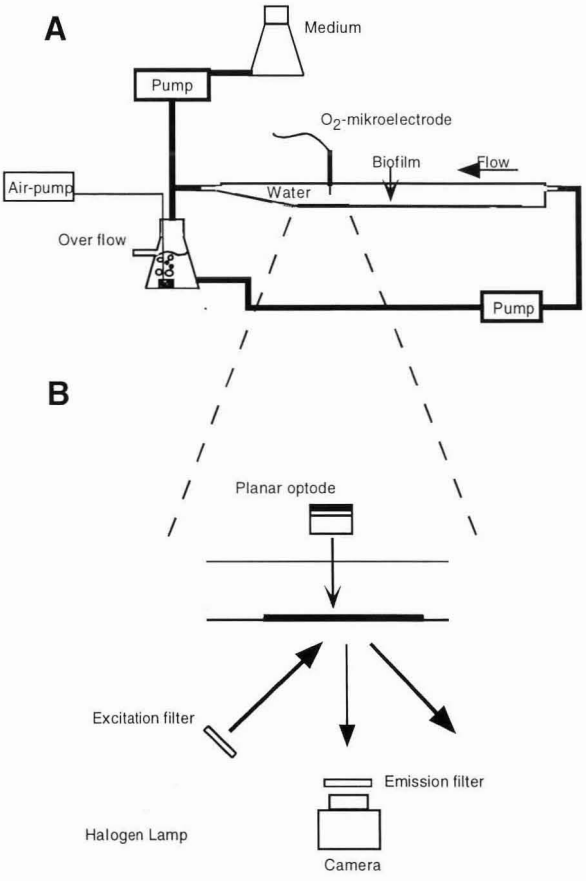

Fig. 1. Schematic drawing of the experimental setup. (B) Enlargement of the area around the planar optode including camera, filters etc., which is omitted in (A). For details see text.

The planar optode was fixed to the bottom of the dry flow-cell by a thin film of transparent silicone and thereafter it cured for 24 h . The planar optode was excited by a halogen lamp equipped with a bandpass glass filter (BG 12, Schott, Germany) in order to eliminate yellow and red light from

the excitation beam (Fig. 1B). A CCD Photometrics™ camera (CH250L) equipped with a 60 mm Nikon macro lens and a longpass glass filter (OG 570, Schott) was positioned below the flow cell at a distance of approximately 15 cm (Fig. 1B). The flow cell, the halogen lamp, and the CCD camera were fixed relative to each other in a custom designed frame, in order to minimize vibration effects. The flow cell was inoculated by 10 ml activated sludge from a waste water treatment plant, and after 10 to 12 d an approximately 400 µm thick biofilm covered the bottom of the flow-cell and the planar optode. Images were obtained by the CCD camera as a function of time (biofilm development), free flow velocity of the overlying water and concentrations of organic substances in the overlying water.

After each series of experiments the biofilm covering the investigated part of the planar optode was removed for calibration purposes. Images were obtained at 3 to 5 different O_2 saturations. The saturation was adjusted by flushing with N_2 gas in the overflow bottle and was measured by the calibrated O_2 microelectrode (Fig. 1A). A stereo microscope allowed visual inspection of the biofilm and capillaries inserted by a micromanipulator were used to measure the thickness of the biofilms. All experiments were performed in a darkened thermostat room at 20°C.

Image recording, calibration and analysis. The camera was equipped with a Peltier cooled CCD chip (KAF 1400, 1317 x 1035 pixels, 6.8 x 6.8 µm) and was controlled by a Macintosh Quadra computer. The images were obtained using an aperture of 2.8 and an exposure time of 0.01 s. The digital pictures were acquired as 12 bit grey-scale images with the program NU-200, Photometrics and stored in a 16 bit TIFF format for later analysis. In order to reduce the time required for calculations, the images were obtained with a binning factor of 2, implying that only an average value for each set of 4 neighboring pixels was stored. This reduced the original number of pixels to 3.4 x 10^5, the images covered 19.7 x 15.6 mm and consequently the spatial resolution in both directions was about 30 µm. The investigated area and the spatial resolution of the obtained images could be adjusted by applying lenses of different focal length.

For most optodes the emitted light intensity (I) can be approached by a modified Stern-Volmer equation (Klimant, et al. (1995)):

$$I = I_0\left[\alpha + (1-\alpha)\left(\frac{1}{1+K_{sv}C}\right)\right] \qquad (1)$$

where α is the non-quenchable fraction of the fluorescence, I_0 is the fluorescence intensity in the absence of O_2, K_{sv} is the quenching constant and C is the O_2 saturation. Due to the relatively heterogeneous planar optodes used in our experiments, each of these parameters were found to be pixel dependent (10). Consequently we had to perform 3 point calibration of each individual pixel. To do so, we used the calibration images obtained after each experiment. The I_0 value of each pixel was determined directly from an image obtained with no O_2 in the overlying water, while the pixel values of α and K_{sv} were calculated based on the 2 additional calibration-images. The necessary equations are derived in Glud et al. (10). Knowing all three calibration constants the pixel dependent O_2 saturation in the acquired images could be derived from Eq. (2):

$$C = \frac{I_0 - I}{K_{sv}(I - I_0\alpha)} \qquad (2)$$

After appropriate calibration the O_2 saturation was depicted on a 8 bit color scale (256 different colors), with a chosen max/min O_2 value.

RESULTS

Biofilm development. After inoculation, the free flow velocity in the flow cell was kept at an intermediary level of approximately 25 cm s^{-1}. A thin opaque layer of polysaccharides soon covered the planar optode, as observed through a stereo microscope. Gradually, flocculent material embedded in the opaque layer and grew into a heterogeneous biofilm. The inoculation was repeated 3 times and every time it took between 10 to12 d for a biofilm with an average thickness of 400 µm to develop. The surface of the biofilm was characterized by an extensive variation in microtopography and generally developed faster further downstream in the flow cell. As the biofilm grew in thickness the average O_2 saturation at the base of the biofilm decreased correspondingly (Fig. 2). For the interpretation of Fig. 2 it is important to notice that the measurements were made on different biofilms and it is therefore not possible to follow the same area during different development stages. The initial measurement just after inoculation resulted in a homogenous signal that corresponded to 100% air saturation (284 µM) (Fig. 2A). After 4 d a thin biofilm covered the optode, but most of the sensor still experienced full air saturation (Fig. 2B). However, at the very left, the biofilm was thicker and the average O_2 saturation at the base of this area was 80.3% (227 µM), while single aggregates resulted in O_2 saturation down to 57.0% (162 µM) (Fig. 2B). After 8 d the planar optode was covered by a 200 µm (on average) thin biofilm and the average O_2 saturation at the base had decreased to 64.1% (182 µM) (Fig. 2C). Figure 2D-F represents 3 different biofilms 11 to 13 d after inoculation. In Fig. 2D the average O_2 saturation had further decreased to 52.3% (149 µM) and areas, with O_2 saturations below 20% (57 µM), were apparent. In Fig. 2E the saturation varied extensively: the central area had an O_2 saturation below 20.0% (57 µM) whereas the surrounding areas had higher O_2 tensions approaching air-saturation. The central area of the biofilm which had developed to an average thickness of 400 µm was anoxic at the base (Fig. 2F) and, as for the biofilm presented in Fig. 2E horizontal O_2 gradients from the center to the periphery of the image had evolved.

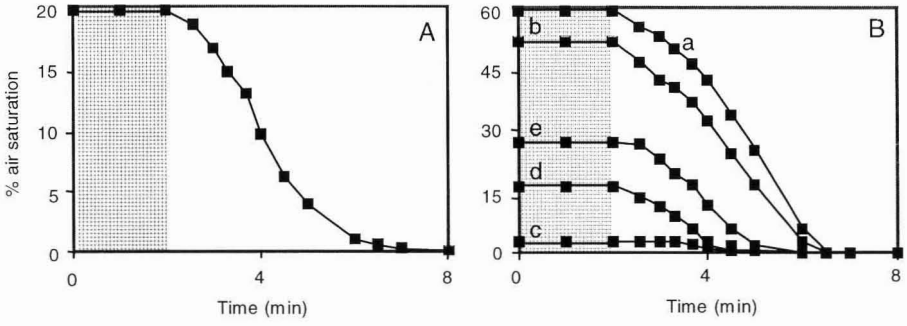

Fig. 3. (A) Average % air saturation at the base of a 12 d old biofilm as the flow velocity of the overlying water was changed from 35.1 cm s^{-1} (shaded) to 6.2 cm s^{-1}. (B) Corresponding data for the 5 individual positions (a-e) indicated in Fig. 2F.

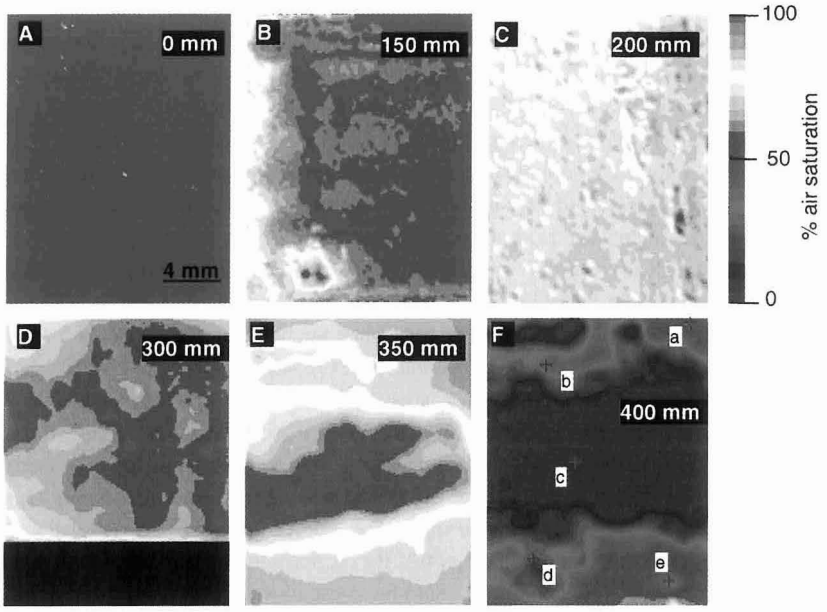

Fig. 2. The O_2 saturation at the base of 6 different biofilms (A) 0 d, (B) 4 d, (C) 8 d and (D-F) 11 to 13 days after inoculation (average thickness indicated). For clarification the original 8 bit color scale is reduced to 26 colors. The flow direction was in all instances from right to left and the velocity approximately 20 cm s^{-1}. The black box in (D) covers an area of the planar optode that was obscured by the reflection from a screw in the bottom of the flow cell. The 5 points indicated in (F) were used in the experiments with changed flow velocities (Figs. 3 &. 5). A scale bar is shown in (A).

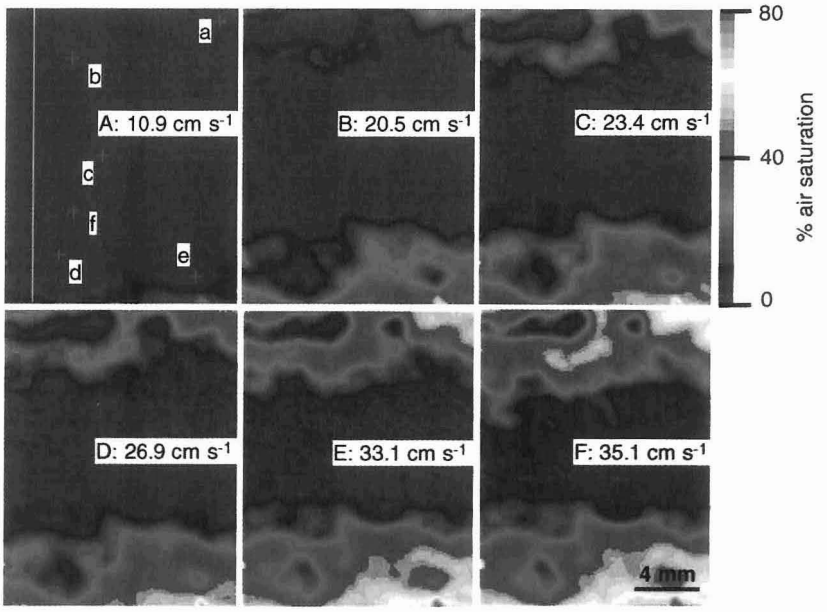

Fig. 4. Oxygen images of the base of a 13 d old biofilm at increasing flow velocities. Positions investigated in greater details in Figs. 5B & 6 are in (A). A scale bar for the dimensions is indicated in (F) and the flow direction was from right to left.

Flow effects on the O_2 distribution at the base of a biofilm. The O_2 saturation at the base of the 12 d old biofilm presented in Fig. 2F was measured after the free flow velocity of the overlying water was reduced from 35.1 to 6.2 cm s^{-1}. After changing the flow velocity, the average O_2 saturation started to decreased and the base of the biofilm reached complete anoxia 6 min. later (Fig. 3A). The average O_2 decrease followed a sigmoidal curve with a maximum rate of decrease after 1.5 min. However, different pixels responded very differently, probably caused by differences in local biofilm thickness, transport coefficients and respiration rates (Fig. 3B).

One day later the steady state O_2 saturation at the base of the same biofilm was measured at different flow velocities of the overlying water, 6 examples are presented in Fig. 4. The average O_2 saturation increased from 0% to 23.1 % (0 to 66 µM) when the free flow velocity was increased from 6.2 to 35.1 cm s^{-1} (Fig. 5A). However, it is apparent from Fig. 4 that some areas in the biofilm were more sensitive to flow than others. At 20.5 cm s^{-1} areas with increased O_2 saturations had developed in the otherwise anoxic surroundings and as the flow increased these areas gradually grew and became connected (Fig. 4). At the highest flow velocities, numerous 'islands' with low O_2 saturations in otherwise O_2-rich surroundings, still remained (Fig. 4F). These islands exhibited steeper O_2 gradients in the direction against the flow as compared to the 'lee' side of the islands. Even at the maximum flow rate no pixels reached full saturation (Fig. 4F). By decreasing the flow velocity in steps, the O_2 conditions prior to increased flow conditions could be re-established, indicating that the biofilm did not change physically during the increased flow scenario (data not shown).

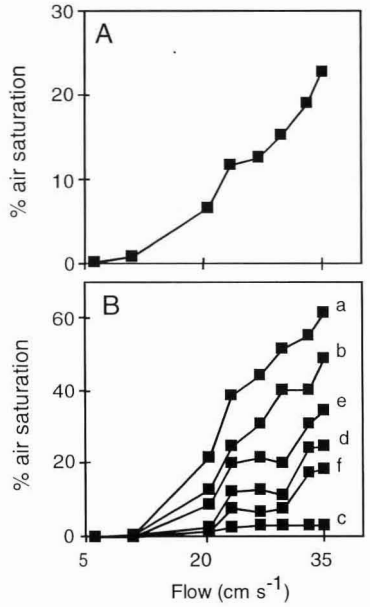

Fig. 5. (A) Average O_2 saturation at the base of a 13 d old biofilm as a function of the flow velocity of the overlying water. (B) Equivalent values for individual pixels indicated in Fig. 4A.

The observations that different areas of the biofilm responded differently to flow increases are emphasized in Figs. 5B & 6. Fig. 5B. shows the O_2 saturation for 6 different pixels (indicated in Fig. 4A) at different flow regimes. The O_2 saturation at pixel c only changed marginally as the flow was

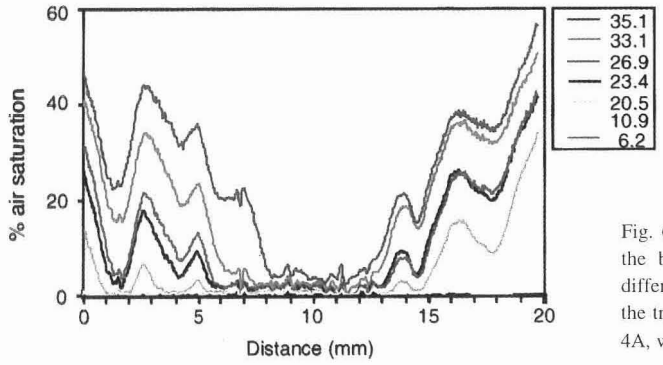

Fig. 6. O_2 saturation along a transect at the base of a 13 d old biofilm at 7 different flow velocities. The position of the transect is indicated by a line in Fig. 4A, where 0 indicates the upper corner.

increased from 10.9 to 20.5 cm s^{-1} and pixel d and f were almost insensitive to the flow until it exceeded 23.4 cm^{-1}. Here the O_2 saturation increased, but then remained at a constant level; this was also found for pixel e until the flow reached 33.1 cm s^{-1}. The O_2 saturation at pixel b and a increased almost linearly with flow and at maximum flow velocity it reached 49.1% (139 µM) and 61.7% air saturation (175 µM), respectively.

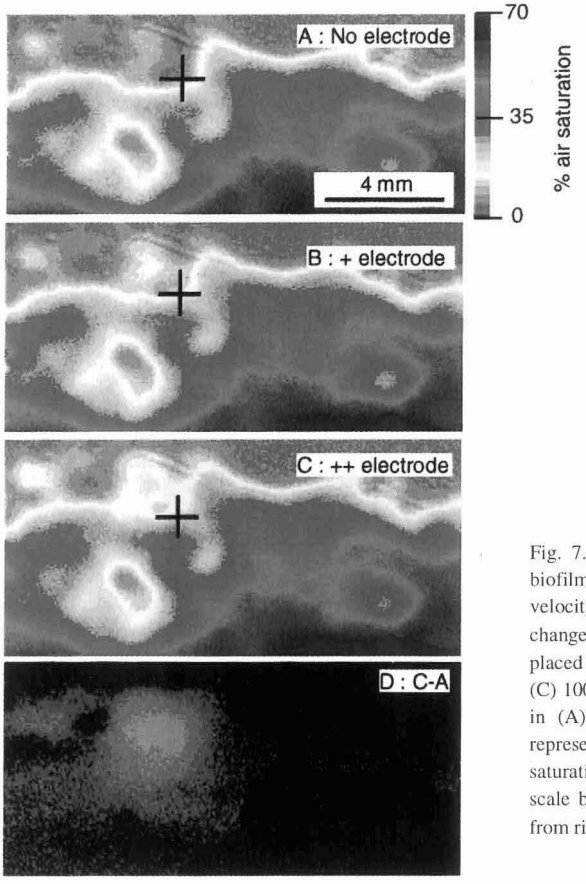

Fig. 7. Enlargement of the lower corner of the biofilm presented in Fig. 4 with a free flow velocity of 29.8 cm s^{-1}. Note that the scale bar is changed. (B) The tip of a microelectrode (+) was placed 200 µm above the surface of a biofilm and (C) 100 µm below the surface. (D) The O_2 images in (A) and (C) are subtracted and red pixels represent positions with an increased O_2 saturation after insertion of the microelectrode. A scale bar is included and the flow direction was from right to left.

Pixel values along a line perpendicular to the flow direction (indicated in Fig. 4A) are presented as a function of flow in Fig. 6. The positions of local maxima and minima appeared flow-insensitive as expected if they corresponded to metabolic hot spots. The O_2 gradients between them were likewise in many cases flow-insensitive. It is apparent that whole areas exhibited the same stepwise response to flow changes as e.g. pixels d, e and f, in Fig. 5B; pixels between 14 and 19.5 mm were almost insensitive to the flow increase between 23.4 to 26.9 and 33.1 to 35.1, while the pixels between 3 and 5 mm clearly showed increased O_2 saturations at the same flow increases. At the highest flow velocity, no positions were anoxic and notably positions from 6 to 8 mm showed a dramatic increase in O_2 saturation during the last flow increase. During all flow experiments the overlying water was fully air saturated. Repeating the flow experiments with the biofilms presented in Fig. 2D and 2E, resulted in similar observations.

Oxygen images were acquired as a microelectrode in the overlying water was inserted into the biofilm (Fig. 7). Below the sensor tip, the O_2 saturation gradually increased as the O_2 microsensor was moved downward. When the sensor was 200 μm above the surface of the biofilm the O_2 saturation had increased by 6.3% air saturation (18 μM) below the sensor tip, and the value further increased to 9.1% (26 μM) as the sensor was inserted into the biofilm (Fig. 7A-C). The horizontal distribution of the disturbance extended approximately 3 mm perpendicular to the flow direction and more than 5 mm downstream from the sensor tip. After removal of the microelectrode, the original O_2 conditions were re-established. The experiment was repeated several times on different biofilms with the same qualitative observations: oxygen saturation increased significantly when an O_2 microsensor tip approached the biofilm and the perturbation affected a large area as compared to the size of the sensor tip (data not shown).

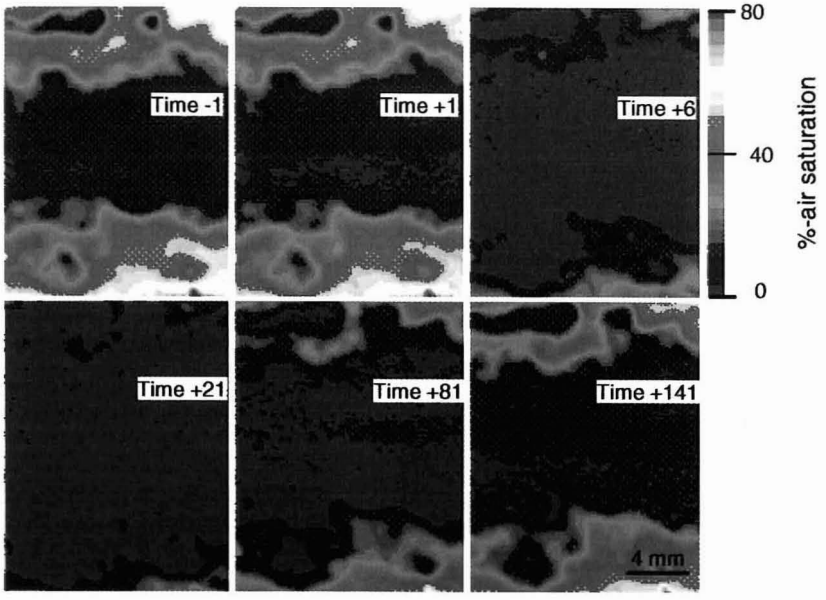

Fig. 8. Oxygen images of the base of a 13 d old biofilm at constant flow velocities before and after the addition of glucose to the free flowing water. Time is indicated in minutes and a positive sign indicates the time after glucose addition. The free flow velocity was 35.1 cm s^{-1} from right to left. A scale bar is shown in the last panel.

Organic carbon addition. Glucose was added to a final concentration of 2 mM in the water overlying the biofilm investigated in Fig. 4F, by injection into the reservoir (see Fig. 1A). The free flow velocity was kept at 35.1 cm s^{-1}. As new medium was continuously added at a rate of 50 ml min^{-1} the concentration of dissolved glucose gradually decreased. By washout the concentration of glucose decreased to < 1 µM after 165 min. The addition of glucose resulted in an immediate decrease of the average O_2 saturation and a minimum value of 2.4% (7 µM) was reached after 11 min (Figs. 8 & 9). The O_2 saturation then stayed constantly low for another 15 min before it gradually increased to a constant level of approximately 11% air saturation (31 µM), after 160 min (Fig. 9). In another experiment acetate was removed from the usual medium during a steady state situation (flow velocity was 35.1 cm s^{-1}), but the O_2 saturation at the base of the 13 d old biofilm was unchanged even after 5 h without acetate (data not shown).

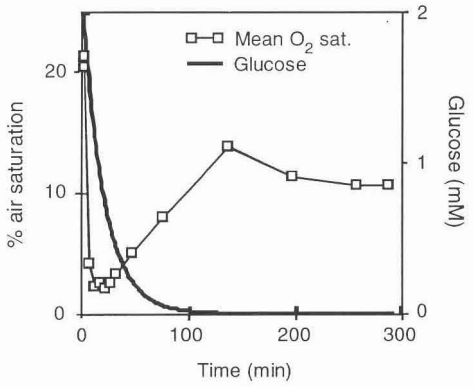

Fig. 9. Average O_2 saturation at the base of a 13 d old biofilm after the addition of glucose to a final concentration of 2 mM. The decrease in glucose concentration is solely estimated from the washout rate.

DISCUSSION

Flow related O_2 dynamic and the physical structure of biofilms. The presented data clearly demonstrate a complex and highly dynamic 2- and 3- dimensional O_2 distribution within a mature biofilm. Visual observations could to some extent relate the physical structure of the biofilms to the O_2 dynamic measured at the base. The investigated biofilms showed an extensive variation in thickness which was caused by dense cell clusters and channel structures, as has also been observed by others (e.g. 3). The location of these clusters and channels corresponded to low and high O_2 values, respectively. Despite the channel structures, well developed biofilms with an average thickness > 350 µm became completely anoxic at the base, at flow velocities below 6 cm s^{-1}, but at higher flow velocities, increased shear stress and pressure gradients, gradually ensured a better ventilation of the biofilms. Oxygen images at higher flow velocities (e.g. Fig. 4) typically depicted areas with large densities of biomass and high O_2 consumptions in relative O_2-rich surroundings. The base of the mature biofilms never reached full saturation, even at the base of the channels, indicating either a poor mixing between water in the channels and the overlying water or that the bottom of the

channels was covered by a thin O_2-consuming community (base film). The development of the O_2-rich channels with increasing flow was incremental and typically a row of microoxic islands developed in otherwise anoxic surroundings and then fused into an O_2-rich channel. The fact that the O_2 channels were very flow sensitive and that reduced islands within channels exhibited step saturation gradients upstream and lower O_2 gradients downstream, indicates that the channels contained flowing liquid (7). Advective flow has been shown to occur in biofilms by a number of studies (e.g. 6, 16). Increasing the flow above our maximum velocity would probably have further increased the O_2 saturation at the base (Fig. 5). However, at a certain point, resuspension and thereby disruption of the biofilm would have occurred.

The ventilation of different channels was not always linearly related to free flow velocity. It was often observed that as free flow velocity was incrementally increased the O_2 saturation in some channels was unaffected during some increments, while it increased significantly in others. These observations probably reflected the complex structure of a mature biofilm where channels made up a complicated network with many intersection points. As the free flow velocity has increased, interaction between changes in pressure gradients and shear stress in the different channels led to a complex enhancement of the biofilm ventilation. It was never observed that the O_2 saturation decreased at any positions with increasing flow velocities, which would have indicated a physical change in the biofilm structure. In younger and less developed biofilm, the same observations were made. Here, however, the O_2 saturation at the base of clusters and channels was higher. At the highest flow velocities the O_2 saturation at the base of the these channels was close to 100%, especially when the channels were broad as in Fig 2E.

Visual inspections showed that hairy structures on the surface of the biofilm moved or vibrated in the flow. The O_2 saturation at the base did not mimic these movements. The response time of the planar optodes was < 1s, indicating that these movements either did not cause fluctuations in the O_2 distribution at the base or that the fluctuation had a frequency faster than 1 Hz. However, even if movement of the hairy structures did not cause O_2 fluctuations at the base, it probably affected the steady state O_2 distribution within the biofilm.

Oxygen dynamic during development of a biofilm. The biofilms investigated here consisted of a very diverse population of bacteria and became established at a flow rate of approximately 20 cm s^{-1} on the surface of a planar optode coated with black silicone. The structure of biofilms varies but, in general, mature biofilms consist of cell clusters embedded in exopolymers that are separated by open voids (3, 20). After reaching an average thickness of approximately 400 µm, the biofilm went into a stationary phase and the O_2 distribution at the base then remained stable for a period.

Unfortunately the frequent calibration that was required by our set-up excluded the possibility of following the same section of the biofilm for a longer time. Construction of more stable planar optodes by integrating the experiences from microoptodes will probably overcome this problem (13). Additionally, developments of fluorescence lifetime based techniques for planar optodes would improve the long-term stability and a simplify the calibration procedures (17).

Carbon limitation of a subpopulation of bacteria in the mature biofilms was illustrated by the immediate increase in O_2 consumption after addition of 2 mM glucose. The result was an extensive anoxia at the base of the biofilm even at maximum flow rate (Fig. 8). The anoxia rapidly expanded from the cell clusters, illustrating that O_2 was extracted from the water percolating the biofilm. The O_2

saturation in the overlying water was unchanged during this experiment, indicating that mixing between the overlying water and the water in the voids was too inefficient to supply electron acceptors for the stimulated respiration. After 160 min, dilution had decreased the concentration of dissolved glucose to less than 1 μM. The new steady state O_2 saturation was significantly lower as compared to before glucose addition, probably due to retained glucose in the biofilm, allowing a higher specific respiration. This indicate a population of bacteria which presumably was living on non-optimal secondary metabolic compounds or on acetate as carbon source, but which could respire at a much higher rate on glucose. The omission of acetate from the medium had no effect on the O_2 distribution at the base of another mature biofilm investigated within a time horizon of 5 h. This show that the acetate utilizing component of the biofilm contained an internal store of carbon which made respiration at the same rate possible for at least 5 h.

Flow and nutrient conditions typically fluctuate in nature and according to the acquired O_2 images this would have a significant impact on the O_2 conditions within a biofilm. Bacteria situated at a given position within a biofilm must experience a variety of oxic and anoxic conditions within relatively short time intervals. The presented data demonstrate the degree of metabolic flexibility which is required by bacteria living in such a dynamic structure.

Microsensor measurements in biofilms. The data presented in Fig. 7 demonstrate how the presence of a microsensor can change the oxic conditions within a biofilm. It has previously been shown that O_2 microsensors can compress the diffusive boundary layer and increase the O_2 saturations in coastal marine sediments (9). The mechanism behind this is not fully understood, but it is connected to local flow accelerations very close to the sensor tip (Glud et al. unpubl. data). The hydrodynamic changes induced by the presence of a sensor interacts in three dimensions with the complex hydrodynamics at the biofilm water interface. The extent of the effect thus depend on the free flow velocity, the microsensor dimensions, and the 3-dimensional structure of the biofilm. The presented example was typical for the mature biofilms we investigated, but it was often observed that when the microsensor tip was placed in a channel between clusters, the disturbed area was more elongated, which again indicate liquid flow. It is clear that O_2 microsensor measurements in biofilms overestimate the O_2 penetration depth and the oxic conditions within a biofilm. In fact the investigated biofilm appeared totally oxic when measurements were carried out by microelectrodes, while the planar optode showed that the approximately 50% of the biofilm basis was anoxic. Since the effect is probably a function of sensor dimensions, great care has to be taken when microprofiles of different solutes, obtained by differently sized sensors, are aligned and interpreted. Likewise experiments with any intruding object e.g. microinjection needles for flow studies have to take the observed effects into account. Presumably the effects can be minimized by inserting sensors or needles from below so that the stem has no contact with the free flowing water (9). The disturbances introduced by microsensors illustrate the importance of local flow accelerations and microturbulences for solute distributions within biofilms. Extrusions or hairy structures typically observed in biofilms may indeed ensure an efficient nutrient exchange several object diameters further downstream. Extensive microtopography may, in addition to channel structures, optimize the solute exchange between biofilm and overlying water through increased turbulence.

Application of the planar optodes techniques to biofilms has for the first time allowed the true O_2 distribution at the basis of biofilms to be resolved. Previously the oxic conditions at the basis were

extrapolated from 1-dimensional approaches that by their presence changed the microenvironment. The extreme spatial and temporal variation in the aerobic conditions within biofilms has been demonstrated together with the large potential of planar optodes for studies of microenvironments in biofilms.

ACKNOWLEDGMENT

Gerhard Holst is thanked for practical help and constructive discussions during the experiments. RNG and OK were partly financed by the Commission of the European Community under MAST III program 'MICROMARE', project no. 950029 and gratefully acknowledge the support.

REFERENCES

1. **Caldwell, D. E., D. R. Korber, and J. R. Lawrence.** 1992. Confocal laser microscopy and computer image analysis. Adv. Microb. Ecol. **12:**1-67.
2. **Canfield, D.E., and D. J. Des Marais.** 1993. Biogeochemical cycles of carbon, sulphur and free oxygen in a microbial mat. Geochim. Cosmochim. **57:**3971-3984.
3. **Costerton, J.W., Z. Lewandowski, D. de Beer, D. Caldwell, D. Korber, and G. James.** 1994. Biofilms, the customized microniche. J. Bact. **176:**2137-2142.
4. **Dalsgaard, T., and N. P. Revsbech.** 1992. Regulating factors of denitrification in trickling filter biofilms as measured with oxygen/nitrous oxide microsensor. FEMS Microb. Ecol. **101:**151-164.
5. **De Beer, D., P. Stoodly, F. Roe, and Z. Lewandowski.** 1994. Effects of biofilm structure on oxygen distribution and mass transport. Biotechnol. Bioeng. **43:**1131-1138.
6. **De Beer, D., P. Stoodly, and Z. Lewandowski.** 1994. Liquid flow in heterogenous biofilms. Biotech. Bioeng. **44:**636-641.
7. **De Beer, D., P. Stoodly, and Z. Lewandowski.** 1996. Liquid flow and mass transport in heterogenous biofilms. Water Res. **30:**2761-2765.
8. **Ford, T., and R. Mitchell.** 1991. The ecology of microbial corrosion. Adv. Microb. Ecol. **11:**231-262.
9. **Glud, R. N., J. K. Gundersen, B. B. Jørgensen, and N. P. Revsbech.** 1994. Effects on the benthic diffusive boundary layer imposed by microelectrodes. Limnol. Oceanogr. **39:**462-467.
10. **Glud, R. N., N. B. Ramsing, J. K. Gundersen, and I. Klimant.** 1996. Planar optodes: A new tool for fine scale measurements of two-dimensional O_2 distribution in benthic communities. Mar. Ecol. Prog. Ser. **140:**217-226.
11. **Glud, R. N., N. B. Ramsing, and N. P. Revsbech.** 1992. Photosynthesis and photosynthesis coupled respiration in natural biofilms quantified with oxygen microsensors. J. Phycol. **28:**51-60.
12. **Kautsky, H.** 1939. Quenching of luminescence by oxygen. Trans. Faraday. Soc. **35:**216-219.
13. **Klimant, I., V. Meyer, and M. Kühl.** 1995. Fiber-optic oxygen microsensors, a new tool in aquatic biology. Limnol. Oceanogr. **40:**1159-165.
14. **Klimant, I., and O. S. Wolbeis.** 1995. Oxygen sensitive luminescent materials based on silicone-soluble ruthenium diimine complexes. Anal. Chem. **34:**3160-3166.
15. **Lawrence, J. R., D. R. Korber, B. D. Hoyle, J. W. Costerton, and D. E. Caldwell.** 1991. Optical sectioning of microbial biofilms. J. Bacteriol. **173:**6558-6567.
16. **Lewandowski, Z., D. E. Altobelli, P. D. Majors, and E. Fukushima.** 1992. NMR imaging of hydrodynamics near microbially colonized surfaces. Water Sci. Technol. **26:**577-584.
17. **Lippitsch, M. E., J. Pusterhoffer, M. J. P. Leiner, and O. S. Wolfbeis.** 1988. Fiber-optic oxygen sensor with the fluorescence decay time as the information carrier. Anal. Chim. Acta **205:**16.
18. **Revsbech, N. P.** 1989. An oxygen microelectrode with a guard cathode. Limnol. Oceanogr. **34:**474-478.
19. **Revsbech, N. P., and B. B. Jørgensen.** 1986. Microelectrodes: Their use in microbial ecology. Adv. Microb. Ecol. **9:**293-352.
20. **Stewart, P. S., R. Murga, R. Srinivasan, and D. de Beer.** 1995. Biofilm structural heterogeneity visualized by three microscopic methods. Water Res. **29:**2006-2009.

Chapter 3

Structural and functional dynamics of sulfate reducing populations in bacterial biofilms

Cecilia M. Santegoeds[1], Timothy G. Ferdelman[1],
Gerard Muyzer[2], and Dirk de Beer[1]

[1] Max Planck Institute for Marine Microbiology, D-28359 Bremen, Germany.
[2] Netherlands Institute for Sea Research (NIOZ), 1790 AB Den Burg, The Netherlands.

This chapter has been published in Applied and Environmental Microbiology 64:3731-3739 (1998).

ABSTRACT

We describe the combined application of microsensors and molecular techniques to investigate the development of sulfate reduction and of sulfate reducing bacterial populations in an aerobic bacterial biofilm. Microsensor measurements for oxygen showed that anaerobic zones developed in the biofilm within one week and that oxygen was depleted in the top 200 to 400 μm during all stages of biofilm development. Sulfate reduction was first detected after 6 weeks of growth, although favorable conditions for growth of sulfate reducing bacteria (SRB) were present from the first week. *In situ* hybridization with a 16S rRNA probe for SRB revealed that sulfate reducers were present in high numbers (approximately 10^8 SRB/ml) in all stages of development, both in the oxic and anoxic zones of the biofilm. Denaturing gradient gel electrophoresis (DGGE) showed that the genetic diversity of the microbial community increased during the development of the biofilm. Hybridization analysis of the DGGE profiles with taxon-specific oligonucleotide probes showed that *Desulfobulbus* and *Desulfovibrio* were the main sulfate reducing bacteria in all biofilm samples, as well as in the bulk activated sludge. However, different *Desulfobulbus* and *Desulfovibrio* species were found in the 6th and 8th week of incubation, respectively, coinciding with the development of sulfate reduction. Our data indicate that not all SRB detected by the molecular analysis were sulfidogenically active in the biofilm.

INTRODUCTION

Although sulfate reduction is thought to be an anaerobic process, sulfate reducing bacteria are also important in aerobic environments, if they can proliferate in anaerobic zones. For example, in marine sediments (16, 17) and in aerobic wastewater treatment systems (18, 20) sulfate reduction accounts for up to 50% of the mineralization of organic matter. Furthermore, sulfate reduction strongly stimulates microbially enhanced corrosion of metals (5, 7). Therefore, the detection of sulfate reducers and sulfate reducing activity in sediments, wastewater treatment plants, and fouling biofilms is of great practical and scientific relevance. Conventional microbial techniques based on selective culturing are of limited usefulness for quantification and characterization of environmental populations, as it is now well recognized that most strains do not grow in vitro, either because cultivation media poorly resemble natural growth conditions or because different strains of microorganisms are interdependent (2, 49). Techniques based on the analysis of bacterial DNA and RNA, may complement the conventional microbiological approach, and nowadays are routinely used to determine the presence and distribution of individual bacterial species, including SRB, in complex communities such as those in bacterial biofilms (1, 33-35).

So far, these studies of microbial communities, i.e., bacterial biofilms have mainly focused on the exploration of bacterial diversity and on the detection of individual bacterial taxa by molecular techniques. Studies relating community structure to community function are scarce, partially because of difficulties in monitoring microbial activities. Within biofilms, the convection of compounds is hindered, and consequently mass transfer to the cells often limits conversion rates. Because of this resistance to mass transfer, biofilms develop various microenvironments, which differ from the bulk

liquid (6, 10, 18). This complicates the interpretation of community function analysis, because extrapolation of the community behavior to that of the individual cells is impossible without knowledge of their microenvironment.

The most direct way to study the different microzonations in biofilms is with microsensors – needle-shaped devices with a tip measuring from <1 to 100 μm, which are sensitive for a specific compound. Due to their small size, microsensor measurements cause minimal disturbance to the system. With microsensors, microenvironments can be examined, and microgradients can be measured. The measured gradients are a function of both the local transport and conversion rates. Thus, if the transport process (usually diffusion) is known, the spatial distribution of microbial activity can be derived from the substrate profiles (38). An important advantage of using microsensors is the capability to unravel closed cycles, such as sulfate reduction coupled to sulfide oxidation, within a biofilm or sediment (18). With these systems, measurements of net substrate consumption or product excretion lead to considerable underestimation of the actual processes within the biofilms. Internal metabolic cycles can be hidden, although they play a crucial role in the biofilm, and will be reflected in the structure of the microbial community.

Ramsing et al. (33) were the first to use both microsensors and molecular techniques to study sulfate reduction in a trickling-filter biofilm, which was used for treating municipal wastewater. Recently, Schramm et al. (42) employed combined microsensor and molecular techniques to study nitrification in a trickling-filter biofilm. In both studies a good correlation was found between microbial conversions (sulfate reduction and nitrification) and microbial population distributions within the biofilms.

The studies described above were performed on well-established and mature biofilms. In this work, we studied the transients of sulfate reduction, using microsensors, and followed the successional changes in microbial species, using molecular techniques, with a developing, multispecies bacterial biofilm. This topic is relevant as biofilms are often subjected to changing conditions and sloughing is followed by recolonization. The aim of our study was to assess how closely the species composition reflects activity in a biofilm with gradually changing microenvironments.

A biofilm developing in an aerobic wastewater treatment plant was used as a model system for biofilms growing in aerobic sulfate containing waters with high organic loads. Microsensors with high spatial resolution were used to measure oxygen and hydrogen sulfide profiles and to infer aerobic respiration and sulfate reducing activities. Molecular techniques for studying SRB were as follows: denaturing gradient gel electrophoresis (DGGE) analysis of PCR-amplified 16S ribosomal DNA (rDNA) fragments to determine the complexity of the microbial community in the biofilm and to monitor its behavior over time; hybridization analysis of these DGGE profiles with group-specific oligonucleotide probes to identify SRB; and *in situ* hybridization with thin sections to quantify the SRB and to determine their spatial distribution within the biofilm.

MATERIALS AND METHODS

Biofilm growth and sampling. An oxygen impermeable plastic foil (Ril-O-Ten 80/100X ; Otto Nielsen Emballage AS, Lyngby, Denmark) was submerged as a substratum for biofilm growth in the activated-sludge basin (first aerated stage) of the Seehausen municipal wastewater treatment plant in Bremen, Germany, during spring 1996. The temperature in the basin during the experiment varied between 17°C and 20°C. In the bulk liquid, the concentration of O_2 and SO_4^{2-} were 1.8 to 2.4 mg/l (55 to 75 µM) and 75 to 115 mg/l (800 to 1,200 µM), respectively. NO_3^- was absent. The biological oxygen demand was approximately 350 mg/l (10 mM). Samples of the foil (ca. 6 by 12 cm each) on which the bacterial biofilm was growing, were taken weekly over a total period of 12 weeks. While submerged in wastewater, samples were transferred to the laboratory and used within 1 h for microelectrode measurements. Replicate samples were frozen at -20°C for molecular analysis.

Biofilm fixation and slicing. Biofilm samples for *in situ* hybridization analysis were fixed by incubation in paraformaldehyde (4% [wt/vol] in phosphate-buffered saline) at 4°C for 1 h and washed subsequently in phosphate-buffered saline. After fixation, samples were embedded in embedding medium (OCT compound; Sakura Finetek USA, Torrance, Calif.) and frozen above evaporating liquid nitrogen. Thin sectioning of the biofilm was performed with a cryomicrotome (Microm model HM 505 E) at -18°C. Vertical slices of about 10 µm thick were collected on gelatin-coated microscopic slides. The slides were air dried and dehydrated in a series of increasing concentrations of ethanol (50, 80 and 96% [vol/vol]).

Biofilm thickness measurement. Biofilm thickness was determined by positioning a thin glass needle mounted on a micromanipulator on the surface of the biofilm. The needle was moved down until it touched the substratum, which was detected by bending the needle, viewed through a dissection microscope. Biofilm thickness was inferred from micro-manipulator readings.

Microsensor measurements. Microsensor measurements were performed at room temperature (20 to 23°C) in a flow cell with aeration and circulation of artificial wastewater containing the following ingredients: 50 mM KH_2PO_4, 400 µM K_2HPO_4, 760 µM $(NH_4)_2SO_4$, 41 µM $MgSO_4 \cdot 7H_2O$ and 200 µM Na-acetate at pH 7.5 (the last ingredient was added as an additional carbon-source to the bound carbon inside the biofilm to ensure that oxygen remained the limiting substrate). The oxygen concentration in the flow cell was kept the same as in the activated sludge basin, i.e., approximately 70 µM O_2, by bubbling with air and nitrogen. The oxygen concentration in the flow cell was continuously monitored with an oxygen microsensor. Microsensors, mounted on micro-manipulators, were positioned on the surface of the biofilm, which was viewed through a dissection microscope. Profiles were recorded by penetrating the biofilm with the microsensor in increments of 50 or 100 µm and using a micromanipulator.

Microsensors were used to measure oxygen (37), hydrogen sulfide (19), and pH (38). The oxygen and pH electrodes were calibrated as described before (37, 38). The H_2S microsensor was calibrated by measuring the signal in dilution series of a standard solution (sulfide dissolved in artificial wastewater with constant pH, flushed with nitrogen to avoid oxidation of the sulfide) (18).

The concentration of total dissolved sulfide (H_2S plus HS^- plus S^{2-}) in the dilution series was determined by a spectrophotometric method (8). The total dissolved sulfide measured in the biofilm was calculated by using the slope and intercept of the calibration curves. The sulfide electrode had a linear response to H_2S concentrations of up to 1,000 μM. The detection limit of the microsensors varied between 1 and 3 μM total sulfide. No pH correction was necessary, since the sensor was calibrated at the same pH as the sample medium and the buffer prevented the development of pH gradients inside the biofilm. The diffusive fluxes were calculated by using Fick's first law, $J = -D * \delta c/\delta x$, where J = flux (in micromoles per square meter per second), D = diffusion coefficient (in square meters per second), and $\delta c/\delta x$ = concentration gradient (in micromoles per cubic meter). Diffusion coefficients inside the biofilm were assumed to equal the molecular diffusion coefficients (7). Values of 2.12×10^{-5} cm^2/s for oxygen (3) and 1.39×10^{-5} cm^2/s for total sulfide (18) at 20°C were used.

Total iron determination. Ten mililiters of 0.5 M HCl and 0.5 g dithionite were added to the biofilm sample to extract Fe oxides, FeS and $FeCO_3$ (46). The total iron concentration in this extract was determined spectrophotometrically at 562 nm after reaction of the extract with Ferrozine solution (1% [wt/vol] hydroxylammoniumchloride and 10% [wt/vol] Ferrozine in 50 mM N-2-hydroxyethylpiperazine-N-2-ethanesulfonic acid buffer, pH 7.0) (46). The detection limit was 1 μM total iron.

Nitrate determination. The nitrate concentration in the bulk liquid of the activated-sludge basin was measured spectroscopically with Spectroquant model 14773 (E. Merck, Darmstadt, Germany). The detection limit was 16 μM (1 mg/liter) NO_3^-.

Net sulfate reduction measurement with radiotracers. The net sulfate reduction (sulfate reduction minus sulfide oxidation) was determined by measuring the accumulation of reduced sulfur compounds in the 7-week-old biofilm. Carrier free $^{35}SO_4^{2-}$ (2.5 MBq; Amersham) was added to the medium in the microsensor set-up after a blank sample of the biofilm was taken for a reference. During the 30-h incubation period, samples were taken from the biofilm (3 to 4 cm^2 each) and from the medium (4 ml each) at intervals of at least 2.5 h to determine total radioactivity and sulfate concentration. The entire sample (foil plus adhering biofilm) was preserved in a 20% (wt/vol) Zn-acetate solution. The fraction of reduced $^{35}SO_4^{2-}$ per square centimeter of plastic foil (i.e., radioactive H_2S, FeS, S^0, and FeS_2) was determined with the foil and biofilm by the hot acidic Cr(II) procedure as described by Fossing et Jørgensen. (13). The net sulfate reduction was expressed as an areal rate, i.e., moles of reduced ^{35}S per square meter per second for comparison with the microsensor flux measurements.

Nucleic acid extraction and PCR amplification. DNA was extracted from the biofilm samples by a combined freeze-thaw (freezing three times in liquid nitrogen and thawing at 37°C) and hot phenol-chloroform-isoamyl alcohol treatment (45). The ribosomal DNA was enzymatically amplified as described by Muyzer et al. (29), with either the universal primer 907R and the bacterial primer GM5F with a GC-clamp, or the universal primer 907R and the SRB385 primer (1) with a GC-

clamp, targeting SRB of the delta subdivision as well as some other bacteria (Table 1.). A hot-start, touch-down PCR program was used for all amplifications to minimize nonspecific amplification (29). The PCR reaction mixture (100 µl) contained 50 pmol of each primer, 25 nmol of each of the four deoxynucleoside triphosphates, 300 µg bovine serum albumin, 10 µl 10× PCR buffer (HT Biotechnology Ltd) and 10 to 20 ng of template DNA.

TABLE 1. Oligonucleotides used in this study.

Oligo-nucleotide	Sequence	Position[a]	Formamide (%)[b]	NaCl (mM)[c]	Specificity
GM5F[d]	5'- CCTACGGGAGGCAGCAG - 3'	341-357	-	-	Bacteria (30)
907R	5' - CCGTCAATTCCTTTGAGTTT - 3'	907-928	-	-	All organisms (universal probe) (30)
SRB385[d]	5' - CGGCGTCGCTGCGTCAGG - 3'	385-402	35	80	SRB of the delta proteobacteria (1) plus several gram-positive bacteria (e.g. *Clostridium*) (32)
NON338	5' - ACTCCTACGGGAGGCAGC - 3'	338-355	0	900	None (negative control probe) (22)
Probe 660	5' - GAATTCCACTTTCCCCTCTG - 3'	660-679	-	-	*Desulfobulbus* (11)
Probe 687	5' - TACGGATTTCACTCCT - 3'	687-702	-	-	*Desulfovibrio* (11) plus some members of the genera *Geobacter*, *Desulfomonas*, *Desulfomicrobium*, *Bilophila* and *Pelobacter*
Probe 804	5'- CAACGTTTACTGCGTGGA - 3'	804-821	-	-	*Desulfobacterium*, *Desulfobacter*, *Desulfococcus*, *Desulfosarcina*, *Desulfobotulus* (11)
NSO1225	5' - CGCGATTGTATTACGTGTGA - 3'	1225-1244	35	80	Ammonium-oxidizing beta proteobacteria (28)
NIT3[e]	5' - CCTGTGCTCCATGCTCCG - 3'	1035-1048	40	56	*Nitrobacter* spp. (50)
NSR1156	5' - CCCGTTCTCCTGGGCAGT - 3'	1156-1173	30	112	Freshwater *Nitrospira* spp. (41)

[a] Position in the 16S rRNA of *Escherichia coli* (4)
[b] Formimide concentration in the hybridization buffer.
[c] Sodium chloride concentration in the washing buffer.
[d] When used for DGGE, this primer has the following GC-clamp at its 5' end: 5'- CGCCCGCCGCGCCCCGCGCCCGTCCCGCCGCCCCCGCCCG-3'.
[e] Used with unlabeled competitor oligonucleotide cNIT3 (5' - CCTGTGCTCCAGGCTCCG - 3') (50).

DGGE analysis of 16S rDNA fragments. DGGE was performed with the D-Gene system (BioRad) and the following ingredients and conditions: 1x TAE (40 mM Tris, 20 mM acetic acid and 1 mM EDTA at pH 8.3), 1-mm-thick gels, and a denaturant gradient from 35% to 65% urea-formamide, at 60°C, with 100 V constantly for 17 h version (29, 30). DGGE gels were photographed on a UV transillumination table (302 nm) with a Polaroid camera. Photos were scanned with the software program Fotolook 2.05 (Agfa), and inverse images were prepared with Photoshop 4.0 (Adobe).

Blotting and hybridization analysis of DGGE gels. DGGE gels were blotted on nylon membranes (Hybond+; Amersham) as described by Muyzer et al. (29). Hybridization analysis was performed with probes specific for different groups of sulfate reducers (Table 1). Probe 660 is specific for *Desulfobulbus* species; probe 687 targets *Desulfovibrio* species as well as some members of the genera *Geobacter*, *Desulfomonas*, *Desulfuromonas*, *Desulfomicrobium*, *Bilophila* and *Pelobacter*; and probe 804 targets *Desulfobacter*, *Desulfobacterium*, *Desulfosarcina*, *Desulfococcus* and *Desulfobotulus* species (11). The probes were end-labeled with radioactive [γ-^{32}P]ATP (New

England Biolabs). The hybridization buffer used was described by Martinez-Picado et Blanch (25) and contained the following: 10x Denhardt solution, 4x SSC (1x SSC is 0.15 M NaCl and 0.015 M sodium citrate at pH 7.0), 0.1% (wt/vol) sodium dodecyl sulfate, 2 mM EDTA and 50 μg salmon sperm DNA per ml. Membrane blots were prehybridized for 3 to 4 hours at 40°C before the radioactively labeled probe was added. Hybridization was performed for about 17 hrs at 40°C. Thereafter, the membranes were washed twice at 40°C for 30 min with 2x SSC-0.1% (wt/vol) sodium dodecyl sulfate. To eliminate non-specific binding, the membranes were washed two more times for 15 min at the appropriate dissociation temperature (56°C for probe 660, 48°C for probe 687, and 52°C for probe 804), determined by the method as described by Raskin et al. (36). The hybridized membranes were dried and exposed for 1 to 2 days to a PhosphoImager screen. These screens were further analyzed with the PhosphoImager and the program ImageQuant (Molecular Dynamics, Inc.).

In situ hybridization. The protocol described by Manz (22) was used for fluorescence *in situ* hybridization (FISH) of the biofilm slices with probe NON338, as a negative control, and probe SRB385 for the detection of sulfate reducers (Table 1). Probes NSO1225, NIT3 and NSR1156 were used to estimate the amount of nitrifying bacteria in the biofilm. The probes were synthesized and labeled with the fluorochrome CY3 (Interactiva GmbH, Ulm, Germany). The hybridization buffer contained 0.9 M NaCl, the percentage (vol/vol) of formamide shown in Table 1, 20 mM Tris-HCl (pH 7.4), and 0.01% (wt/vol) sodium dodecyl sulfate. The probe concentration was 5 ng/μl. Hybridization was performed for 1 to 2 hours at 46°C. The biofilm was washed at 48°C for 15 min in a washing buffer containing 20 mM Tris-HCl (pH 7.4), 5 mM EDTA, the NaCl concentration indicated in Table 1, and 0.01% (wt/vol) sodium dodecyl sulfate. The specimens were examined with an Axioplan epifluorescence microscope (Carl Zeiss, Oberkochen, Germany). CY3-stained cells were counted in 20 to 22 areas of 125 x 625 μm^2, both at the bottom and at the top of the biofilm. The density of cells in the biofilm was too high to allow enumeration of the total number stained with 4',6 diamidino-2-phenylindole (DAPI). Therefore, the number of stained bacteria was expressed per unit of volume of biofilm.

RESULTS

Biofilm growth and development process. Within 1 week, a patchy biofilm ca. 400 μm thick developed on the plastic foil in the activated-sludge basin (Fig. 1). The thickness of the biofilm increased until the eighth week, after which it remained more or less constant at 1,000 to 1,200 μm.

Oxygen and sulfide profiles measured at different stages of biofilm development are shown in Fig. 2. The graphs show mean values of four to six profiles measured at different positions in the biofilm. pH values measured in the biofilm were within 0.05 U of the pH in the bulk liquid (data not shown), because of the buffering capacity of the medium used for measuring the profiles. Within 1 week the biofilm developed anaerobic zones, which grew thicker during the following weeks. Oxygen was depleted within the top 200 to 400 μm in all stages of biofilm development (except in some profiles of the 1-week-old biofilm). Although the anaerobic environment in the biofilm would

have allowed for sulfate reduction, as there was enough substrate and sulfate available, no sulfide production was measured until the sixth week.

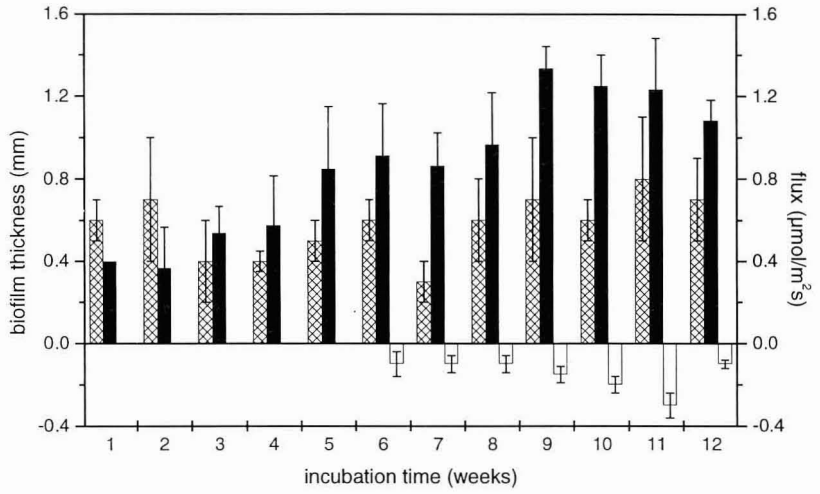

FIG. 1. Development of biofilm thickness (black bars), and fluxes of oxygen into the biofilm (hatched bars) and sulfide into the oxic zone (white bars) calculated from the microprofiles.

In the sixth week, a total sulfide concentration of 40 µM was detected, which increased to approximately 100 µM in the 10- and 12-week-old biofilm (Fig. 2). No sulfide diffused out of the biofilm, and oxygen and sulfide profiles overlapped, indicating that all sulfide produced by sulfate reduction was oxidized in the aerobic part of the biofilm.

Iron, which could have bound the sulfide, was not detected, either in biofilm samples (measured at weeks 5 and 11), nor in the activated sludge (data not shown).

Sulfate reduction rates measured by a radiotracer method using $^{35}SO_4^{2-}$ showed much lower values (approximately 0.017 µmol/m^2.s^1) than the rates calculated with microsensor data (Fig. 1). Also, the radioactive tracer technique showed that no reduced S compounds accumulated inside the biofilm or bulk water.

Community development. To determine how the structure of the community developed with time and to identify the presence of SRB, DGGE of PCR-amplified DNA fragments and hybridization analysis of these DGGE profiles with group-specific probes were performed. Fig. 3 shows the DGGE pattern of 16S rRNA gene fragments obtained after PCR amplification with a primer pair which amplifies members of the domain *Bacteria*. Figure 4 shows a graph of the total number of bands, as well as new bands appearing relative to the activated sludge and the total number of bands remaining from the activated sludge. Nearly all bands obtained from the activated sludge remained in the biofilm samples. However, new bands also appeared during the maturation of the biofilm.

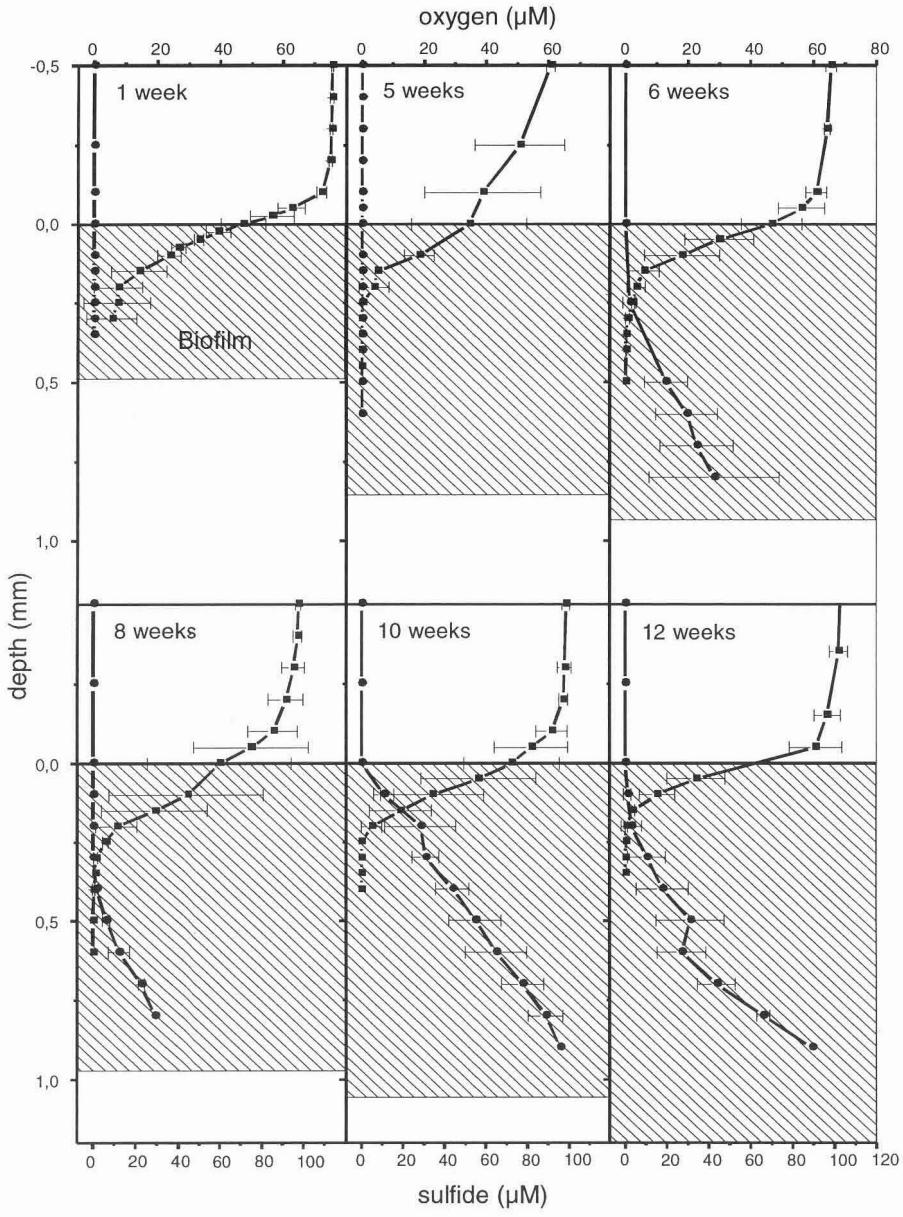

FIG. 2. Oxygen (■) and total sulfide (●) microprofiles in a 1-, 5-, 6-, 8-, 10- and 12-week-old biofilms. Biofilm thickness is indicated by the shaded areas. The biofilm surface is at a depth of 0 mm, the water phase is indicated by negative values, and the biofilm by positive values.

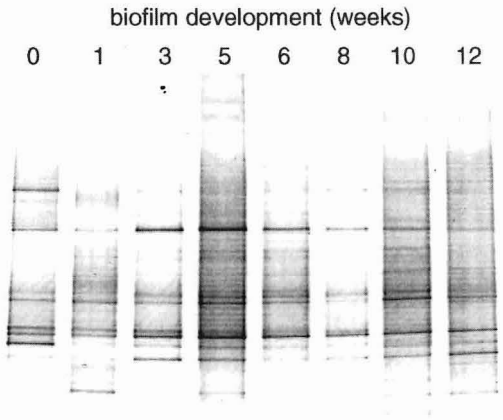

FIG. 3. DGGE analysis of 16S rDNA fragments obtained after PCR-amplification with primer pair GM5F-907R and genomic DNA from bacterial biofilm samples taken at different time points. From left to right: sample taken directly from the activated sludge (t = 0 weeks); samples taken from the 1-, 3-, 5-, 6-, 8-, 10- and 12-week-old biofilm (as indicated above the lanes).

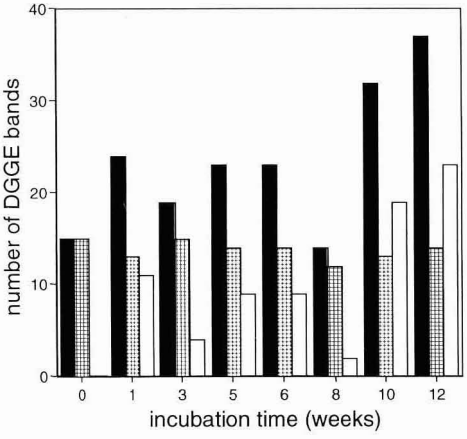

FIG. 4. Graphical representation of the number of bands in the denaturing gradient gel shown in Fig. 3. Total number of DGGE bands, the black bars, total bands remaining from week 0 (activated sludge), hatched bars; new bands after week 0, white bars.

Detection of SRB in DGGE profiles. DGGE gels with DNA fragments amplified with primers for members of the domain *Bacteria* were blotted and hybridized with probes specific for different groups of SRB (probes 660, 687 and 804). No hybridization was observed, probably due to the small ratio of each SRB strain to the total number of bacteria in the biofilm.

To increase the sensitivity of SRB detection in our samples, we used the SRB385 sequence with a GC-clamp as a forward primer, which targets sulfate reducers, as well as some other delta proteobacteria and gram-positive bacteria, and the 907R sequence as the reverse primer. In this way,

we excluded the amplification of 16S rDNA fragments of most of the *Bacteria*, and enriched PCR products from SRB. These DGGE profiles were subsequently blotted and hybridized with radioactively-labeled oligonucleotide probes specific for different groups of SRB.

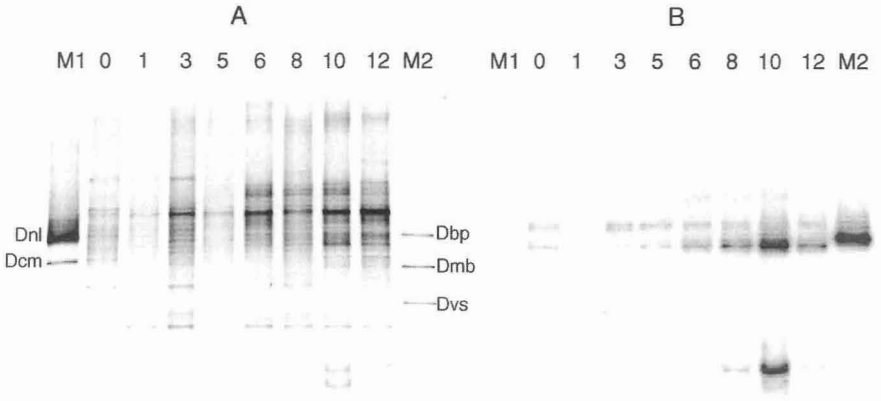

FIG. 5. (A) DGGE analysis of PCR-amplified 16S rDNA fragments obtained with primers 385F and 907R and bacterial genomic DNA from biofilm samples taken at different time points. From left to right, marker 1 (M1), *Desulfonema limicola* (Dnl) and *Desulfococcus multivorans* (Dcm); sample taken from the activated sludge (t = 0 weeks); samples from the 1-, 3-, 5-, 6-, 8-, 10- and 12-week-old biofilm (as indicated above the lanes); marker 2 (M2), *Desulfobulbus propionicus* (Dbp, positive control for probe 660), *Desulfomicrobium baculatum* and *Desulfovibrio salexigenes* (Dmb and Dvs, both positive control for probe 687). (B) Hybridization results of the same DGGE pattern hybridized with probe 660, which is specific for *Desulfobulbus* species. The 'smiling' bands in the lower parts of the gels are single stranded DNA, and should be disregarded.

In these SRB-enriched DGGE gels clear hybridization was obtained with probe 660 and 687 (Fig. 5B and 6B), but not with 804 (data not shown). This indicates the presence of *Desulfobulbus* (probe 660) and possibly *Desulfovibrio* (probe 687, which also targets members of the genera *Geobacter*, *Desulfomonas*, *Desulfuromonas*, *Desulfomicrobium*, *Bilophila* and *Pelobacter*) and the absence of all species targeted by probe 804 (*Desulfobacter*, *Desulfobacterium*, *Desulfosarcina*, *Desulfococcus* and *Desulfobotulus)* in all stages of biofilm development and in the activated sludge. Furthermore, hybridization analysis of the DGGE profiles with probe 660 showed the initial presence of two *Desulfobulbus* strains, and the appearance of another strain after week 6 (compare lanes 2 to 5, Fig. 5B, with lanes 6 to 9), coinciding with the first detection of sulfide production by microsensors. The result for probe 687 was simular; initially two *Desulfovibrio* strains were present, and a third appeared during week 8 (compare lanes 2 to 6, Fig. 6B, with lanes 7 to 9).

The DGGE patterns obtained with primers targeting sulfate reducers (Fig. 5 and 6) show less variation with time than those obtained with bacterial primers (Fig. 3). This trend can be seen more clearly in Fig. 7, which contains a graph of the number of total, new, and remaining DGGE bands. The number of bands representing SRB varies only between 14 and 21, whereas Fig. 4 shows a variation of 14 to 37 bands from all bacteria during biofilm development.

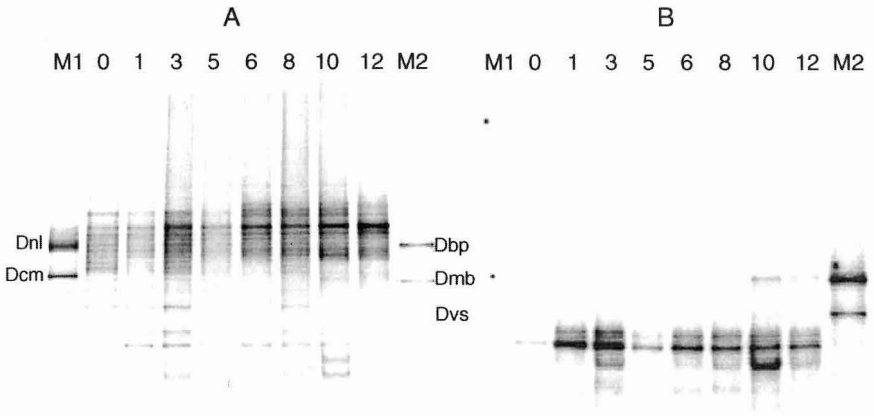

FIG. 6. (A) DGGE analysis of PCR amplified 16S rDNA fragments obtained with primers set 385F and 907R. From left to right: marker 1 (M1), *Desulfonema limicola* (Dnl) and *Desulfococcus multivorans* (Dcm); sample taken from the activated sludge (t = 0 weeks); samples from the 1-, 3-, 5-, 6-, 8-, 10- and 12-week-old biofilm (as indicated above the lanes); marker 2 (M2), *Desulfobulbus propionicus* (Dbp, positive control for probe 660), *Desulfomicrobium baculatum* and *Desulfovibrio salexigenes* (Dmb and Dvs, both positive control for probe 687). (B) Hybridization results of the same DGGE pattern hybridized with probe 687, which is specific for *Desulfovibrio* species. The bands in the lower parts of the gels are single stranded DNA, and should be disregarded.

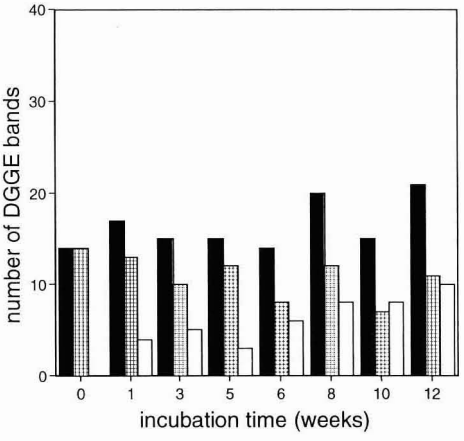

FIG. 7. Graphical representation of the number of bands in the denaturing gel shown in Fig. 5A and 6A. Total number of DGGE bands, black bars; total bands remaining from week 0 (activated sludge), hatched bars; new bands, white bars.

In situ hybridization of sulfate reducing and nitrifying bacteria. *In situ* hybridization with the SRB385 probe of thin sections of biofilms taken at weeks 2 and 11 stained *Vibrio*-shaped bacteria and short fat rods. Both morphotypes, resembling *Desulfovibrio* and *Desulfobulbus* cells, were present over the whole thickness of the biofilm. In the 2-week-old biofilm, the number of SRB was (64 ± 23 [mean ± standard deviation]) x 10^6 SRB/ml at the surface and (114 ± 33) x 10^6 SRB/ml at the

bottom of the biofilm. In the 11-week-old biofilm, the SRB varied from (201 ± 78) x 10^6 SRB/ml to (358 ± 127) x 10^6 SRB/ml on the surface and at the bottom of the biofilm, respectively.

In situ hybridization with probes specific for nitrifying bacteria revealed the presence of ammonia-oxidizing bacteria (30 x 10^6 to 90 x 10^6 cells per ml) and nitrite-oxidizing bacteria, *Nitrobacter* species (0.6 x 10^6 to 1 x 10^6 cells per ml) and *Nitrospira* species (50 x 10^6 to 100 x 10^6 cells per ml), respectively in the 2- and 6-week-old biofilm.

DISCUSSION

Process and biofilm development. The thickness and community characteristics of the biofilm developed gradually during 12 weeks without large scale-sloughing. The biofilm had a heterogeneous structure during the whole experimental period, as was reported in other studies (10, 26), explaining the variations in the amounts of oxygen and sulfide (Fig. 1). Heterogeneity may increase the surface area exchange, therefore allowing more efficient transport of substrates and products. In determining the fluxes, we assumed that diffusion was the only transport mechanism; thus, the fluxes might be underestimated. However, the fluxes measured in this study are close to those calculated by Kühl et Jørgensen (18) for a trickling-filter biofilm.

The microprofiles (Fig. 2) showed that no sulfide diffused out of the biofilm. Since iron was absent, iron sulfide precipitation can be excluded. The low value for the sulfate reduction rate, determined with radiotracers, as compared to the rates calculated from microsensor data, can be explained only by the cycling between reduced and oxidized ^{35}S compounds. Most of the $^{35}S^{2-}$ formed is rapidly oxidized to $^{35}SO_4^{2-}$ or other oxidized ^{35}S compounds, which are not detectable by our radiotracer method (H_2S, S^0, FeS_2, FeS). Examination of the specific activity of the reduced sulfur pool during the course of the experiment showed that the pool rapidly became equilibrated (within 3 h) with the initially labeled sulfate. This indicates, that a small reduced sulfur pool (sulfide) with a high turnover rate is present in the biofilm.

We concluded that all sulfide, produced by sulfate reduction in the anoxic zone, was oxidized in the oxic layer in the biofilm. Thus, at the point of the steepest gradient, the sulfide flux in the zone adjacent to the aerobic zone, can be used as a conservative measure of the SRB activity. Diffusive fluxes of oxygen into the biofilm and sulfide from the anaerobic zone into the aerobic zone, calculated from the microprofiles, are given in Fig. 1. Sulfide fluxes ranged from 15% in week 6 to 35% in week 11 of the oxygen fluxes (Fig. 1). Since oxidation of 1 mol of sulfide to sulfate requires 2 mol of oxygen, a large part (up to 70%) of the oxygen diffusing into the biofilm was used for the reoxidation of sulfide. Thus, sulfate reduction may be as important as aerobic mineralization in the biofilm. Since the biomass yield by sulfate reduction is much lower than by aerobic mineralization (21), rates of biomass production in wastewater treatment plants based on biofilms may be affected significantly. The turnover of the sulfide pool in the biofilm, calculated by dividing the pool size with the fluxes (both determined from microsensor profiles), lasted only minutes. Consequently sulfate reduction rates in biofilms can be reliably measured *in situ* only by microsensors.

The development of anaerobic zones in the biofilm created an optimal environment for sulfate reducers. However, sulfide production could not be measured during the first 6 weeks of biofilm development. In theory, sulfide could have been oxidized anaerobically, e.g., by Fe^{3+} or NO_3^- as an electron acceptor. However, neither Fe^{3+} nor NO_3^- was present in the bulk liquid of the activated-sludge basin. *In situ* hybridization showed the presence of ammonia and nitrite oxidizers in the 2- and 6-week-old biofilm; consequently, some nitrate could have been formed by nitrification inside the biofilm. However, even if sulfide reduction was coupled to anaerobic sulfide oxidation in the initial stages of biofilm development, some sulfide should have been detected by the sensitive sulfide microsensor. We, therefore, conclude that no sulfate reduction occurred in the biofilm during the first 6 weeks. Similar lag phases in developing biofilms have been detected for sulfate reducing (48) and other slow-growing bacteria, such as nitrifiers (47) and methanogens (14). Slow adaptation of the sulfate reducing population to the biofilm microenvironment might explain the lag phase in sulfate reduction that was found in our study.

Community development. Comparative DGGE analysis of PCR products obtained with primers for the 16S rDNA of all bacteria showed that the species composition of the biofilm changed within 1 week from that of the activated sludge (Fig. 3). The original strains remained, but new bands appeared each week (Fig. 4), leading to a more complex bacterial community. Exceptions were week 8, and to a lesser degree week 3, where fewer bands were detected. These exceptions might have been caused by a lower amount of DNA loaded on the gel. Our results show that biofilms can harbor a much wider range of microbial species than the bulk liquid. The increase in bacterial diversity, shown by the increasing number of DGGE bands, was the result of development of different microhabitats inside the biofilm. Due to resistance to mass transfer and conversions, microzonations develop within the biofilm, providing a broader range of niches for bacteria with different physiological characteristics.

DGGE analysis of PCR products obtained with primers specific for sulfate reducers, i.e., primer pair SRB385F/907R, showed that the community of delta proteobacteria, including the sulfate reducers, was more stable during biofilm development than the total community (compare Fig. 4 and 7). *Desulfobulbus* and *Desulfovibrio* species were present from the beginning. Additional populations of *Desulfobulbus* and of *Desulfovibrio* appeared, respectively, after 6 and 8 weeks of incubation. We speculate that the additional strains from week 6 and week 8 are responsible for the sulfide production in the biofilm.

The question of the metabolic activity of the species identified as SRB, present in the first 5 weeks, is unresolved. Our FISH data indicate that a significant portion of the SRB are present and proliferate in the oxic part of the biofilm. The ability of *Desulfobulbus* and *Desulfovibrio* species to respire oxygen (12, 24) could explain their presence in activated sludge and the initial biofilm. As the activated-sludge basin is aerated, other nonrespiring sulfate reducers may be unable to survive in this aerobic environment. Also, the finding of Teske et al. (45), that *Desulfobulbus* and *Desulfovibrio* are the main SRB species in the aerobic layers of a stratified fjord, underlines their ability to survive (and maybe thrive) in the presence of oxygen. Alternatively, SRB could use a different metabolic pathway. Some *Desulfobulbus* and *Desulfovibrio* species can utilize nitrate instead of sulfate as a terminal electron acceptor (27, 43, 52). There is conflicting evidence whether or not nitrate is used in the presence of sulfate. It has been reported that nitrate can suppress sulfate reduction (43) and,

conversely, that sulfate inhibits the use of nitrate as terminal electron acceptor (9). However, no nitrate was found in the bulk liquid of the activated-sludge basin. Another metabolic rol of SRB could be the fermentation of organics, such as fumarate or malate (51).

With *in situ* hybridization we found 10^7 to 10^8 SRB/ml of biofilm volume. Considering the total cell density of 10^{10} to 10^{11} cells per ml of biofilm reported by others (7, 31), we estimate that the relative percentage of bacteria that are SRB is less than 1%. This, however, contradicts our finding that a large part of the oxygen diffusing into the biofilm is used for oxidation of the formed sulfide and that sulfate reduction, therefore, plays an important role in the biofilm. An explanation for this discrepancy is that either the SRB are extremely active or our FISH technique underestimates the number of SRB. From the H_2S fluxes and the number of SRB (determined by FISH), the specific sulfate reduction rate (moles of SO_4^{2-} $cell^{-1}$ day^{-1}) was calculated to be 70 x 10^{-15} mol SO_4^{2-} $cell^{-1}$ day^{-1} (at week 11). This value is in the upper range of the specific sulfate reduction rates reported by Jørgensen (15).

By using the molecular techniques described in this paper we were able to follow community development, and to detect different groups of SRB in complex biofilms, with many species. This would be difficult with conventional cultivation techniques. However, molecular techniques also have biases and limitations. First, PCR amplification is not quantitative, as preferential amplification can occur (39, 44). Therefore, band intensities cannot be extrapolated to indicate the abundance of a particular bacterial population. Second, the number of DGGE bands is dependent on the amount of DNA that is applied to the gel as well as on the number of different DNA fragments. Third, some of the oligonucleotides, i.e., SRB385 and probe 687, which were used in this study, are not as specific as originally described. However, we only used the primer SRB385 in our PCR reactions to exclude most non-SRB and to enrich the SRB populations. Probe SRB385 was also used for *in situ* hybridization analysis. For this application, the specificity of the probe is increased as the gram-positive cells, targeted by SRB385, are not accessible for the oligonucleotide when paraformaldehyde is used as fixative (40). These biases demonstrate the importance of combining different molecular methods and to compare them with activity measurements.

Relating community analysis obtained by molecular techniques to processes occurring within microbial consortia is of great practical relevance. However, the molecular techniques currently available, and used in this study, seem insufficient to accurately predict the behavior of a gradually changing but complex microbial community. More specific techniques, perhaps involving the detection or expression of specific genes, are needed so that molecular techniques caan be used as reliable diagnostic tools. Further analysis of the biofilm samples, nitrate microsensor measurements, and *in situ* hybridization with more specific probes (23), might give a more detailed picture of the abundance, distribution and functioning of the sulfate reducing bacterial groups.

ACKNOWLEDGMENTS

This work was financially supported by the Körber Foundation (Hamburg, Germany) and the Max Planck Society (München, Germany). We thank Dror Minz and Kerstin Sahm for their help with the hybridization analysis and T_d determination; Ronnie Glud for his help with the radiotracer experiment; Susanne Klöser for the total iron detection; and Gaby Eickert, Anja Eggers and Vera Hübner for technical assistance with the microsensors.

REFERENCES

1. **Amann, R., J. Stromley, R. Devereux, R. Key, and D. A. Stahl.** 1992. Molecular and microscopic identification of sulfate-reducing bacteria in multispecies biofilms. Appl. Environ. Microbiol. **58:**614-623.
2. **Brock, T. D.** 1987. The study of microorganisms in situ: progress and problems. Symp. Soc. Gen. Microbiol. **41:**1-17.
3. **Broecker, W. S., and T.-H. Peng.** 1974. Gas exchange rates between air and sea. Tellus. **26:**21-35.
4. **Brosius, J., T. J. Dull, D. D. Sleeter, and H. F. Noller.** 1981. Gene organization and primary structure of a ribosomal RNA operon from *Escherichia coli*. J. Mol. Biol. **148:**107-127.
5. **Bryant, R. D., W. Jansen, J. Boivin, E. J. Laishley, and J. W. Costerton.** 1991. Effect of hydrogenase and mixed sulfate-reducing bacterial populations on the corrosion of steel. Appl. Environ. Microbiol. **57:**2804-2809.
6. **Bungay, H. R., W. J. Whalen, and W. M. Sanders.** 1969. Microprobe techniques for determining diffusivities and respiration rates in microbial slimes. Biotechnol. Bioeng. **11:**765-772.
7. **Characklis, W. G., and K. C. Marshall** (eds.). 1989. Biofilms. 1st ed. John Wiley & Sons, Inc., New York.
8. **Cline, J. D.** 1969. Spectrophotometric determination of hydrogen sulfide in natural waters. Limnol. Oceanogr. **14:**454-458.
9. **Dalsgaard, T., and F. Bak.** 1994. Nitrate reduction in a sulfate-reducing bacterium, *Desulfovibrio desulfuricans*, isolated from rice paddy soil: sulfide inhibition, kinetics, and regulation. Appl. Environ. Microbiol. **60:**291-297.
10. **De Beer, D., P. Stoodley, F. Roe, and Z. Lewandowski.** 1994. Effect of biofilm structures on oxygen distribution and mass transfer. Biotechnol. Bioeng. **43:**1131-1138.
11. **Devereux, R., M. D. Kane, J. Wilfrey, and D. A. Stahl.** 1992. Genus- and group-specific hybridization probes for determinative and environmental studies of sulfate-reducing bacteria. System. Appl. Microbiol. **15:**601-609.
12. **Dilling, W., and H. Cypionka.** 1990. Aerobic respiration in sulfate reducing bacteria. FEMS Microbiol. Lett. **71:**123-128.
13. **Fossing, H., and B. B. Jørgensen.** 1989. Measurement of bacterial sulfate reduction in sediments evaluation of single-step chromium reduction method. Biogeochem. **8:**205-222.
14. **Gorris, L. G. M., J. M. A. van Deursen, C. van der Drift, and G. D. Vogels.** 1988. Influence of waste water composition on biofilm development in laboratory methanogenic fluidized bed reactors. Appl. Microbiol. Biotechnol. **29:**95-102.
15. **Jørgensen, B. B.** 1978. A comparison of methods for the quantification of bacterial sulfate reduction in coastal marine sediments. Geomicrobiol. **1:**49-64.
16. **Jørgensen, B. B.** 1982. Mineralization of organic matter in the sea bed - the role of sulphate reduction. Nature (London). **296:**643-645.
17. **Jørgensen, B. B., and F. Bak.** 1991. Pathways and microbiology of thiosulfate transformations and sulfate reduction in a marine sediment (Kattegat, Denmark). Appl. Environ. Microbiol. **57:**847-856.

18. **Kühl, M., and B. B. Jørgensen.** 1992. Microsensor measurements of sulfate reduction and sulfide oxidation in compact microbial communities of aerobic biofilms. Appl. Environ. Microbiol. **58:**1164-1174.
19. **Kühl, M., C. Steuckart, G. Eickert, and P. Jeroschewski.** 1998. A H_2S microsensor for profiling biofilms and sediments: Application in an acidic lake sediment. Aquat. Microb. Ecol. **15:**201-209.
20. **Lens, P. N., M.-P. de Poorter, C. C. Cronenberg, and W. H. Verstraete.** 1995. Sulfate reducing and methane producing bacteria in aerobic wastewater treatment systems. Water Res. **29:**871-880.
21. **Lens, P. N., A. Massone, A. Rozzi, and W. H. Verstraete.** 1995. Effect of sulfate concentration and scraping on aerobic fixed biofilm reactors. Water Res. **29:**857-870.
22. **Manz, W., R. Amann, W. Ludwig, M. Wagner, and K.-H. Schleifer.** 1992. Phylogenetic oligodeoxynucleotide probes for the major subclasses of proteobacteria: problems and solutions. Syst. Appl. Microbiol. **15:**593-600.
23. **Manz, W., M. Eisenbrecher, T. R. Neu, and U. Szewzyk.** 1998. Abundance and spatial organization of Gram-negative sulfate-reducing bacteria in activated sludge investigated by in situ probing with specific 16S rRNA targeted oligonucleotides. FEMS Microbiol. Ecol. **25:**43-61.
24. **Marschall, C., P. Frenzel, and H. Cypionka.** 1993. Influence of oxygen on sulfate reduction and growth of sulfate-reducing bacteria. Arch. Microbiol. **159:**168-173.
25. **Martinez-Picado, J., and A. R. Blanch.** 1994. Rapid detection and identification of *Vibrio anguillarum* by using a specific oligonucleotide probe complementary to 16S rRNA. Appl. Environ. Microbiol. **60:**732-737.
26. **Massol-Deyá, A., J. Whallon, R. F. Hickey, and J. M. Tiedje.** 1995. Channel structures in aerobic biofilms of fixed-film reactors treating contaminated groundwater. Appl. Environ. Microbiol. **61:**769-777.
27. **McCready, R. G. L., W. D. Gould, and F. D. Cook.** 1983. Respiratory nitrate reduction by *Desulfovibrio* sp. Arch. Microbiol. **135:**182-185.
28. **Mobarry, B. K., M. Wagner, V. Urbain, B. E. Rittmann, and D. A. Stahl.** 1996. Phylogenetic probes for analyzing abundance and spatial organization of nitrifying bacteria. Appl. Environ. Microbiol. **62:**2156-2162.
29. **Muyzer, G., T. Brinkhoff, U. Nübel, C. Santegoeds, H. Schäfer, and C. Wawer.** 1997. Denaturing gradient gel electrophoresis (DGGE) in microbial ecology, p. 1-27. *In* A. D. L. Akkermans, J. D. van Elsas, and F. J. de Bruijn (eds.), Molecular Microbial Ecology Manual, vol. 3.4.4. Kluwer, Dordrecht, The Netherlands.
30. **Muyzer, G., E. C. de Waal, and A. G. Uitterlinden.** 1993. Profiling of complex microbial populations by denaturing gradient gel electrophoresis analysis of polymerase chain reaction-amplified genes encoding for 16S rRNA. Appl. Environ. Microbiol. **59:**695-700.
31. **Okabe, S., T. Yasuda, and Y. Watanabe.** 1997. Uptake and release of inert fluorescence particles by mixed population biofilms. Biotechnol. Bioeng. **53:**459-469.
32. **Ramsing, N. B., H. Fossing, T. G. Ferdelman, F. Andersen, and B. Thamdrup.** 1996. Distribution of bacterial populations in a stratified fjord (Mariager Fjord, Danmark) quantified by in situ hybridization and related to chemical gradients in the water column. Appl. Environ. Microbiol. **62:**1391-1404.
33. **Ramsing, N. B., M. Kühl, and B. B. Jørgensen.** 1993. Distribution of sulfate-reducing bacteria, O_2, and H_2S in photosynthetic biofilms determined by oligonucleotide probes and microelectrodes. Appl. Environ. Microbiol. **59:**3840-3849.
34. **Raskin, L., R. Amann, L. K. Poulsen, B. E. Rittmann, and D. A. Stahl.** 1995. Use of ribosomal RNA-based molecular probes for characterization of complex microbial communities in anaerobic biofilms. Water Sci. Technol. **31:**261-272.
35. **Raskin, L., B. E. Rittmann, and D. A. Stahl.** 1996. Competition and coexistance of sulfate-reducing and methanogenic populations in anaerobic biofilms. Appl. Environ. Microbiol. **62:**3847-3857.
36. **Raskin, L., J. M. Stromley, B. E. Rittmann, and D. A. Stahl.** 1994. Group-specific 16S rRNA hybridization probes to describe natural communities of methanogens. Appl. Environ. Microbiol. **60:**1232-1240.
37. **Revsbech, N. P.** 1989. An oxygen microelectrode with a guard cathode. Limnol. Oceanogr. **55:**1907-1910.
38. **Revsbech, N. P., and B. B. Jørgensen.** 1986. Microelectrodes: their use in microbial ecology. Adv. Microb. Ecol. **9:**293-352.

39. **Reysenbach, A.-L., L. J. Giver, G. S. Wickham, and N. R. Pace.** 1992. Differential amplification of rRNA genes by polymerase chain reaction. Appl. Environ. Microbiol. **58:**3417-3418.

40. **Roller, C., M. Wagner, R. Amann, W. Ludwig, and K.-H. Schleifer.** 1994. *In situ* probing of Gram-positive bacteria with high DNA G+C content using 23S rRNA-targeted oligonucleotides. Microbiol. **140:**2849-2858.

41. **Schramm, A., D. de Beer, M. Wagner, and R. Amann.** 1998. *Nitrosospira* sp. and *Nitrospira* sp. as dominant populations in a nitrifying fluidized bed reactor: Identification and activiy in situ. Appl. Environ. Microbiol. **in press**.

42. **Schramm, A., L. H. Larsen, N. P. Revsbech, N. B. Ramsing, R. Amann, and K.-H. Schleifer.** 1996. Structure and function of a nitrifying biofilm as determined by in situ hybridization and the use of microelectrodes. Appl. Environ. Microbiol. **62:**4641-4647.

43. **Seitz, H.-J., and H. Cypionka.** 1986. Chemolithotrophic growth of *Desulfovibrio desulfuricans* with hydrogen coupled to ammonification of nitrate or nitrite. Arch. Microbiol. **146:**63-67.

44. **Suzuki, M. T., and S. J. Giovannoni.** 1996. Bias caused by template annealing in the amplification of mixtures of 16S rRNA genes by PCR. Appl. Environ. Microbiol. **62:**625-630.

45. **Teske, A., C. Wawer, G. Muyzer, and N. B. Ramsing.** 1996. Distribution of sulfate-reducing bacteria in a stratified fjord (Mariager Fjord, Denmark) as evaluated by most-probable-number counts and denaturing gradient gel electrophoresis of PCR-amplified ribosomal DNA fragments. Appl. Environ. Microbiol. **62:**1405-1415.

46. **Thamdrup, B., H. Fossing, and B. B. Jørgensen.** 1994. Manganese, iron, and sulfur cycling in a coastal marine sediment, Aarhus Bay, Denmark. Geochim. Cosmochim. Acta. **58:**5115-5129.

47. **Thörn, M., A. Mattsson, and F. Sörensson.** 1996. Biofilm development in a nitrifying trickling filter. Water Sci. Technol. **34:**83-89.

48. **Van Houten, R. T., L. W. Hulshoff Pol, and G. Lettinga.** 1994. Biological sulphate reduction using gas-lift reactors fed with hydrogen and carbon dioxide as energy and carbon source. Biotechnol. Bioeng. **44:**586-594.

49. **Wagner, M., R. Amann, H. Lemmer, and K.-H. Schleifer.** 1993. Probing activated sludge with oligonucleotides specific for proteobacteria: inadequacy of culture-dependent methods for describing microbial community structure. Appl. Environ. Microbiol. **59:**1520-1525.

50. **Wagner, M., G. Rath, H.-P. Koops, J. Flood, and R. Amann.** 1996. *In situ* analysis of nitrifying bacteria in sewage treatment plants. Water Sci. Technol. **34:**237-244.

51. **Widdel, F., and T. A. Hansen.** 1992. The dissimilatory sulfate- and sulfur-reducing bacteria, p. 583-616. *In* A. Balows, H. G. Trüper, M. Dworkin, W. Harder, and K.-H. Schleifer (eds.), The Prokaryotes, 2nd ed, vol. I. Springer-Verlag, New York Inc.

52. **Widdel, F., and N. Pfennig.** 1982. Studies on dissimilatory sulfate-reducing bacteria that decompose fatty acids. II. Incomplete oxidation of propionate by *Desulfobulbus propionicus* gen. nov., sp. nov. Arch. Microbiol. **131:**360-365.

Chapter 4

Diversity and distribution of sulfate reducing bacteria in a developing biofilm

Cecilia M. Santegoeds,[1] Dror Minz,[2] Werner Manz,[3]
Michael Wagner,[4] Dirk de Beer,[1] and Gerard Muyzer[5]

[1]Max Planck Institute for Marine Microbiology, D-28359 Bremen, Germany.
[2]Volcani Research Center, 50-250 Israel.
[3]Technische Universität Berlin, Institut für Technische Umweltschutz, Fachgebiet Ökologie der Mikroorganismen, D-10587 Berlin, Germany.
[4]Technische Universität München, Lehrstuhl für Mikrobiologie, D-80290 Munich, Germany.
[5]Netherlands Institute for Sea Research, NL-1790 AB Den Burg, The Netherlands.

This chapter will be submitted to FEMS Microbial Ecology.

ABSTRACT

It was recently shown (21) that sulfate reducing bacteria (SRB) were present in the oxic as well as anoxic zones of a bacterial biofilm, growing in the aeration basin of a wastewater treatment plant. These SRB were, however, not sulfidogenically active during the first 6 weeks of biofilm development. Different molecular biological methods, such as PCR specific for the functional genes dissimilatory sulfite reductase (DSR) and [NiFe] hydrogenase and fluorescence *in situ* hybridization (FISH) with SRB-group specific 16S rRNA probes, were now combined to reveal the diversity and distribution of SRB within the growing biofilm. Although the number of *in situ* detected Gram negative SRB did not drastically change over time (from 2.7 x 10^8 SRB/ml in the 2 week old biofilm to 3.1 x 10^9 SRB/ml in the 11 week old biofilm), the DSR gene content did increase during biofilm development, coinciding with the increase of sulfide flux within the biofilm. The discrepancy between the results obtained with the two different molecular methods can be explained by the presence and increase of sulfate reducing populations, which were not detectable by the probes used for FISH. Different SRB, belonging to the genera *Desulfovibrio*, *Desulfomicrobium*, *Desulfobacterium*, *Desulfobacter*, and *Desulforhopalus* were detected with FISH in both the oxic and anoxic zones, and during all stages of biofilm development. Denaturing gradient gel electrophoresis (DGGE) of [NiFe] hydrogenase gene fragments, showed only minor changes in the *Desulfovibrio* community during biofilm development. Phylogenetic analysis of biofilm derived DSR sequences and of excised [NiFe] hydrogenase DGGE bands revealed a high genetic diversity among the *Desulfovibrio* species, which corresponds with the various microenvironments present in biofilms.

INTRODUCTION

Sulfate reducing bacteria are widely distributed in natural and engineered systems and for example have been detected in sediments (9), fresh and marine water columns (18, 26), microbial mats (25), and in biofilms and activated sludge of wastewater treatment systems (10, 11, 13, 20), where they play an important role in the mineralization process of organic matter. However, their presence does not necessarily imply sulfate reducing activity, since they could also be using other metabolic pathways, like nitrate reduction (15, 22), iron reduction (4), oxygen respiration (6, 14), fermentation of fatty acids (31), or they might not be metabolically active at all.

Lacking sulfate reducing activity by SRB was recently observed in a developing biofilm by Santegoeds *et al.* (21). It was shown that although anoxic zones were present from the first week on in the biofilm, sulfide could not be detected in the first 6 weeks of biofilm development. Oxygen was depleted in the first 200 - 400 μm of the biofilm during all stages of development and any other suitable electron acceptor such as nitrate or iron was absent. Hybridization analysis of DGGE gels and *in situ* hybridization of sliced biofilm samples, however, demonstrated that significant amounts of sulfate reducing bacteria were actually present from the beginning on, and that additional *Desulfobulbus* and *Desulfovibrio* species appeared after 6 - 8 weeks, but that the observed slight

increase in total number of SRB could not explain the sudden onset of sulfide production after the 6th week of biofilm development. Therefore, further research was needed. In the present study different molecular techniques were applied to investigate the diversity and spatial distribution of SRB in the biofilm system.

Over the last decade a battery of molecular tools were developed for directly studying SRB within complex environments. rRNA-targeted oligonucleotide probes developed by Devereux *et al.* (5) and Manz *et al.* (13) are well suited to study the abundance and spatial distribution of SRB using dot blot or *in situ* hybridization techniques. Recently, Wagner *et al.* (28) described PCR-primers specific for the dissimilatory sulfite reductase genes, which encode a key-enzyme in the sulfate reduction process. These genes could be amplified from all SRB investigated, and phylogenetic analysis based on DSR sequences gave a similar phylogeny as that based on 16S rRNA sequences, which makes these genes excellent molecular markers for detection and identification of SRB in natural samples. Primers for another functional gene, the [NiFe] hydrogenase gene that plays an important role in the hydrogen metabolism of *Desulfovibrio* species, were developed by Wawer *et al.* (30). The [NiFe] hydrogenase gene is present in all *Desulfovibrio* species and is therefore an excellent marker for these species.

The objective of this study was to examine the dynamics and genetic diversity of SRB and in particular of *Desulfovibrio* in the growing biofilm by using the [NiFe] hydrogenase marker in parallel with the DSR gene primers. Fluorescence *in situ* hybridization (FISH) with group specific probes was performed to unravel the spatial distribution of SRB and to quantify their abundance.

MATERIALS AND METHODS

Biofilm growth and sampling. An oxygen impermeable plastic foil (Ril-O-Ten 80/100 X manufactured by Otto Nielsen Emballage AS, Lyngby, Denmark (3)) was submerged as a substratum for biofilm growth in the first aerated stage of an activated sludge basin of the municipal wastewater treatment plant Seehausen in Bremen, Germany. A description of the basin conditions can be found in Santegoeds *et al.* (21). Samples of the foil on which the bacterial biofilm was growing, were taken weekly, over a total period of 12 weeks. The samples were fixed or frozen on site and kept at -20°C until further analysis.

Biofilm fixation and slicing. For *in situ* hybridization analysis biofilm samples were fixed by incubation in paraformaldehyde (4% [w/v] in phosphate-buffered saline [PBS]) at 4°C for 1 h and washed subsequently in PBS. After fixation, the samples were embedded in embedding medium (OCT compound; Sakura Finetek USA, Torrance, California) and frozen above evaporating liquid nitrogen. Thin sectioning of the biofilm was performed with a cryomicrotome (Microm HM 505 E) at -18°C. The vertical slices of about 10 µm thickness were collected on gelatin-coated microscopic slides. The specimens were air dried and dehydrated in a series of increasing concentrations of ethanol (50, 80 and 96% [v/v]).

Nucleic acid extraction and PCR amplification. DNA was extracted from the biofilm samples by freeze-thawing and hot phenol-chloroform-isoamyl alcohol treatment (26). A ca. 1.9 kb fragment of the dissimilatory sulfite reductase genes was amplified using primer pair DSR1F and DSR4R (28) (Table 1). A ca. 440 bp DNA fragment of the [NiFe] hydrogenase gene was amplified with the primer pair Hyd1F with GC-clamp and Hyd5R (30) (Table 1). A hot-start PCR program was used, where 1 unit of SuperTaq DNA polymerase (HT Biotechnology Ltd., Germany) was added at 80°C after 5 min heating at 94°C, and with 35 cycles, each cycle consisting of 1 min at 94°C, 1 min at 60°C for primer pair DSR1F-DSR4R and 65°C for primer pair Hyd1F-Hyd5R, and 3 min at 72°C. The PCR reaction mixture (100 µl) contained 50 pmol of each primer, 25 nmol of all four deoxynucleoside triphosphates, 200 µg of bovine serum albumin, 10 µl 10× PCR buffer (HT Biotechnology Ltd., Germany) and 10-100 ng of template DNA. To compare the different biofilm samples among each other with regard to their DSR content the same concentration of template DNA was used for the DSR gene amplification. The PCR products were evaluated on a 1% (w/v) agarose gel.

Table 1. Oligonucleotide probes used in this study.

Probe	Position[a]	Sequence, 5' → 3'	Target	Formamide (%)[b]	NaCl (mM)[c]
DSR1F	-	AC[C/G]CACTGGAAGCACG	Dissimilatory sulfite reductase gene (28)	-	-
DSR4R	-	GTGTAGCAGTTACCGCA	Dissimilatory sulfite reductase gene (28)	-	-
Hyd1F[d]	-	CGCGACGCCCAGCACTTCACCCAGCGC	[NiFe] hydrogenase gene (30)	-	-
Hyd5R	-	GCAGGGCTTCCAGGTAGTGGGCGGTGGCGATGAGGT	[NiFe] hydrogenase gene (30)	-	-
SRB385	338-355	CGGCGTCGCTGCGTCAGG	SRB of the delta proteobacteria (1) plus several Gram-positive bacteria (e.g. *Clostridium*) (19)	35	80[e]
NON338	338-355	ACTCCTACGGGAGGCAGC	none (negative control) (12)	0	900
DSV698	698-717	GTTCCTCCAGATATCTACGG	*Desulfovibrio* (13)	35	88
DSD131	131-148	CCCGATCGTCTGGGCAGG	*Desulfovibrio* (13)	20	250
DSV407	407-424	CCGAAGGCCTTCTTCCCT	*Desulfovibrio* (13)	50	31.2
DSV1292	1292-1309	CAATCCGGACTGGGACGC	*Desulfovibrio* (13)	35	88
DSV214	214-230	CATCCTCGGACGAATGC	*Desulfomicrobium* (13)	10	500
DSS658	658-678	TCCACTTCCCTCTCCCAT	*Desulfosarcina* (13)	60	15.6
DSB985	985-1004	CACAGGATGTCAAACCCAG	*Desulfobacter* (13)	20	250
DSBO224	224-242	GGGACGCGGACTCATCCTC	*Desulfobotulus* (13)	60	15.6
DSMA488	488-507	GCCGGTGCTTCCTTTGGCGG	*Desulfomonile* (13)	60	15.6
DSR651	651-668	CCCCCTCCAGTACTCAAG	*Desulforhopalus* (13)	35	88
221	221-240	TGCGCGGACTCATCTTCAAA	*Desulfobacterium* (5)	35	88
660	660-679	GAATTCCACTTTCCCCTCTG	*Desulfobulbus* (5)	60	15.6

[a] Position in the 16S rRNA of *Escherichia coli* (2).
[b] Formamide concentration in hybridization buffer.
[c] Sodium chloride concentration in washing buffer.
[d] This primer has the following GC-clamp at the 5' end: 5'- CGCCCGCCGCGCCCCGCGCCCGTCCCGCCGCCCCCGCCCG-3'.
[e] Plus 5 mM EDTA in washing buffer.

DGGE analysis of [NiFe] hydrogenase gene fragments. DGGE was performed using the D-Gene™ system (BioRad) and the following specifications: 1x TAE (40 mM Tris, 20 mM acetic acid and 1 mM EDTA at pH 8.3), 1 mm thick gels, a denaturant gradient from 30% to 70%

urea/formamide, a temperature of 60°C, and a constant voltage of 200V for 3.5 hours (16, 30). DGGE gels were photographed on a UV transillumination table (302 nm) with a Polaroid camera. The photos were scanned and inversed with Photoshop 4.0 (Adobe).

Excision amplification of DGGE bands. DGGE bands were carefully excised on a UV and transilluminator with a scalpel and subsequently transferred to a 1.5 ml tube with 500 µl water and approximately 500 µl glass beads of 0.75-1.0 mm diameter. The acrylamide bands were disrupted by bead beating at maximum speed twice for 1 min. The samples were left overnight at 4°C and thereafter 1-10 µl of the supernatant was used for reamplification of the DNA fragment. A second DGGE was run to confirm that only one band was reamplified, and that it had the same position in the gel as the excised band. Prior to sequencing the PCR products were purified using the QIAquick Spin PCR purification kit (Qiagen GmbH, Hilden, Germany).

Cloning of DSR PCR products. The pGEM®-T Easy Vector System of Promega (Wisconsin, USA) was used for cloning dissimilatory sulfite reductase PCR products. Ligation and transformation reactions were performed according to the pGEM®-T Easy Vector System Technical Manual. Restriction enzyme analysis with enzyme *Eco*RI was used to identify clones harboring 1.9 kb inserts. Observed insert restriction patterns were also used for a rough discrimination between the different clones. One to three representative clones of each different restriction pattern were purified with the Wizard™ *Plus* Minipreps DNA Purification System of Promega (Wisconsin, USA) as described in the manual.

Sequencing. Clones and reamplified DGGE bands were sequenced using the Applied Biosystems PRISM Dye Terminator Cycle Sequencing Ready reaction kit supplied with Ampli*Taq* DNA polymerase. Sequencing was performed with the DSR primers (DSR1F-DSR4R) for the DSR clones and with the [NiFe] hydrogenase gene primers (Hyd1F-Hyd5R) for the reamplified DGGE bands. Both ends of the DSR clones were sequenced yielding ca. 400 basepairs from either direction. The sequencing products were analyzed with the Applied Biosystems 377 DNA sequencer.

Phylogenetic analysis. [NiFe] hydrogenase nucleotide sequences were manually aligned to other sequences obtained from nucleotide databases with the program SeqApp (8). The nucleotide sequences were aligned according to the alignment of the deduced amino acid sequences. A distance matrix from the aligned sequences was obtained by using the "show distance matrix" option in the software program PAUP (test version 4) developed by Swofford (24). In estimates of evolutionary relationships, regions with missing data were omitted from the alignment. Matrices of evolutionary distances were computed by using DNADIST (Kimura option) for nucleotide sequences. An evolutionary tree was constructed from the evolutionary distances with the program FITCH. All programs are implemented in the software package PHYLIP 3.5 (7). The reliability of tree nodes was determined by bootstrap analysis (100 resamplings) with parsimony (PAUP).

Deduced DSR amino acid sequences were aligned using the GDE 2.2 sequence editor (S. Smith, unpublished) implemented in the ARB software environment (23). Distance matrix (with

FITCH, PHYLIP version 3.5 (7), and with Neighbour Joining, ARB (23)), parsimony (PROTPARS, PHYLIP version 3.5), and maximum likelihood analyses (PROTML, PHYLIP version 3.5) were performed on a concatenated α- and β-DSR-subunit amino acid data set. For phylogenetic analysis missing sequence information was coded as missing data, yielding 330 positions for the α- (166 positions) and β-subunit (164 positions) data set. Bootstrap analysis (100 resamplings) was performed for the parsimony method using the respective program in the PHYLIP package.

***In situ* hybridization.** The protocol described by Manz (12) was used for fluorescence *in situ* hybridization (FISH) of the biofilm slices with probe NON338, as a negative control, probe SRB385 for general detection of sulfate reducers, and probes DSV698, DSD131, DSV407, DSV1292, DSV214, DSS658, DSB985, DSBO224, DSMA488, DSR651 (13), 221 and 660 (5) for the detection of different SRB groups (Table 1). The probes were synthesized and labeled with the fluorochrome CY3 by Interactiva GmbH (Ulm, Germany). The hybridization buffer contained 0.9 M NaCl, a percentage (v/v) of formamide (see Table 1), 20 mM Tris-HCl (pH 7.4) and 0.01% (w/v) SDS. The probe concentrations were 50 ng/µl hybridization buffer. Hybridization was performed for 2 hours at 46°C, after which the biofilm slices were washed at 48°C for 15 min in a washing buffer containing 20 mM Tris-HCl (pH 7.4), a concentration of NaCl as given in Table 1 and 0.01% (w/v) SDS. The specimens were microscopically examined with an Axioplan epifluorescence microscope (Carl Zeiss, Oberkochen, Germany). CY3-stained cells were counted in 6-15 areas of 315 x 315 μm^2 at the bottom of the biofilm. The density of cells in the biofilm was too high to count the total cell number using DAPI staining. Therefore, the number of stained bacteria was expressed per volume (ml) of biofilm, instead per percentage of the total cell number.

RESULTS

Diversity of SRB based on DSR gene sequence analysis. Using a specific PCR for the amplification of the dissimilatory sulfite reductase genes with the same amount of DNA for all samples, we found that the gene was present in the activated sludge as well as in all biofilm samples (Fig. 1A). However, the amount of the DSR gene in each sample varied. We obtained lesser PCR product from samples of the first 5 weeks of the biofilm, than from the activated sludge. More DSR-PCR products were obtained from week 6 on with a maximum in week 10. The increase in DSR-PCR products from the 6th week on correlates well with the increase in sulfide flux (Fig. 1B), which was determined previously (21).

DSR PCR products from the activated sludge sample, the samples of 3-, 5- and 10-week old biofilms were cloned Approximately 70 clones were screened for the right insert, and characterized by restriction fragment length polymorphism (RFLP) analysis to reduce redundancy prior to sequence analysis. We found 6 different patterns (type A to F patterns, data not shown). From each pattern 1-3 clones were sequenced and used for phylogenetic analysis. Clones 3 (type A), 4 (type B), 7 (type E), 9 (type F) and 11 (type E) originate from the activated sludge, clone 16 (type A) from the

3 weeks old biofilm, clone 68 (type B) from the 5 weeks old biofilm and clones 40 (type E), 41 (type A), 42 (type B), 43 (type D) and 44 (type C) from the 10 week old biofilm. The phylogenetic affiliation of these 12 DSR clone sequences is shown in Fig. 2. In general, stable tree topologies were observed using the different treeing methods. All treeing methods suggested that the DSR clone sequences 3, 11, 41, 42, and 68 are related to but not identical with *Desulfobulbus propionicus* while the remaining analyzed DSR clone sequences clustered together with members of the genus *Desulfovibrio*. DSR sequences indicative for SRB which do not belong to the delta-subclass of *Proteobacteria* were not retrieved from the activated sludge and biofilm samples.

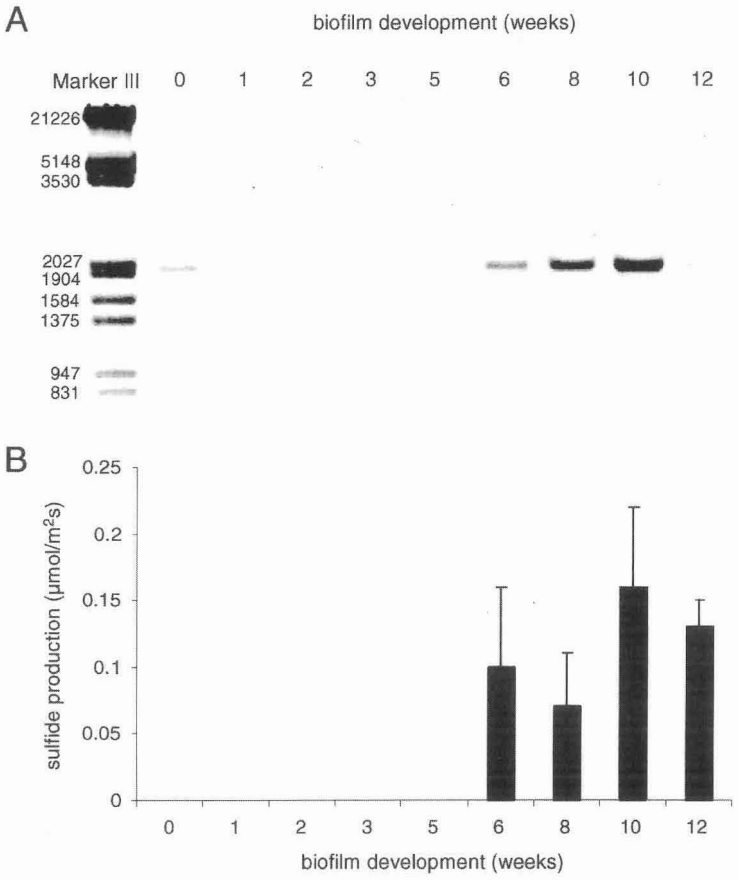

Fig. 1. (A) The 1.9 kb fragment of the dissimilatory sulfite reductase genes, PCR amplified from DNA of activated sludge (t = 0 weeks), and of 1-, 2-, 3- 5-, 6-, 8-, 10- and 12-week old biofilm samples. The same amount of DNA was used for all samples. A molecular weight marker is shown in the left lane. (B) Flux measurements of sulfide being produced within the biofilm and determined by microsensor measurements (21).

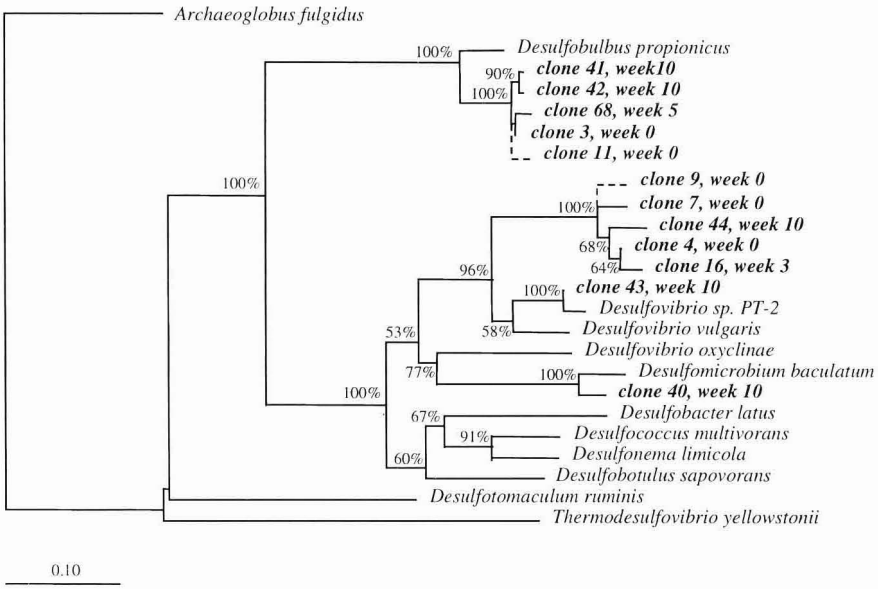

Fig. 2. Phylogenetic tree reflecting the relationships of the analyzed DSR clones (retrieved from the activated sludge and biofilm samples) with the DSR from sulfate reducing prokaryotes (28). Dashed lines are used for clones with partial sequences. The DSR sequences of *Desulfobulbus propionicus* and *Desulfomicrobium baculatum* (27) were added to the dataset to be able to more accurately define delta-subclass SRB in the DSR tree. Tree topology was obtained from FITCH distance matrix analysis of the DSR alpha- and beta-subunit amino acid dataset. Bootstrap values were determined from parsimony analysis on an identical dataset. Branches for which no bootstrap value is indicated were not recovered in the majority of bootstrap replicates by the parsimony method. The scale bar indicates the number of expected amino acid substitutions per site per unit of branch length.

Genetic diversity of *Desulfovibrio* species. [NiFe] hydrogenase gene PCR products were retrieved from the activated sludge sample as well as from most biofilm samples. To determine the genetic diversity and the development of the *Desulfovibrio* community with time a DGGE analysis was performed on the [NiFe] hydrogenase PCR products. From this DGGE gel (Fig. 3) it can be seen that the activated sludge contained at least 10 different *Desulfovibrio*-like hydrogenase genes. Most of these gene fragments remained in the biofilm and some new bands appeared during the biofilm development. There is, however, no drastic change in the DGGE pattern after the 6th week, i.e. after sulfide production started. However, the DGGE patterns indicate a community change after the 10th week. This community change did not coincide with a change in sulfate reducing activity.

We were able to excise and successfully amplify 6 DGGE bands, which are marked and numbered in Fig. 3. The phylogenetic affiliation of these sequences is depicted in Fig. 4. From this tree it can be seen that the *Desulfovibrio* species present in the biofilm are highly diverse, and are not identical to any known sequence.

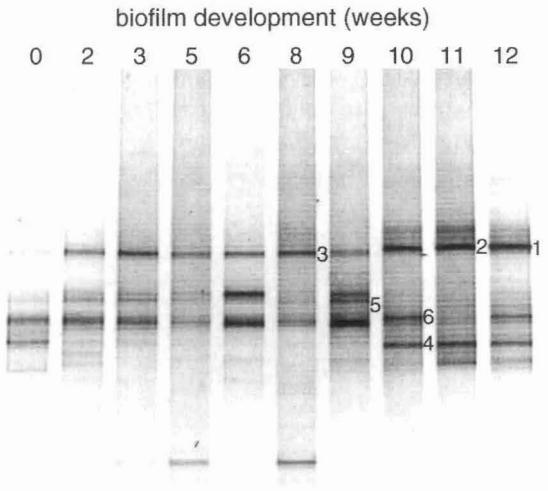

Fig. 3. DGGE analysis of PCR-amplified [NiFe] hydrogenase gene fragments obtained with primers Hyd1F + GC clamp and Hyd5R and genomic DNA from biofilm samples taken at different time points. From left to right, sample taken from the activated sludge (t = 0 weeks), and samples from the 2-, 3-, 5-, 6-, 8-, 9-, 10-, 11- and 12-week old biofilm (as indicated above the lanes). Excised bands are numbered on the right side.

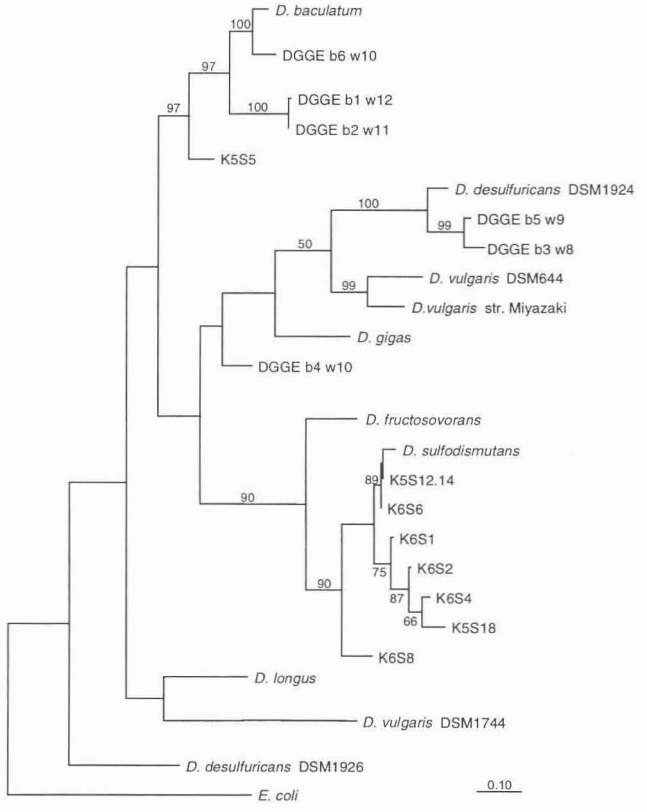

Fig. 4. Phylogenetic tree of [NiFe] hydrogenase sequences obtained from excised bands of the DGGE gel shown in Fig. 3. The first number refers to the number of the excised DGGE band and the second number indicates the age of the biofilm sample in weeks. The tree was calculated using the distance matrix method from the nucleotide sequences. Bootstrap values, indicated on the nodes of the tree, were determined from parsimony analysis (PAUP). The scale bar represents 10% estimated change per nucleotide.

Abundance and distribution of sulfate reducing bacteria. Among all probes used for FISH to detect different groups of sulfate reducing bacteria within the activated sludge and biofilms only the probes DSV698, DSV214, DSB985, DSR651 and 221 gave a hybridization signal. Most of these SRB were present at higher numbers at the substratum than at the biofilm surface (Fig. 5A). Only *Desulfovibrio* species detected with probe DSV698 were spread more evenly over the biofilm (Fig. 5B).

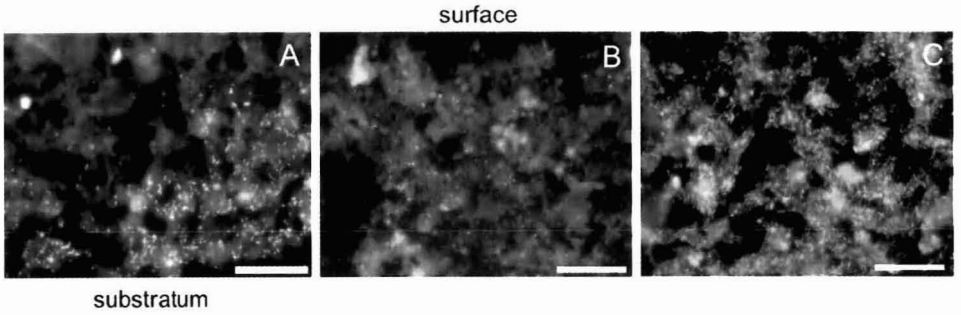

Fig. 5. Microscopic photographs of vertical cross sections of biofilm samples after *in situ* hybridization with CY3-labeled probes. For size comparison a 50 μm bar is shown in the right corner. (A) The bottom part of a 9 week old biofilm hybridized with probe DSV214. The substratum can be seen at the bottom of the photograph. (B) The top part of a 10 week old biofilm hybridized with probe DSV698. The biofilm surface can be seen at the top of the photograph. (C) The middle part of a 11 week old biofilm hybridized with probe SRB385. Neither the biofilm surface nor the substratum can be seen on this photograph.

The total number of detected SRB (determined by counts of all group specific probes) increased during biofilm development from week 2 to week 6 (from 2.7 x 10^8 SRB/ml to 2.5 x 10^9 SRB/ml) and remained thereafter between 2.4 x 10^9 SRB/ml and 3.4 x 10^9 SRB/ml (Fig. 6). It was found that the number of *Desulfovibrio* and *Desulfomicrobium* species detected with probes DSV698 and DSV214 remained more or less constant during biofilm development (Fig. 6). Whereas the SRB targeted with the *Desulforhopalus* probe DSR651 developed steadily, and the number of *Desulfobacter* and *Desulfobacterium* species (probe DSB985 and 221, respectively) showed a more pronounced increase during biofilm growth (Fig. 6).

DISCUSSION

Diversity of SRB based on DSR gene sequence analysis. As the dissimilatory sulfite reductase is a key-enzyme in dissimilatory sulfate reduction, it can be concluded from Fig. 1A that the activated sludge, as well as all biofilm samples contained DNA from sulfate reducing bacteria. The same DNA concentration was used for all samples, as well as the same PCR conditions,

therefore the samples underwent the same treatment and thus most PCR biases might be assumed to be the same for all samples. Although we can not exclude that (i) DNA extraction efficiency is different for different SRB and (ii) that different DSR genes from different SRB do not amplify equally well, we believe that we can compare the PCR products among each other in a semi-quantitative way and infer from the data the dynamics of the DSR gene content during biofilm development. Figure 1A shows that the DSR gene was more abundant in the activated sludge than in the first five weeks of biofilm development, indicating that the number of SRB in the sludge was higher than in the biofilm. After week 6, however, the DSR gene band became more distinct and the amount of DSR gene increased until the 10th week of incubation, after which the concentration decreased again. To check whether the maximum at week 10 was caused by DNA inhibition of PCR amplification in samples from other dates, we repeated the PCR amplification diluting the DNA for each sample from week 8 till week 12. This resulted in the same maximum as before (data not shown). We therefore have to conclude that the relative number of SRB (detectable by using the DSR primers) increased until the 10th week of incubation and that it thereafter decreased again. However, we can not say anything about the actual numbers of the SRB present in the biofilm. The relative numbers might have decreased through dilution with other non-SRB, but also a community shift might result in a lower DSR amplification through the presence of bacteria whose DSR gene is not readily amplified.

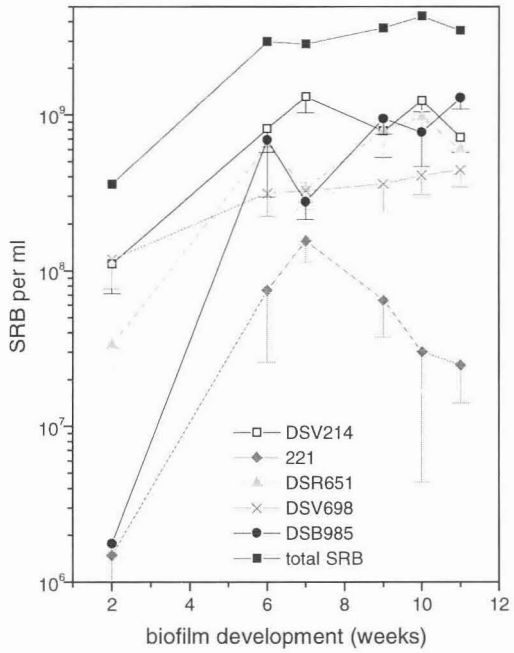

Fig. 6. The number of SRB that are counted in the 2, 6, 7, 9, 10 and 11 week old biofilm by FISH using probes DSV698 (cross), DSV214 (open square), DSB985 (circle), 221 (diamond) and DSR651 (triangle). The total number of detected SRB (the sum of all probes) is indicated by the solid squares. FISH analysis with probes DSD131, DSV407, DSV1292, DSS658, DSBO224, DSMA488 and 660 did not result in any hybridization signal in the biofilm samples.

The phylogenetic analysis of the DSR gene clones revealed the presence of *Desulfovibrio* and *Desulfobulbus* relatives in the activated sludge and in different biofilm samples. This confirms former DGGE hybridization data from blotted DGGE gels (21), showing predominance of *Desulfovibrio* and *Desulfobulbus* species during all stages of biofilm development. The number of sequenced clones is too low to draw solid conclusions about a community shift. As preferential amplification might have occurred, these sequences may not represent the predominant ones. But taking previous DGGE hybridization results (21) into account together with the *in situ* hybridization data (which will be discussed later), it seems that *Desulfovibrio* strains are the numerically dominant representatives of the sulfate reducing populations in the biofilm.

Genetic diversity of *Desulfovibrio* species. The DGGE gel of the PCR amplified [NiFe] hydrogenase gene fragments (Fig. 3) depicts a complex pattern with only slight changes in the *Desulfovibrio* community during the first 9 weeks of biofilm development. At week 10, coinciding with the maximum of sulfide production and of DSR gene abundance, a community shift occurred.

Comparing the detected [NiFe] hydrogenase diversity with other studies (29, 30), we find that the genetic diversity of *Desulfovibrio*-like species in the biofilm is greater than that in anaerobic bioreactors. This high genetic diversity in biofilms can be explained by the various chemical microzonations in the biofilm, due to mass transfer resistance and conversions, which result in a broad range of niches for bacteria with different physiological characteristics.

If we compare the [NiFe] hydrogenase DGGE with earlier hybridization results (21) of a DGGE using general and SRB specific 16S rDNA primers (primers 907 (17) and SRB385 (1)) and the probe 687 for hybridizing *Desulfovibrio* species (5), we find a much lower number of hybridized bands belonging to *Desulfovibrio* (4 bands maximum, data not shown here) than bands of the [NiFe] hydrogenase gene fragments (10 to 13 bands during all stages of biofilm development, Fig. 3), suggesting the presence of less *Desulfovibrio* species. However, this discrepancy is caused by the more specific PCR reaction for the [NiFe] hydrogenase gene fragments, amplifying only the gene from *Desulfovibrio* species, whereas the PCR with primers 907-SRB385 amplifies a fragment of the 16S rRNA gene from all Gram negative sulfate reducing bacteria and even some Gram positive bacteria targeted by the SRB385 primer. Therefore the fraction of some individual *Desulfovibrio* species in the total pool of 16S rDNA fragments might be too low to be detected on a DGGE gel. Another explanation might be, that there is more than one [NiFe] hydrogenase gene present in the *Desulfovibrio* species from the biofilm, or that [NiFe] hydrogenase genes exist also in other species.

The phylogeny of the amplified [NiFe] hydrogenase gene fragments (Fig. 4) reveals a high diversity among the *Desulfovibrio* species. The sequenced DGGE bands do not cluster together, but are wide spread over the tree, which is in contrast to sequences retrieved from anaerobic bioreactors (the K5S and K6S sequences in the tree (29)), which form close clusters. This heterogeneity of [NiFe] hydrogenase sequences from the biofilm samples might be related to existence of a high number of different microenvironments in the biofilms.

Abundance and distribution of sulfate reducing bacteria. FISH analysis with group specific probes showed a 10-fold increase of the total detectable Gram negative SRB population in the

biofilm from week 2 to week 6, when sulfide production started. As the *Desulfovibrio* - *Desulfomicrobium* numbers remained more or less constant during this time, we might assume that these species had to adapt to their new environment before they could reduce sulfate, or that the *Desulfobacter*, *Desulfobacterium*, and to a lesser extent, *Desulforhopalus* species are responsible for the sulfide production after week 5. The change in SRB numbers was, however, not as major as was expected from the increase of DSR gene amplification products and sulfide production. It could well be that this increase and also the start of sulfide production at week 6 was caused by the increase of yet another SRB population, not detected with the SRB probes used for FISH or for hybridization of DGGE patterns. Potential candidates for such a SRB population could be SRB of the delta-subclass which are not targeted by the probes used for FISH or members belonging to the Gram positive sulfate reducing bacterial genus *Desulfotomaculum*, which are known to be present in anaerobic wastewater treatment systems. The presence of Gram positive SRB, however, appears to be unlikely, since all DSR clones analyzed were related to the genera *Desulfovibrio* and *Desulfobulbus*.

Hybridization of DGGE patterns (21) and comparative DSR sequence analysis revealed the presence of *Desulfovibrio* as well as *Desulfobulbus* species, but no *Desulfobacter* or *Desulfobacterium* species. In contrast, FISH analysis identified *Desulfovibrio* species as well as *Desulfobacter*, *Desulfobacterium*, and *Desulforhopalus*, but no *Desulfobulbus* species. This discrepancy in results of the three molecular methods can be caused by for instance preferential amplification, resulting in only minor fractions of 16S rDNA PCR products from *Desulfobacter* and *Desulfobacterium* (many of these species have mismatches with the primer SRB385) and thus no hybridization signal from these species on the DGGE blots. Similar biases may occur during amplification of the DSR genes. Relatives of *Desulfobulbus* on the other hand might not have been detected *in situ* because their number could have been below the detection limit of FISH, although still detectable by PCR. Another explanation would be, that yet, not recognized members of the genus *Desulfobulbus*, are present in the biofilm, which do possess mismatches with probe 660, but can be amplified with the DSR primers. It could, however, also be that the *Desulforhopalus* relatives shown by FISH (which is a close relative of *Desulfobulbus*) hybridized under less stringent conditions on the DGGE blots with the 660 probe.

The total numbers of SRB, calculated from the group specific probes, are one order of magnitude larger than the total SRB numbers counted with probe SRB385 (data shown earlier (21)). This difference might be explained by the presence of very thin and small SRB cells that hybridized especially with probes DSV214 and DSV698. These cells might have been overlooked when the total SRB community was hybridized with probe SRB385 (see Fig. 5). Another explanation could be that several SRB (belonging among others to the genera *Desulfobacter* and *Desulfomicrobium*) are missed in the SRB385 hybridization analysis because of their known mismatch with the probe.

In conclusion, the *in situ* hybridization data revealed a minor change in abundance of SRB over the examined time period. Although the observed increase of SRB is only slight, it might explain the lag in sulfate reducing activity during the first 6 weeks of biofilm development. The presence of sulfidogenically inactive SRB during the first 6 weeks of biofilm development can be due to attachment of inactive SRB originated from the activated sludge, which might have to adapt first to

their new environment before becoming active. Another explanation for the lag in sulfate reduction can be an increase of an important undetected sulfate reducing population during biofilm development.

The results of this study illustrate that SRB community structure and dynamics in complex environments can most accurately be examined by combined application of different molecular techniques. Resolution and reliability of cultivation independent SRB analysis could be significantly increased by targeting the 16S rRNA, the DSR genes, and the [NiFe] hydrogenase gene in parallel.

ACKNOWLEDGMENTS

We like to thank Heike Abicht for sequencing and phylogenetic analysis of the dissimilatory sulfite reductase gene of *Desulfobulbus propionicus*. Bo Barker Jørgensen, as Körber price recipient, and Rudi Amann are thanked for their kind support. This work was sponsored by the Körber Foundation, and the Max Planck Society, Germany. M.W. was also supported by the DFG grant "Bioremediation of marine pollutants by marine cyanobacterial mats - an interdisciplinary approach", and W.M. by a grant of the Technical University Berlin (FIP 6/41).

REFERENCES

1. **Amann, R., J. Stromley, R. Devereux, R. Key, and D. A. Stahl.** 1992. Molecular and microscopic identification of sulfate-reducing bacteria in multispecies biofilms. Appl. Environ. Microbiol. **58:**614-623.
2. **Brosius, J., T. J. Dull, D. D. Sleeter, and H. F. Noller.** 1981. Gene organization and primary structure of a ribosomal RNA operon from *Escherichia coli*. J. Mol. Biol. **148:**107-127.
3. **Canfield, D. E., B. Thamdrup, and J. W. Hansen.** 1993. The anaerobic degradation of organic matter in Danish coastal sediments: Fe reduction, Mn reduction and sulfate reduction. Geochim. Cosmochim. Acta. **57:**3867-3883.
4. **Coleman, M. L., D. B. Hedrick, D. R. Lovley, D. C. White, and K. Pye.** 1993. Reduction of Fe(III) in sediments by sulphate-reducing bacteria. Nature. **361:**436-438.
5. **Devereux, R., M. D. Kane, J. Wilfrey, and D. A. Stahl.** 1992. Genus- and group-specific hybridization probes for determinative and environmental studies of sulfate-reducing bacteria. System. Appl. Microbiol. **15:**601-609.
6. **Dilling, W., and H. Cypionka.** 1990. Aerobic respiration in sulfate reducing bacteria. FEMS Microbiol. Lett. **71:**123-128.
7. **Felsenstein, J.** 1993. PHYLIP (Phylogeny Inference Package) version 3.5c. Department of Genetics, University of Washington, Seattle.
8. **Gilbert, D. G.** 1992. SeqApp - A bio-sequence analysis application. Indiana University, Bloomington.
9. **Jørgensen, B. B.** 1982. Mineralization of organic matter in the sea bed - the role of sulphate reduction. Nature (London). **296:**643-645.
10. **Kühl, M., and B. B. Jørgensen.** 1992. Microsensor measurements of sulfate reduction and sulfide oxidation in compact microbial communities of aerobic biofilms. Appl. Environ. Microbiol. **58:**1164-1174.

11. **Lens, P. N., M.-P. De Poorter, C. C. Cronenberg, and W. H. Verstraete.** 1995. Sulfate reducing and methane producing bacteria in aerobic wastewater treatment systems. Water Res. **29:**871-880.
12. **Manz, W., R. Amann, W. Ludwig, M. Wagner, and K.-H. Schleifer.** 1992. Phylogenetic oligodeoxynucleotide probes for the major subclasses of proteobacteria: problems and solutions. Syst. Appl. Microbiol. **15:**593-600.
13. **Manz, W., M. Eisenbrecher, T. R. Neu, and U. Szewzyk.** 1998. Abundance and spatial organization of Gram-negative sulfate-reducing bacteria in activated sludge investigated by in situ probing with specific 16S rRNA targeted oligonucleotides. FEMS Microbiol. Ecol. **25:**43-61.
14. **Marschall, C., P. Frenzel, and H. Cypionka.** 1993. Influence of oxygen on sulfate reduction and growth of sulfate-reducing bacteria. Arch. Microbiol. **159:**168-173.
15. **McCready, R. G. L., W. D. Gould, and F. D. Cook.** 1983. Respiratory nitrate reduction by *Desulfovibrio* sp. Arch. Microbiol. **135:**182-185.
16. **Muyzer, G., T. Brinkhoff, U. Nübel, C. Santegoeds, H. Schäfer, and C. Wawer.** 1998. Denaturing gradient gel electrophoresis (DGGE) in microbial ecology, p. 1-27. *In* A. D. L. Akkermans, J. D. van Elsas, and F. J. de Bruijn (eds.), Molecular Microbial Ecology Manual, vol. 3.4.4. Kluwer, Dordrecht, The Netherlands.
17. **Muyzer, G., E. C. de Waal, and A. G. Uitterlinden.** 1993. Profiling of complex microbial populations by denaturing gradient gel electrophoresis analysis of polymerase chain reaction-amplified genes encoding for 16S rRNA. Appl. Environ. Microbiol. **59:**695-700.
18. **Pedersen, K., and S. Ekendahl.** 1990. Distribution and activity of bacteria in deep granitic groundwaters of southeastern Sweden. Microb. Ecol. **20:**37-52.
19. **Ramsing, N. B., H. Fossing, T. G. Ferdelman, F. Andersen, and B. Thamdrup.** 1996. Distribution of bacterial populations in a stratified fjord (Mariager Fjord, Danmark) quantified by in situ hybridization and related to chemical gradients in the water column. Appl. Environ. Microbiol. **62:**1391-1404.
20. **Ramsing, N. B., M. Kühl, and B. B. Jørgensen.** 1993. Distribution of sulfate-reducing bacteria, O_2, and H_2S in photosynthetic biofilms determined by oligonucleotide probes and microelectrodes. Appl. Environ. Microbiol. **59:**3840-3849.
21. **Santegoeds, C. M., T. G. Ferdelman, G. Muyzer, and D. de Beer.** 1998. Structural and functional dynamics of sulfate-reducing populations in bacterial biofilms. Appl. Environ. Microbiol. **64:**3731-3739.
22. **Seitz, H.-J., and H. Cypionka.** 1986. Chemolithotrophic growth of *Desulfovibrio desulfuricans* with hydrogen coupled to ammonification of nitrate or nitrite. Arch. Microbiol. **146:**63-67.
23. **Strunk, O., O. Gross, B. Reichel, M. May, S. Hermann, N. Stuckmann, B. Nonhoff, M. Lenke, T. Ginhart, A. Vilbig, T. Ludwig, A. Bode, K.-H. Schleifer, and W. Ludwig.** 1998. ARB: a software environment for sequence data. http://www.mikro.biologie.tu-muenchen.de/pub/ARB. Department of Miocrobiology, Technische Universität München, Munich, Germany.
24. **Swofford, D. L.** 1991. PAUP: Phylogenetic Analysis Using Parsimony. Illinois Natural History Survey, Illinois, USA.
25. **Teske, A., N. B. Ramsing, K. Habicht, M. Fukui, J. Küver, B. B. Jørgensen, and Y. Cohen.** 1998. Sulfate-reducing bacteria and their activities in cyanobacterial mats of Solar Lake (Sinai, Egypt). Appl. Environ. Microbiol. **64:**2943-2951.
26. **Teske, A., C. Wawer, G. Muyzer, and N. B. Ramsing.** 1996. Distribution of sulfate-reducing bacteria in a stratified fjord (Mariager Fjord, Denmark) as evaluated by most-probable-number counts and denaturing gradient gel electrophoresis of PCR-amplified ribosomal DNA fragments. Appl. Environ. Microbiol. **62:**1405-1415.
27. **Wagner, M., H. Abicht, M. Klein, and D. A. Stahl.** 1999. DSR sequences of *Desulfobulbus propionicus* and *Desulfomicrobium baculatum*. in preparation.
28. **Wagner, M., A. J. Roger, J. L. Flax, G. A. Brusseau, and D. A. Stahl.** 1998. Phylogeny of dissimilatory sulfite reductases supports an early origin of sulfate respiration. J. Bacteriol. **180:**2975-2982.
29. **Wawer, C., M. S. M. Jetten, and G. Muyzer.** 1997. Genetic diversity and expression of the [NiFe] hydrogenase large-subunit gene of *Desulfovibrio* spp. in environmental samples. Appl. Environ. Microbiol. **63:**4360-4369.

30. **Wawer, C., and G. Muyzer.** 1995. Genetic diversity of *Desulfovibrio* spp. in environmental samples analyzed by denaturing gradient gel electrophoresis of [NiFe] hydrogenase gene fragments. Appl. Environ. Microbiol. **61:**2203-2210.

31. **Widdel, F., and T. A. Hansen.** 1992. The dissimilatory sulfate- and sulfur-reducing bacteria, p. 583-616. *In* A. Balows, H. G. Trüper, M. Dworkin, W. Harder, and K.-H. Schleifer (eds.), The Prokaryotes, 2nd ed, vol. I. Springer-Verlag, New York Inc.

Chapter 5

An interdisciplinary approach to the occurrence of anoxic microniches, denitrification, and sulfate reduction in aerated activated sludge

Andreas Schramm[1], Cecilia M. Santegoeds[1],
Helle K. Nielsen[2], Helle Ploug[1], Michael Wagner[3], Milan Pribyl[4],
Jiri Wanner[4], Rudolf Amann[1], and Dirk de Beer[1]

[1]Max Planck Institute for Marine Microbiology, D-28359 Bremen, Germany.
[2]University of Aarhus, Dept. of Microbial Ecology, DK-8000 Aarhus C, Denmark.
[3]Technische Universität München, Lehrstuhl für Mikrobiologie,D-80290 Munich, Germany.
[4]Prague Institute of Chemical Technology, Dept. of Water Technology and Environmental Engineering, CZ-166 28 Prague 6, Czech Republic.

This chapter has been submitted to Applied and Environmental Microbiology (1999).

ABSTRACT

A combination of different methods was applied to investigate the occurrence of anoxic processes in aerated activated sludge. Microsensor measurements (O_2, NO_2^-, NO_3^-, H_2S) were performed on single sludge flocs to detect anoxic niches, denitrification, or sulfate reduction on a microscale. Incubations of activated sludge with $^{15}NO_3^-$ and $^{35}SO_4^{2-}$ were used to determine denitrification and sulfate reduction on a batch scale. In five out of seven investigated sludges, no anoxic zones developed during aeration, and consequently denitrification rates were very low. However, in two sludges anoxia in flocs coincided with significant denitrification rates. No sulfate reduction was found in any sludge by neither microsensor nor batch investigations, not even under totally anoxic conditions. In contrast, the presence of sulfate reducing bacteria could be shown by fluorescence in situ hybridization with 16S rRNA-targeted oligonucleotide probes and by PCR-based detection of genes encoding for the dissimilatory sulfite reductase. A possible explanation for the absence of anoxia even in most of the larger flocs is that oxygen transport is not only diffusional but enhanced by advection, facilitated by flow through pores and channels. This is indicated by the irregularity of some oxygen profiles and further supported by confocal laser scanning microscopy of the three-dimensional floc structure which showed that flocs from the two sludges in which anoxic zones were found were apparently denser than flocs from the other sludges.

INTRODUCTION

Activated sludge is currently the most widely used process for the treatment of both domestic and industrial wastewaters and, at least by scale, one of the most important microbiological technologies (18). It primarily relies on the degradation and uptake of organic matter by a microbial community under aerobic conditions. Modern plants are often supplemented with anoxic/anaerobic reactor stages to enhance nitrogen and phosphorous removal. The biomass is finally separated from the purified water by gravitational settling prior to recirculating part of it back into the aeration basin. The process, therefore, selects for microorganisms that remain in the system due to their growth in flocs.

This immobilized growth leads to conditions that markedly differ from conditions of suspended growth in the bulk water phase. Closer interactions of different physiological types of microorganisms are possible (i.e. ammonia and nitrite oxidizers (22)), and bacteria are better protected from protozoan grazing (13) or harmful substances. On the other hand, the transport of solutes (e.g. oxygen and nutrients) in flocs is expected to be mainly diffusional (50, 51). Although the vast majority of activated sludge flocs has been reported to be smaller than 20 µm, i.e. of a size where diffusion limitation is unlikely, flocs larger than 50 µm contribute most to surface area, volume and mass (28). In those larger flocs, the development of anoxic zones has been postulated due to diffusion limitation (e.g. (50)). This would allow for combined nitrification-denitrification in quasi-stratified flocs, hence saving reaction space and time (e.g. (16, 51) and references therein). Less beneficial, anoxic microniches could also support the survival and activity of sulfate reducing bacteria (SRB) in

aerated activated sludge, resulting in the production of H_2S and subsequent problems with sludge bulking (58) or floc disintegration (38).

These hypotheses have been supported indirectly by several reports of nitrogen losses from aeration basins (e.g. (16, 20, 51)), and by the detection of SRB in activated sludge by cultivation (26), (58) and fluorescence in situ hybridization (FISH) (34). In contrast, no anoxic zones could be detected by microsensor measurements in large activated sludge flocs (diameter 1.6 mm) at air saturation (26).

Recently, a flow system was developed for microelectrode measurements in freely sinking aggregates ('marine snow') that also enables the analysis of smaller and more fragile flocs in a natural flow field (40, 41). We used this setup for microsensor measurements of oxygen, nitrate, nitrite and hydrogen sulfide in individual activated sludge flocs. These single floc measurements were complemented with $^{15}NO_3^-$ and $^{35}SO_4^{2-}$ incubation experiments (15, 37) to determine overall rates of denitrification and sulfate reduction in the different sludges tested. Finally, the 3D structure, that is critical for the transport mechanism in a floc (diffusion or advection), was recorded by confocal laser scanning microscopy (CLSM), and the samples were screened for SRB by FISH with rRNA-targeted oligonucleotide probes (4, 34) and by PCR specific for the dissimilatory sulfite reductase gene (53). By this interdisciplinary approach we hoped to achieve a more comprehensive picture of the occurrence and preconditions of anoxic processes in activated sludge flocs.

MATERIAL AND METHODS

Samples. Activated sludge samples were obtained from the aeration basins of municipal wastewater treatment plants (WWTP) in Bremen-Seehausen (Germany), Aarhus-Marselisborg, Odder (both Denmark), and Prague (Czech Republic), from a pilot plant in Aarhus (Denmark), and from two lab-scale sequencing batch reactors (SBR) receiving artificial wastewater (peptone 1000 mg COD l^{-1}, acetic acid 300 mg COD l^{-1}, glucose 400 mg COD l^{-1}, ethanol 300 mg COD l^{-1}, N-NH_4^+ 0.2 mg l^{-1}, P_{total} 14 mg l^{-1}). Both SBR were operated with rapid filling periods (5-10 min) to simulate the conditions in a plug-flow reactor with high substrate concentration gradients. SBR1 was operated with a complete oxic cycle (23 h aeration, 1 h settling), whereas SBR2 was subjected to an alternating cycle (3 h anoxic, 8 h aeration, 1 h settling). Some operational data of the investigated sludges are summarized in Table 1.

For microsensor measurements a small portion of sludge was diluted to avoid massive agglomeration of flocs after sampling, and single flocs were carefully transferred to the measuring setup by means of a pipette with the tip cut open. For the batch experiments freshly collected sludge was allowed to settle, the supernatant was discarded, and the concentrated sludge was used for the incubations.

Microsensor measurements. Clark-type microsensors for O_2 (42), LIX-type microsensors for NO_2^- and NO_3^- (8), and amperometric H_2S microsensors (25) were constructed, calibrated, and used for measurements as previously described. The lower detection limits of NO_2^- and H_2S were 0,1 µM

and 1 µM, respectively. Microprofiles of single activated sludge flocs were recorded by keeping the flocs freely suspended in a vertical flow system, where the flow velocity opposed and balanced the sinking velocity of the individual floc. To create a parallel, non-turbulent, uniform flow a nylon stocking was mounted in the flow chamber horizontally to the flow, and the flocs were positioned just above this net (40, 41). By this net-jet system the flocs could be stabilized in the upward flowing water column allowing microsensor measurements with a spatial resolution of 25 - 50 µm inside the flocs. For practical reasons microprofiles of different chemical species were usually recorded in different flocs.

TABLE 1. Operational data of the investigated activated sludge plants.

	WWTP Aarhus	**WWTP Bremen**	**WWTP Odder**	**WWTP Prague**	**Pilotplant Aarhus**	**SBR1**	**SBR2**
*COD (mg l^{-1})	419	476	450	242	n.d.	2000	2000
*N-NH_4 (mg l^{-1})	33.1	37.5	34	20	n.d.	0.2	0.2
*P_{total} (mg l^{-1})	3.2	7.0	12	3.65	n.d.	14	14
MLSS (g l^{-1})	4.3	3.04	3.14	2.7	n.d.	7.4	3.2
reaction time (h)	5.7	6.5	n.d.	3.3	n.d.	46	33
sludge age (d)	25	10	n.d.	3.3	n.d.	25	8

*influent values; n.d. not determined

The artificial wastewater used in the flow chamber contained 200 µM sodium acetate, 760 µM $(NH_4)_2SO_4$, 220 µM KH_2PO_4, 400 µM K_2HPO_4, and 41 µM $MgSO_4$, representing an F:M (food to microorganism) ratio of approximately 0.1, which is a value typical for most nutrient removal plants (47). For measurements of NO_2^- and NO_3^- profiles this medium was supplemented with 100 µM KNO_3. Microsensor measurements were performed at 20°C at three different oxygen concentrations: air saturation (~ 280 µM), 2 mg l^{-1} (~ 60 µM), the oxygen set-point of most aeration basins, and anoxic conditions.

Additionally, 10 ml of activated sludge were amended with a mixture of acetate, propionate and butyrate (final concentration 1 mM each) in a test-tube and incubated for approximately 1 h without aeration. After oxygen was depleted (proven by microsensor measurements) an H_2S microsensor was repeatedly introduced into the sludge.

Calculations. The volumetric oxygen respiration rate R of a sphere with zero order kinetics at steady state is described by (41):

$$R = \frac{4\pi r_0^{\,2}}{\frac{4}{3}\pi(r_0^{\,3} - r_c^{\,3})} \cdot \frac{D_{W(ox)}(C_\infty - C_0)}{\delta_{eff}} \qquad (1)$$

where r_0 is the radius of the sphere, $4\pi r_0^2$ and $\frac{4}{3}\pi r_0^3$ are the surface area and volume, respectively, r_c is the radial distance from the center at which the oxygen concentration becomes zero (if there is no anoxic zone $r_c = 0$), $D_{W(ox)}$ is the molecular diffusion coefficient of oxygen in water, C_∞ and C_0 are the concentrations of oxygen in the bulk water phase and at the floc surface, respectively, and δ_{eff} is the effective diffusive boundary layer (DBL) thickness. The same formula was used to calculate denitrification rates of single flocs from nitrate microprofiles. D_W for oxygen at 20°C is $2.12 \cdot 10^{-5}$ cm^2

s^{-1} (5), for nitrate $1.66 \cdot 10^{-5}$ cm^2 s^{-1} (29). Determination of $\delta_{eff.}$ and data processing was done by a simple diffusion-reaction model assuming zero order kinetics as described in detail by Ploug et al. (41).

Acetate concentration at the floc center was estimated from the volumetric oxygen respiration rates R using (41):

$$C_c = -\frac{R}{3} \cdot \left(\frac{r_0^2}{2D_{agg(ac)}} + \frac{r_0 \cdot \delta_{eff}}{D_{W(ac)}} \right) + C_\infty \qquad (2)$$

where C_c is the acetate concentration at the floc center, δ_{eff} is the effective DBL thickness determined from the oxygen profiles, and $D_{agg(ac)}$ and $D_{W(ac)}$ are the molecular diffusion coefficients of acetate in the floc and in water which were assumed to be the same. $D_{W(ac)}$ was calculated using standard tables and formulas (30) and corrected for co-diffusion of NH_4^+ (the cation with the highest concentration in the medium) to a value of $1.00 \cdot 10^{-5}$ cm^2 s^{-1} (29). The same formula was also applied with respect to oxygen, where C and D are concentrations and diffusion coefficients of oxygen, respectively (41). Thereby, the respiration rates required to create anoxic conditions at the floc center (i.e. $C_c = 0$) were calculated as a function of floc size at different bulk water concentrations of oxygen (Fig. 5).

$^{15}NO_3^-$-incubations. Denitrification rates were determined using a batch reactor with a liquid volume of 1.2 l and a gas volume of 0.5 l (including tubing). The reactor was cylindrical with a diameter of 10 cm and a height of 17 cm. The bottom section was funnel shaped with a porous glass grid in the center, through which gas was supplied. This arrangement prevented the development of stagnant zones. The gas flow rate was just sufficient to keep the flocs in suspension. Oxygen concentration measurements at different positions within the reactor showed that it was well mixed under test conditions. Prior to the incubations, N_2 in the reactor was exchanged by argon to lower the background, thereby improving the detection of ^{15}N-enriched N_2. Rate measurements were performed at air saturation, at an oxygen concentration of 40-60 µM, and in the absence of oxygen by adjusting the oxygen/argon ratio in the gas supply. An oxygen microelectrode was inserted in the reactor for continuous monitoring during the experiments. 300 ml of concentrated activated sludge was added to the reactor, which was then filled up with 1 l of artificial wastewater (as described for the microsensor measurements) and amended with sodium acetate to a concentration of 7.8 mM. The reactor contained 2 - 4 g TSS l^{-1} (TSS = total suspended solids). After the oxygen concentration was adjusted, 8.3 ml of $Na^{15}NO_3$ was added from a 12 mM stock solution of 99.2 atom% $^{15}NO_3^-$, corresponding to a final concentration of 100 µM $^{15}NO_3^-$. During the 30 min incubation experiment, gas samples of 1 ml were taken from the reactor headspace every 3 minutes through a septum with a gas-tight syringe (Hamilton, 1001RN) and transferred to gas-tight exetainers (Labco), that had been filled with N_2-free destilled water. Subsamples of gas (250 µl) were analyzed on an isotope ratio mass spectrometer with collectors for $^{28}N_2$, $^{29}N_2$, and $^{30}N_2$ (Sira Series II, VG Isotech, Middlewich, Chesire, UK) as described previously (37, 44). Total denitrification rates were calculated as the sum of denitrification of $^{15}NO_3^-$ and $^{14}NO_3^-$, that were derived from the measured production of $^{14}N^{15}N$ and $^{15}N^{15}N$ as described in detail by Nielsen (37).

$^{35}SO_4^{2-}$-incubations. Sulfate reduction rates were determined by the ^{35}S-radiotracer method (15) in samples from SBR1, SBR2, and from the WWTP Prague. Reactor design, incubation conditions, and filling of the reactor were as described for the ^{15}N-experiments. After the oxygen concentration was adjusted, 20 ml of tracer was added ($Na_2{}^{35}SO4$, 2 Mbeq). Through a septum samples of 5 ml were taken from the reactor during the first 10 minutes once per minute, then for another 10 minutes once every two minutes. Subsequently, samples were taken every 10 minutes until one hour after the start of the test. To each sample, 5 ml of fixation solution (20% ZnAc, 1% formaline, pH 5) were added and shaken well. Samples to which 0.1 ml of tracer was added after fixation were used as blanks for each incubation. Fixed samples were stored at 4°C until further analysis within two months. The samples were then centrifuged at 10,000 g and the reduced sulfur species in the pellet were determined with the single-step chromate distillation according to Fossing and Jørgensen (15). The detection limit of the method was a sulfate reduction rate of 5 μmol S g^{-1} TSS h^{-1}.

SRB screening. Activated sludge samples were fixed with paraformaldehyde, immobilized on microscopic slides and dehydrated as described previously (3). For fluorescence in situ hybridization (FISH), a set of oligonucleotide probes specific for SRB was used, i.e. SRB385, targeting a broad range of SRB but also numerous non-sulfate-reducing bacteria (2), probes DSV698, DSV407, DSV1292, and DSV214, specific for the family *Desulfovibrionaceae* (34), probes 221 and 660, specific for the genus *Desulfobacterium* and *Desulfobulbus*, respectively (10), and probes DSB985 and DSS658, specific for the genus *Desulfobacter* and the taxon *Desulfosarcina-Desulfococcus* (34), respectively. All probes were purchased labeled with the fluorescent dye CY3 (Interactiva Biotechnologie Ulm, Germany) and applied for FISH using the protocol and the conditions recently described by Manz et al. (34). After the hybridization procedure the samples were stained with 4',6-diamidino-2-phenylindole (DAPI) according to Wagner et al. (52), mounted with antifading reagent (Vectashield, Vector Laboratories Inc., Burlingame, CA) and examined under an epifluorescence microscope (Zeiss, Jena, Germnany). Independent testing for the presence of SRB was done by amplification of a 1.9 kb DNA fragment encoding most of the α and β subunits of the dissimilatory sulfite reductase (DSR). DNA was extracted from four activated sludge samples (WWTP Bremen and Prague, SBR1, SBR2) by a combined freeze-thaw (3 times freezing in liquid nitrogen and heating at 37°C) and hot phenol-chloroform-isoamyl alcohol treatment (49). The DSR gene fragments were then amplified using the primer pair DSR1F (5'- ACSCACTGGAAGCACG-3') and DSR4R (5'-GTGTAGCAGTTACCGCA-3') described by Wagner et al.(53). The PCR reaction mixture (100 μl) contained 100 pmol of each primer, 25 nmol of all four deoxynucleoside triphosphates, 200 μg of bovine serum albumin, 10 μl 10× PCR buffer (HT Biotechnology Ltd) and 10 - 100 ng of template DNA. A hot-start PCR program was used, in which 1 U of SuperTaq DNA polymerase (HT Biotechnology Ltd) was added at 80°C after 5 min heating at 94°C, with 35 cycles, each cycle consisting of 1 min at 94°C, 1 min at 60°C, and 3 min at 72°C. The PCR products were loaded and evaluated on a 1% agarose gel. As a positive control for proper PCR performance with DNA from activated sludge samples, a 550-bp-long 16S rDNA fragment was amplified with universal primers as described by Muyzer et al. (36).

3D analysis of flocs. For the staining with fluorescein-isothiocyanate (FITC) which covalently binds to proteins (19), 0.2 ml of settled flocs were added to 15 ml staining solution (0.1 M sodium phosphate, pH 7.0 and 4 mg l^{-1} FITC). After 5 minutes of gentle mixing the aggregates were allowed to settle, the solution was decanted and the flocs were washed twice with 0.1 M sodium phosphate, pH 7.0. The aggregates were stored at 4°C in 0.1 M sodium phosphate, pH 7.0, with 4% paraformaldehyde. For CLSM analysis the pH was raised to 9 by the addition of 1 M carbonate buffer. Staining with calcofluor to visualize polysaccharides was performed similarly in the same buffer with 300 mg l^{-1} calcofluor (7). The staining time was 2 hours. Washing and storage was as described above. The aggregates were microscopically examined at pH 7.0. DNA within the flocs was stained with ethidiumbromide (1 µg ml^{-1}) for 15 min in the same buffer. The flocs were washed as described above, and immediately observed under the CLSM.

CLSM-analysis. FITC-, calcofluor- and ethidiumbromide-stained flocs were transferred into 1 ml buffer to a chamber sealed on the bottom with a cover glass and analyzed with an inverse confocal laser scanning microscope (LSM510, Carl Zeiss, Jena, Germany). A 40x Plan-Neofluar 1.3 lens was used, and three different lasers (Argon-ion: UV [351-364 nm], 458 nm and 488 nm; HeNe: 543 nm) were applied for excitation. Image processing, including three-dimensional reconstruction, was performed with the standard software package delivered with the instrument (version 2.01, service pack 2). Images were printed on a Kodak printer 8650 by use of the software package Microsoft Power Point (version 7.0, Microsoft, Redmont, USA).

RESULTS

Microprofiles. Microsensor measurements for the different parameters were performed in different activated sludge flocs, all in all in 250 individual flocs with a size range of 400 - 2300 µm (maximum length as observed by dissection microscopy). Larger flocs often consisted of a loose agglomeration of compact subunits of 50 - 100 µm, suggesting a dynamic aggregation and disintegration. Flocs smaller than 400 µm could not be sufficiently stabilized in the flow chamber for profiling.

When incubated under air saturation (~280 µM) oxygen was never depleted but showed values of 90-200 µM in the floc center. In several flocs (indicated by arrows in Fig. 3) oxygen gradients were somewhat irregular or weak, and oxygen increased locally inside a floc. This might result from advective transport of oxygen-rich bulk medium through pores into the floc. Nitrite concentrations slightly increased towards the center reaching 0.5-2 µM, probably due to nitrification. Nitrate concentrations increased to above bulk water concentrations in some flocs indicating nitrifying activity, appeared unchanged in other flocs, and in only three large flocs (SBR2) a decrease of 5-10 µM was observed.

Incubation under 40-60 µM oxygen, resembling the conditions in aeration basins, lead to oxygen concentrations of typically less than 20 µM in the floc center. Complete depletion of oxygen was observed within 12 out of 14 flocs from the two SBR and within 2 out of 8 flocs from the WWTP

Bremen but not within flocs from any other sample. Accordingly, a significant decrease of nitrate towards the floc center was only detected within the SBR flocs, and denitrification rates of individual flocs were calculated in the range of 2-14 nmol·mm^{-3}·h^{-1} (average SBR1 5.9 nmol mm^{-3} h^{-1}, SBR2 10.2 nmol·mm^{-3}·h^{-1}). All other samples showed no or very little nitrate consumption (maximum denitrification rate 1.7 nmol·mm^{-3}·h^{-1}, averages 0-0.7 nmol·mm^{-3}·h^{-1}). Most nitrite gradients were insignificant. In some flocs nitrite accumulated to concentrations of 5-20 µM, possibly because nitrite oxidation was inhibited by low oxygen concentrations. Typical profiles of oxygen, nitrate and nitrite in activated sludge flocs from the WWTP samples and from SBR samples are displayed in Fig. 1 A and B, respectively.

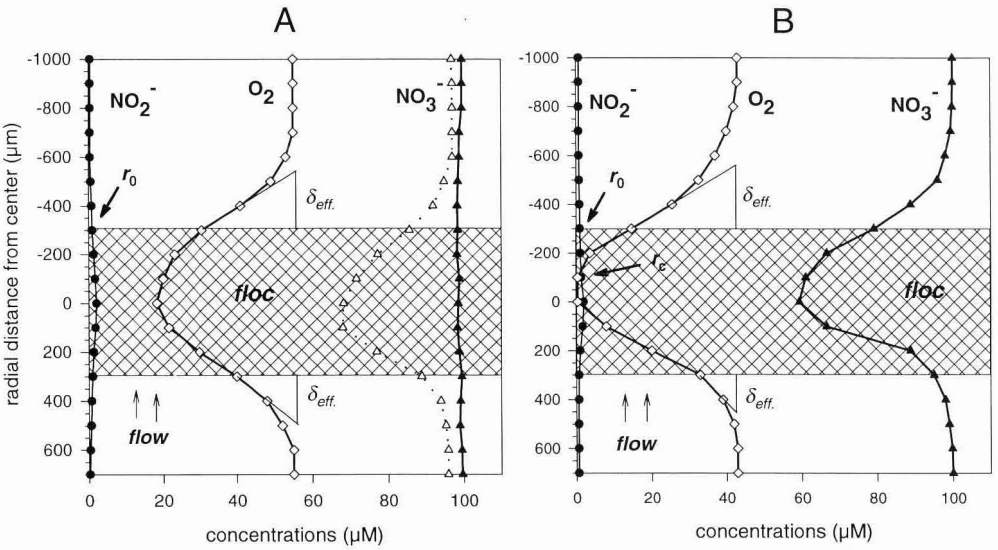

FIG. 1. Typical microprofiles of oxygen, nitrite, and nitrate in activated sludge flocs from WWTP Prague (A) and SBR1 (B), measured in the net-jet flow chamber at 2 mg O_2 l^{-1}. Shaded area = floc, r_0 = floc surface, r_c = distance from floc center where oxygen disappears, $\delta_{eff.}$ = effective diffusion boundary layer (DBL). The dotted nitrate profile in Fig 1A was recorded under anoxic conditions and displays the denitrification potential of the floc.

To test the samples for their denitrification capacity we also recorded nitrate and nitrite profiles while oxygen was absent. A decrease of nitrate was measured in virtually all tested flocs from all sludges. The derived denitrification rates were quite heterogeneous, spanning a range of 0.5-27 nmol·mm^{-3}·h^{-1}. Nitrite profiles were similar to the ones measured under 40-60 µM oxygen, although nitrite production in this case must be attributed to nitrate reduction.

No H_2S was detectable by microsensor measurements in any floc from any sample, not even after prolonged anoxic incubations (1 h) at stagnant conditions in a test-tube.

Respiration rate. Volumetric respiration rates R of individual flocs were calculated from the oxygen profiles assuming diffusion to be the only transport process. They were between 0 and 18 nmol O_2 $mm^{-3}h^{-1}$, with the highest R values found in those sludges in which anoxic microniches had been detected, i.e. in SBR1, SBR2, and WWTP Bremen (Fig. 2).

Under 40-60 µM oxygen the respiration rates obviously decreased with floc size (Fig. 3B), while this trend was not as pronounced under air saturation (Fig. 3A).

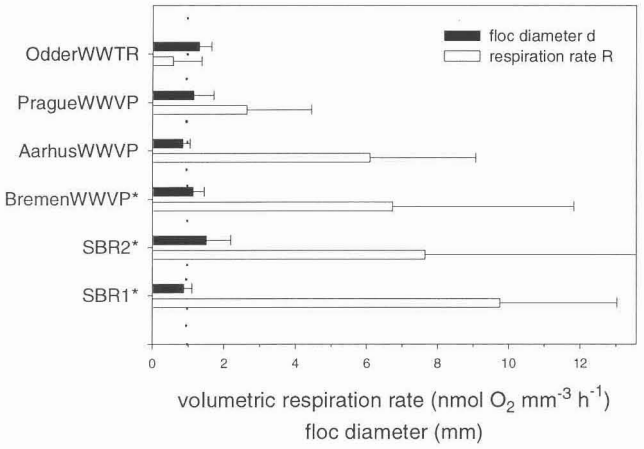

FIG. 2. Mean volumetric respiration rates R and mean floc sizes d with standard deviations of all flocs from all samples in which oxygen gradients have been measured. The dotted line indicates a floc diameter of 1 mm.

Incubation experiments. Batch experiments to determine denitrification and sulfate reduction rates using stable and radio-isotope techniques were performed under the same conditions, and with similar results, as the microsensor measurements (Table 2). Under air saturation virtually no denitrification occurred, and the rates under reactor conditions were extremely low except for the SBR samples. All sludges were, however, capable of denitrification under anoxic conditions, at rather diverse rates. Sulfate reduction could not be detected neither in sludge from Prague WWTP nor in sludges from the SBR, regardless of the aeration conditions applied (air saturation, reactor conditions, or anoxia).

TABLE 2. Denitrification rates as determined by $^{15}NO_3$ incubations.

	air saturation	20% air saturation	anoxic conditions
WWTP Aarhus	0.003±0.001	0.114±0.058	1.496±0.151
WWTP Bremen	n.d.	0.046±0.013	3.212±1.690
WWTP Odder	0.007±0.004	0.040±0.003	1.592±0.401
WWTP Prague	0.005±0.003	0.038±0.005	1.198±0.358
Pilotplant Aarhus	n.d.	n.d.	n.d.
SBR1	0.191±0.12	0.470±0.234	1.257±0.128
SBR2	0.101±0.022	0.940±0.282	1.826±0.246

all values in µmol N g^{-1} TSS min^{-1}

SRB screening. FISH with probe SRB385 suggested the presence of SRB in all tested sludges. The abundance of specifically hybridized cells was roughly estimated to be 1-2% in the SBR and in the Aarhus pilot plant, and 3-5% of total cells stained by DAPI in all other samples. Of the more specific probes only DSV698 and DSV1292, complementary to the majority of *Desulfovibrio* species, detected significant numbers of target cells, i.e. 0.5-1% in the SBR and in the Aarhus pilot plant, and 2-4% of total cells in the other samples. In comparison, members of the genera *Desulfobacterium, Desulfobacter, Desulfobulbus, Desulfomicrobium,* and *Desulfosarcina* detected by FISH together made up less than 0.2% in all samples. Additionally, DNA was extracted from activated sludge samples of the SBR as well as from samples of the WWTP Prague and Bremen. Using the same amount of DNA (ca. 20 ng) for the PCR reaction we obtained no PCR product of the DSR gene fragments from the SBR samples, but distinct PCR products of the expected size were retrieved from the WWTP samples (data not shown). As dissimilatory sulfite reductase is a key-enzyme for sulfate reduction, the detection of its genes indicates the presence of sulfate reducing bacteria (or of at least their DNA) in the WWTP activated sludges but not in the SBR.

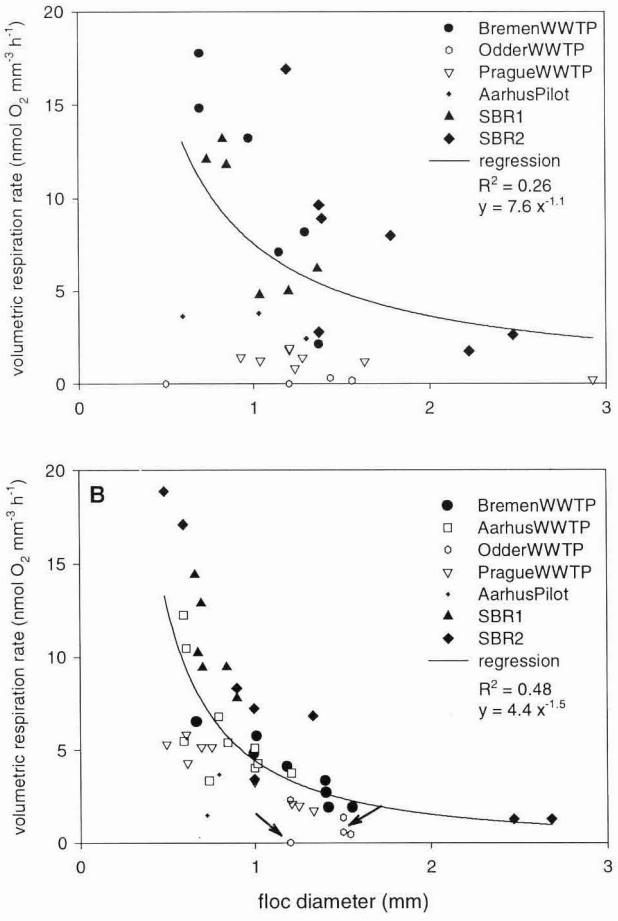

FIG. 3. Volumetric oxygen respiration rates versus floc diameter as measured under air saturation (A) and under 2 mg O_2 l^{-1} (B). Arrows indicate flocs where the oxygen profile was most likely influenced by advective transport (liquid flow). These data points were excluded from the regression curve, as the respiration rates are most probably underestimates (see discussion).

3D analysis of activated sludge flocs. For a qualitative analysis of the three-dimensional floc structure of different sludges (WWTP Prague, Bremen, SBR1, SBR2), flocs were stained either with FITC, calcofluor or ethidium bromide. These fluorescent dyes bind to proteins, polysaccharides and DNA, respectively, which represent the main compounds of extracellular polymeric substance (EPS) of activated sludge flocs (50). Staining of these substances should therefore give a good impression of its structure. A comparison of the different stains revealed that, at the low resolution needed to visualize complete flocs, all three yielded approximately the same picture, i.e. the same ratio of stained floc material to unstained pore volume. However, as FITC-conferred fluorescence of the flocs was brightest and gave best CLSM images, all further 3D analyses were performed on FITC-stained flocs. CLSM analysis revealed clear differences of the floc structure between the different sludge types. WWTP flocs appeared to have a more fluffy structure with more and larger pores (i.e. the unstained part), which were estimated to comprise 50-80% of the entire floc volume. In contrast, SBR flocs seemed to be denser and more compact (pore volume 30-65%). An example of each kind of floc is shown in Fig. 4. It should be mentioned, however, that the numbers must be treated as estimates after examination of 52 flocs rather than as quantitative description of pore volumes and floc populations. Nevertheless, the qualitative difference in porosity and structure was evident.

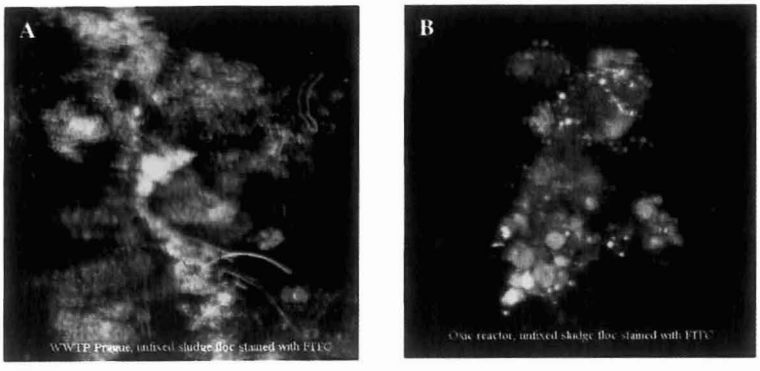

FIG. 4. CLSM image (red-green overlay, use red-green glasses) of the 3D structure of activated sludge flocs from WWTP Prague (A) and SBR1 (2) after FITC staining. 300 x 300 µm.

DISCUSSION

Anoxic microniches and denitrification. When incubated under air saturation anoxia was never detected inside activated sludge flocs which is in agreement with the measurements of Lens et al. (26). Calculation of acetate concentrations in the center of the flocs, based on the measured oxygen respiration rates (equation 2), showed that only in 2 out of 35 flocs acetate could be completely depleted. Therefore, assuming that acetate (this study) or glucose and starch (26) were

suitable substrates for the microbial community in activated sludge, respiration was most likely not limited by the availability of organic carbon. This indicates that the respiration capacity of activated sludge is simply not sufficient to consume such high amounts of oxygen. However, even when incubated under more realistic conditions (2 mg O_2 l^{-1}) no anoxic zones and no denitrification were detected in activated sludge flocs except of the SBR and few flocs from Bremen WWTP. The question has to be raised how representative the microsensor measurements in single flocs have been, i.e. if the measuring approach was suited to detect anoxic microniches, and if the results are meaningful for a complete activated sludge basin. In our study we only analyzed flocs larger than 400 µm. From literature data, this seems to be not an important fraction in terms of number but might be most relevant in terms of volume or mass (12, 28), and hence the fraction that contributes most to the activity of a plant. Furthermore, anoxic zones due to diffusion limitation are primarily to be expected in larger flocs since the volumetric respiration rates required to create anoxia exactly at the center of a floc increase with the square of the floc radius (equation 2, Fig. 5; (41)). Therefore, under reactor conditions volumetric respiration rates of more than 70 nmol·mm^{-3}·h^{-1} are necessary for anoxia in flocs with a diameter of 400 µm or less. Such high rates have only been found in microbial mats (21) and nitrifying aggregates (9) while the rates reported from various other systems such as detritus pellets (41), trickling filter biofilms (23, 24), or sediments (14, 43) are all in the same range (1.2 - 39.6 nmol·mm^{-3} h^{-1}) as the values measured in this study (0 - 19 nmol·mm^{-3}·h^{-1}). It is thus questionable if the respiration rates required for anoxia in flocs smaller than 400 µm can be ever reached in activated sludge. Furthermore, microprofiles were investigated simulating sinking flocs, i.e. in a flow chamber with laminar flow, where no turbulent mixing or collisions of flocs occur. The latter processes, however, are typical for aerated activated sludge basins. They might enhance advective transport of oxygen towards the floc center and obviously lead to a steady aggregation and disintegration of flocs. Gradients and flocs are consequently dynamic features, e.g. the center of a floc might become exposed to oxygen again after a anoxic period by the disruption of the floc. For these two reasons, the size of the studied flocs and the measuring conditions, it is more likely that we overestimated anoxic processes in the activated sludges by microsensor analysis rather than to overlook them.

The isotope incubation experiments yield independent control for the microsensor data as they averaged over all flocs present in a large sample and were better simulated the mixing regime in an activated sludge basin. Consistent with the microprofiles, significant denitrification under 2 mg O_2 l^{-1} was only measured in the SBR, while under anoxic conditions all sludges showed rates of 1.2 - 3.2 µmol N g^{-1} TSS min^{-1}, comparable to conventional anoxic activated sludge basins designed for denitrification (6, 50). This shows that denitrifiers were present in all sludges, and the virtual absence of denitrification in most sludges during aeration can be indeed explained by the absence of anoxic niches inside the activated sludge flocs. Furthermore, denitrification under 2 mg O_2 l^{-1} represented a similar percentage of maximum denitrification activity in both, ^{15}N-incubations and microsensor measurements (data not shown). This indicates that microprofiles actually were recorded under realistic conditions and show data relevant for the whole aeration basin. Some nitrate microprofiles showed denitrification under air saturation, and also denitrification rates determined by ^{15}N-incubations are slightly above the detection limit in samples where no anoxic zones were found.

Thus, one may speculate about the occurrence of aerobic denitrifiers (31, 39, 45). However, their contribution to overall denitrification seems to be almost negligible in the analyzed systems.

Another considerable factor is the bulk water concentration of oxygen. Obviously, reducing the aeration of activated sludge will immediately increase the probability of anoxic microniches and processes inside a diffusion controlled floc (Fig. 5). Indeed there have been reports on enhanced denitrification rates in aerated activated sludges when the bulk oxygen concentration was set to 0.5 - 1.5 mg l^{-1} (17, 20, 57). However, nitrification might be less effective or become incomplete; therefore attempts to achieve nitrogen removal by simultaneous nitrification-denitrification by simply lowering the bulk oxygen concentration would require continuous monitoring and careful balance of both processes.

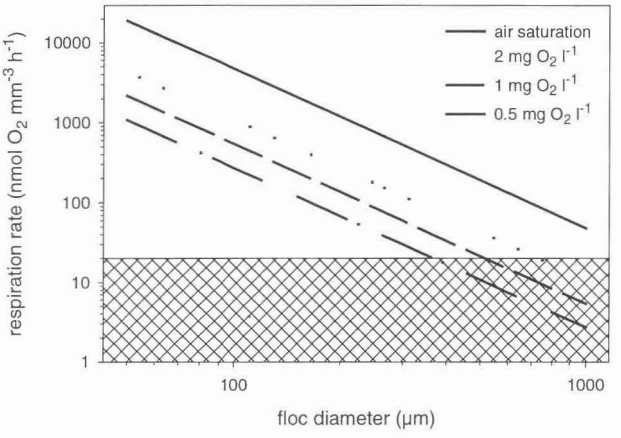

FIG. 5. Volumetric oxygen respiration rates R required to create anoxic conditions exactly at the center of a floc with a maximum DBL under different bulk oxygen concentrations (calculated from equation 2). Under such diffusion limited conditions R decreases with the square of the floc radius. The shaded area represents respiration rates that have been measured during this study.

Respiration rates. Valuable information can be derived from the measured volumetric respiration rates R of individual flocs in relation to their size. As displayed in Fig. 5, smaller flocs require higher respiration rates to become anoxic because of their higher surface to volume ratio. This also applies to the investigated samples (Fig. 2). For example, the mean floc sizes of analyzed flocs from SBR1, Aarhus WWTP and Aarhus Pilot are almost the same, however only the respiration rates of SBR1 are sufficient to create anoxic zones. Furthermore, the volumetric respiration rate R was negatively correlated with floc size d (Fig. 3). This was more pronounced for flocs under reactor conditions than for flocs under air saturation. A decrease of R with d^2 usually would indicate diffusion limitation within the floc (Fig. 5). The observed decrease of R with $d^{1.5}$ at 40-60 µM oxygen (Fig. 3B) might be explained by the different extent of oxygen limitation in the different flocs that contributed to the regression analysis: (i) flocs with anoxic centers, which are truly diffusion limited, (ii) flocs with rather low oxygen concentrations (1-10 µM), that might already slow down respiration rates, and (iii) flocs with higher oxygen levels that should allow for maximum respiration rates since the K_m for oxygen consumption by heterotrophic bacteria is about 1 µM (56). In contrast, diffusion limitation can be excluded to account for this trend under air saturation (Fig. 3A). Oxygen as well as organic carbon are present in concentrations high enough to prevent any limitations as has been

discussed before. An alternative explanation lies in the structure and the geometry of the floc. Larger flocs might be less dense than smaller ones, i.e. contain less active cells per volume and more voids and dead material. This seems to be partially the case, as large flocs (> 1 mm) often enclose bigger particles which do not contribute to respiration. Furthermore, activated sludge flocs are fractal in their geometry, with fractal dimensions of 1.0 - 1.8 (27, 33, 48). As is typical of fractal aggregates, the porosity of flocs increases with increasing floc size (1), resulting in reduced mass and hence respiration rate per volume as the aggregates get larger. The same applies of course also under the lower oxygen concentrations but this weak correlation is covered by the more pronounced diffusion limitation. Fractal geometry of the activated sludge flocs might therefore provide an explanation why the volumetric respiration rates of most sludges have been too low to create anoxic conditions even in the larger flocs. Alternatively, this might be due to advective transport through pores and channel-like structures (32) since larger flocs often consist of dense subunits that are only loosely connected. Flow might have been detected in some of our oxygen profiles that showed a local increase in oxygen concentration (data points marked with an arrow in Fig. 3). Flow could substantially enhance oxygen transfer compared to diffusion. In this case, our calculations of volumetric respiration rates (and denitrification rates) based on diffusional transport underestimate R. If advection is important as transport mechanism in activated sludge flocs, a reduced oxygen bulk concentration does not necessarily result in anoxic zones and enhanced denitrification as discussed above.

Considering fractal geometry and advective transport might help to understand the differences between the flocs from the SBR and the other samples. SBR have been reported to form more compact (and larger) flocs (54) which would allow for higher volumetric respiration rates compared to conventional WWTP flocs and prevent advective transport of oxygen inside the floc. This hypothesis is supported by CLSM analysis of the 3D floc structure that demonstrated SBR flocs to be more compact than WWTP flocs (Fig. 4). However, further research is needed to better understand the impact of floc structure, i.e. fractal geometry and advective transport, on the floc's function.

Sulfate reduction. Low numbers of SRB were detected by FISH in all samples, and the amplification of the DSR gene fragments indicated the presence of SRB in samples from WWTP Bremen and Prague. In contrast, no sulfate reduction was detected in any experiment by microsensor or radioisotope analysis. The sensitivity of the applied techniques was high (1µM H_2S and 5 µmol S g^{-1} TSS·h^{-1}, respectively). Re-oxidation was excluded during anoxic incubations, and by the ^{35}S analysis even immediate precipitation of H_2S, e.g., as FeS (38), would have been detected. Consequently, sulfate reduction did not occur during oxic incubations and no sulfate reduction potential was apparent in the anaerobic incubations. However, a shortcoming of the approach was the use of acetate as sole carbon source in almost all experiments. Acetate is not utilized as electron donor by incompletely oxidizing SRB including *Desulfovibrio* sp. (55), which were detected by far as the main component of the SRB community in the analyzed samples. Most likely, sulfate reduction in our experiments had therefore to rely on endogenous electron donors of the activated sludge that were either produced from the acetate added or had been stored within the flocs. Whereas this assumption is doubtful for the microsensor experiments, due to the small volume of a single floc compared to incubation volume and time, it is well sound for the radiotracer and the test-tube incubations. Here, about one third of the reactor volume consisted of concentrated activated sludge, and only two third

of the sludge bulk water had been replaced by the artificial medium. Essentially, the substrate spectrum was similar to the original activated sludge sample but slightly diluted. Therefore, we are convinced that we would have been able to detect sulfate reduction in the observed systems if it had occurred. The complete absence of sulfate reduction, and the detection of significantly lower numbers of SRB in the pilot plant and SBR compared to the WWTP samples most likely indicate unfavorable conditions for SRB in the investigated sludges. It might be possible that SRB are not able to grow and multiply in the aerated activated sludge but rely on the continuous re-inoculation via sewer, biofilm wall growth in the basin (46), or backwash from settler and anaerobic digester. The lack of these sources in the lab-scale SBR and the pilot plant might explain the low numbers of SRB detected there by FISH. This low amount of SRB might also explain the failure to detect the DSR gene fragment in samples from the SBR. Possibly, the same amount of DNA that resulted in reliable amplifications from the other samples might have been to low to yield PCR products from the SBR. Considering the reported occurrence of higher numbers of SRB in activated sludge (e.g. 26, 34, 58) in the light of our results, we would suggest that the actual function of these SRB in the aeration basins might not be sulfate reduction. For instance, oxygen (11) and nitrate (35) have been described as alternative electron acceptors. However, also plant-to-plant differences have to be kept in mind, and sulfate reduction may occur in other activated sludge systems.

Conclusion. We found that anoxic microniches and denitrification are possible and detectable in aerated activated sludge. The structure of the activated sludge flocs plays an important role for the occurrence of this phenomenon. However, anoxia seems to be rather the exception than the rule in conventional wastewater treatment plants, and sulfate reduction seems to be almost fully absent. The exact interrelations between structure and function of the activated sludge floc require further investigation, especially to describe on a quantitative basis the fractal geometry - respiration correlation.

ACKNOWLEDGMENTS

We thank G. Eickert, A. Eggers, and V. Hübner for constructing oxygen and hydrogen sulfide microsensors. This work was supported by the Körber Foundation and the Max-Planck Society.

REFERENCES

1. **Alldredge, A.** 1998. The carbon, nitrogen and mass content of marine snow as function of aggregate size. Deep Sea Res. **45:**529-541.
2. **Amann, R. I., B. J. Binder, R. J. Olson, S. W. Chisholm, R. Devereux, and D. A. Stahl.** 1990. Combination of 16S rRNA-targeted oligonucleotide probes with flow cytometry for analyzing mixed microbial populations. Appl.Environ.Microbiol. **56:**1919-1925.
3. **Amann, R. I., L. Krumholz, and D. A. Stahl.** 1990. Fluorescent-oligonucleotide probing of whole cells for determinative, phylogenetic, and environmental studies in microbiology. J.Bacteriol. **172:**762-770.
4. **Amann, R. I., W. Ludwig, and K. H. Schleifer.** 1995. Phylogenetic identification and in situ detection of individual microbial cells without cultivation. Microb.Rev. **59:**143-169.
5. **Broecker, W. S., and T.-H. Peng.** 1974. Gas exchange rates between air and sea. Tellus. **26:**21-35.
6. **Christensen, M. H., and P. Harremoes.** 1977. Biological denitrification of sewage: a literature review. Prog. Watet Technol. **8:**509-555.
7. **De Beer, D., V. O'Flaharty, J. Thaveesri, P. Lens, and W. Verstraete.** 1996. Distribution of extracellular polysaccharides and flotation of anaerobic sludge. Appl.Microbiol.Biotech. **46:**197-201.
8. **De Beer, D., A. Schramm, C. M. Santegoeds, and M. Kühl.** 1997. A nitrite microsensor for profiling environmental biofilms. Appl.Environ.Microbiol. **63:**973-977.
9. **De Beer, D., J. C. van den Heuvel, and S. P. P. Ottengraf.** 1993. Microelectrode measurements of the activity distribution in nitrifying bacterial aggregates. Appl.Environ.Microbiol. **59:**573-579.
10. **Devereux, R., M. D. Kane, J. Winfrey, and D. A. Stahl.** 1992. Genus- and group-specific hybridization probes for determinative and environmental studies of sulfate-reducing bacteria. Syst.Appl.Microbiol. **15:**601-609.
11. **Dilling, W., and H. Cypionka.** 1990. Aerobic respiration in sulfate reducing bacteria. FEMS Microbiol. Letters. **71:**123-128.
12. **Droppo, I. G., D. T. Flannigan, G. G. Leppard, C. Jaskot, and S. N. Liss.** 1996. Floc stabilization for multiple microscopic techniques. Appl.Environ.Microbiol. **62:**3508-3515.
13. **Eberl, L., R. Schulze, A. Ammendola, O. Geisenberger, R. Erhart, C. Sternberg, S. Molin, and R. Amann.** 1997. Use of green fluorescent protein as a marker for ecological studies of activated sludge communities. FEMS Microbiol. Letters. **149:**77-83.
14. **Epping, E. H. G., and B. B. Jørgensen.** 1996. Light enhanced oxygen respiration in benthic phototrophic communities. Mar.Ecol.Prog.Ser. **139:**193-203.
15. **Fossing, H., and B. B. Jørgensen.** 1989. Measurement of bacterial sulfate reduction in sediments: evaluation of a single-step chromium reduction method. Biogeochem. **8:**205-222.
16. **Goronszy, M. C., G. Demoulin, and M. Newland.** 1996. Aerated denitrification in full-scale activated sludge facilities. Wat.Sci.Tech. **34:**487-491.
17. **Goronszy, M. C., G. Demoulin, and M. Newland.** 1997. Aerated denitrification in full-scale activated sludge facilities. Wat.Sci.Tech. **35:**103-110.
18. **Gray, N. F.** 1990. Activated sludge. Theorie and practice. Oxford University Press, Oxford.
19. **Griebe, T.** 1991. Ph.D. thesis University of Hamburg, Hamburg, Germany.
20. **Hao, X., H. J. Doddema, and J. W. van Groenestijn.** 1997. Conditions and mechanisms affecting simultaneous nitrification and denitrification in a Pasveer oxidation ditch. Biores. Technol. **59:**207-215.
21. **Jørgensen, B. B., and D. J. Des Marais.** 1990. The diffusive boundary layer of sediments: oxygen microgradients over a microbial mat. Limnol.Oceanogr. **35:**1343-1355.
22. **Juretschko, S., G. Timmermann, M. Schmidt, K.-H. Schleifer, A. Pommerening-Röser, H.-P. Koops, and M. Wagner.** 1998. Combined molecular and conventional analysis of nitrifying bacterial diversity in activated sludge: *Nitrosococcus mobilis* and *Nitrospira*-like bacteria as dominant populations. Appl.Environ.Microbiol. **64:**3042-3051.
23. **Kühl, M., R. N. Glud, H. Ploug, and N. B. Ramsing.** 1996. Microenvironmental control of photosynthesis and photosynthesis-coupled respiration in an epilithic cyanobacterial biofilm. J.Phycol. **32:**799-812.
24. **Kühl, M., and B. B. Jørgensen.** 1992. Microsensor measurement of sulfate reduction and sulfide oxidation in compact microbial communities of aerobic biofilms. Appl.Environ.Microbiol. **58:**1164-1174.

25. **Kühl, M., C. Steuckart, G. Eickert, and P. Jeroschewski.** 1998. A H_2S microsensor for profiling biofilms and sediments: application in an acidic lake sediment. Aquat.Microb.Ecol. **15:**201-209.
26. **Lens, P. N., M.-P. de Poorter, C. C. Cronenberg, and W. H. Verstraete.** 1995. Sulfate reducing and methane producing bacteria in aerobic wastewater treatment systems. Wat.Res. **29:**871-880.
27. **Li, D., and J. J. Ganczaczyk.** 1989. Fractal geometry of particle aggregates generated in water and wastewater treatment process. Environ. Sci. Technol. **23:**1385-1389.
28. **Li, D., and J. Ganczarczyk.** 1991. Size distribution of activated sludge flocs. J.WPCF. **63:**806-814.
29. **Li, Y. H., and S. Gregory.** 1974. Diffusion of ions in sea water and in deep-sea sediments. Geochim.Cosm.Acta. **38:**703-714.
30. **Lide, D. R.** (ed.). 1992. CRC Handbook of chemistry and physics, 73 ed. CRC Press, Boca Raton.
31. **Lloyd, D., L. Boddy, and K. J. P. Davies.** 1987. Persistence of bacterial denitrification capacity under aerobic conditions: the rule rather than the exception. FEMS Microbiol.Ecol. **45:**185-190.
32. **Logan, B. E., and J. R. Hunt.** 1988. Bioflocculation as a microbial response to substrate limitations. Biotech.Bioeng. **31:**91-101.
33. **Logan, B. E., and D. B. Wilkinson.** 1990. Fractal geometry of marine snow and other biological aggregates. Limnol.Oceanogr. **35:**130-136.
34. **Manz, W., M. Eisenbrecher, T. R. Neu, and U. Szewzyk.** 1998. Abundance and spatial organization of Gram-negative sulfate-reducing bacteria in activated sludge investigated by in situ probing with specific 16S rRNA targeted oligonucleotides. FEMS Microbiol.Ecol. **25:**43-61.
35. **McCready, R. G. L., W. D. Gould, and F. D. Cook.** 1983. Respiratory nitrate reduction by *Desulfovibrio* sp. Arch.Microbiol. **135:**182-185.
36. **Muyzer, G., T. Brinkhoff, U. Nübel, C. M. Santegoeds, H. Schäfer, and C. Wawer.** 1998. Denaturing gradient gel electrophoresis (DGGE) in microbial ecology, p. 1-27. *In* A. D. L. Akkermans, J. D. van Elsas, and F. J. de Bruijn (eds.), Molecular microbial ecology manual, 3rd ed, vol. 3.4.4. Kluwer Academic Publishers, Dordrecht, The Netherlands.
37. **Nielsen, L. P.** 1992. Denitrification in sediment determined from nitrogen isotope pairing. FEMS Microbiol.Ecol. **86:**357-362.
38. **Nielsen, P. H., and K. Keiding.** 1998. Disintegration of activated sludge flocs in presence of sulfide. Wat.Res. **32:**313-320.
39. **Patureau, D., N. Bernet, and R. Moletta.** 1997. Combined nitrification and denitrification in a single aerated reactor using the aerobic denitrifier *Comamonas* sp. strain SGLY2. Wat.Res. **31:**1363-1370.
40. **Ploug, H., and B. B. Jørgensen.** 1999. A net-jet flow system for mass transfer and microsensor studies of sinking aggregates. Mar.Ecol.Prog.Ser. **176:**279-290.
41. **Ploug, H., M. Kühl, B. Buchholz-Cleven, and B. B. Jørgensen.** 1997. Anoxic aggregates - an ephemeral phenomenon in the pelagic environment? Aquat.Microb.Ecol. **13:**285-294.
42. **Revsbech, N. P.** 1989. An oxygen microelectrode with a guard cathode. Limnol.Oceanogr. **34:**474-478.
43. **Revsbech, N. P., B. Madsen, and B. B. Jørgensen.** 1986. Oxygen production and consumption in sediments determined at high spatial resolution by computer simulation of oxygen microelectrode data. Limnol.Oceanogr. **31:**293-304.
44. **Risgaard-Petersen, N., and S. Rysgaard.** 1995. Nitrate reductionin sediments and waterlogged soil measured by 15N techniques, p. 287-295. *In* K. Alef and P. Namijaeri (eds.), Methods in Applied SOil Microbiology and Biochemistry. Academic Press.
45. **Robertson, L. A., R. Cornelisse, P. de Vos, R. Hadioetomo, and J. G. Kuenen.** 1989. Aerobic denitrification in various heterotrophic nitrifiers. Antonie van Leeuwenhoek. **56:**289-299.
46. **Santegoeds, C. M., T. G. Ferdelman, G. Muyzer, and D. de Beer.** 1998. Structural and functional dynamics of sulfate-reducing populations in bacterial biofilms. Appl.Environ.Microbiol. **64:**3731-3739.
47. **Sedlak, R.** 1991. Phosphorus and nitrogen removal from municipal wastewater. Principle and prectice, 2nd ed. Lewis publishers, Boca Raton, FL.
48. **Tambo, N., and Y. Watanabe.** 1979. Physical characteristics of flocs 1: The floc density function and aluminum floc. Wat.Res. **13:**409-419.

49. **Teske, A., C. Wawer, G. Muyzer, and N. B. Ramsing.** 1996. Distribution of sulfate-reducing bacteria in a stratified fjord (Mariager Fjord, Denmark) as evaluated by most-probable-number counts and denaturing gradient gel electrophoresis of PCR-amplified ribosomal DNA fragments. Appl.Environ.Microbiol. **62:**1405-1415.
50. **Verstraete, W., and E. van Vaerenbergh.** 1986. Aerobic activated sludge, p. 43-112. *In* W. Schönborn (ed.), Microbial Degradations, 1st ed, vol. 8. VCH, Weinheim, Germany.
51. **Von Münch, E., P. Lant, and J. Keller.** 1996. Simultaneous nitrification and denitrification in bench-scale sequencing batch reactors. Wat.Res. **30:**277-284.
52. **Wagner, M., R. Amann, H. Lemmer, and K.-H. Schleifer.** 1993. Probing activated sludge with oligonucleotides specific for proteobacteria: inadequacy of culture-dependent methods for describing microbial community structure. Appl.Environ.Microbiol. **59:**1520-1525.
53. **Wagner, M., A. M. Roger, J. L. Flax, G. A. Brusseau, and D. A. Stahl.** 1998. Phylogeny of dissimilatory sulfite reductases supports an early origin of sulfate respiration. J.Bacteriol. **180:**2975-2982.
54. **Wanner, J.** 1994. Activated slufge bulking and foaming control. Technomic Publishing Company, Lancaster.
55. **Widdel, F., and F. Bak.** 1992. Gram-negative mesophilic sulfate-reducing bacteria, p. 3352-3378. *In* A. Balows, H. G. Trüper, M. Dworkin, W. Harder, and K.-H. Schleifer (eds.), The Prokaryotes, 2nd ed. Springer Verlag, New York.
56. **Wimpenny, J. W.** 1969. Oxygen and carbon dioxide as regulators of microbial growth and metabolism, p. 161-198. *In* P. M. Meadow and S. J. Pirt (eds.), Microbial Growth. Cambridge University Press, Cambridge.
57. **Wistrom, A. O., and E. D. Schroeder.** 1996. Enhanced nutrient removal by limiting dissolved oxygen concentration in a continously fed, intermittently decanted, activated sludge plant. Environ. Technol. **17:**371-380.
58. **Zietz, U.** 1995. The formation of sludge bulking in the activated sludge process. Eur. Water Pollut.Contr. **5:**21-27.

Chapter 6

Distribution of sulfate reducing and methanogenic bacteria in UASB aggregates determined by microsensor and molecular analysis

Cecilia M. Santegoeds[1], Lars Riis Damgaard[2], Gijs Hesselink[3], Jakob Zopfi[1], Piet Lens[4], Gerard Muyzer[5], and Dirk de Beer[1]

[1] Max Planck Institute for Marine Microbiology, D-28359 Bremen, Germany.
[2] Dept. of Microbial Ecology, Institute of Biology, DK-8000 Aarhus C, Denmark.
[3] Paques Bio Systems BV, 8560 AB Balk, Netherlands.
[4] Sub-department of Environmental Technology, Wageningen Agricultural University, 6700 EV Wageningen, Netherlands.
[5] Netherlands Institute for Sea Research, 1790 AB Den Burg, Netherlands.

This chapter is submitted to Applied and Environmental Microbiology.

ABSTRACT

Using molecular techniques (DGGE and FISH analysis) and microsensors for H_2S and CH_4, we studied the population structure of and the activity distribution in anaerobic aggregates. The aggregates originated from three different types of UASB reactors: a methanogenic reactor where mainly methane was produced, a methanogenic/sulfidogenic reactor with methane as well as sulfide production and a sulfidogenic reactor where mainly sulfide was formed. Microsensor measurements in methanogenic/sulfidogenic aggregates revealed that the activity of sulfate reducing bacteria (2-3 mmol S^{2-}_{tot} m^{-3} s^{-1}) was located at the granular surface in a layer of 50 - 100 µm thickness. The sulfidogenic aggregates contained a wider zone of sulfate reducing bacteria (the first 200 - 300 µm from the aggregate surface) with a higher activity (1-6 mmol S^{2-}_{tot} m^{-3} s^{-1}). The methanogenic aggregates did not show any sulfate reducing activity. Methanogenic activity in the methanogenic/sulfidogenic aggregates and the methanogenic aggregates (1-4 mmol CH_4 m^{-3} s^{-1}) was located more inward, starting at ca. 100 µm distance from the aggregate surface. The methanogenic activity was not affected by the addition of 10 mM sulfate during the CH_4 microprofile measurements. The measured sulfidogenic and methanogenic activities were independent of the type of electron donor (acetate, propionate, ethanol or hydrogen) at the concentrations applied, although the populations metabolizing these substrates were located in different zones in the sulfidogenic aggregates. Molecular analysis of the aggregates showed that the localization of the anaerobic populations corresponded to the microsensor data. A distinct layered structure was found for the methanogenic/sulfidogenic aggregates, with sulfate reducing bacteria in a compact outer shell of 50-100 µm thickness, methanogens in the inner part and *Eubacteria* (some of them hybridizing with a probe specific for syntrophic bacteria) filling the gap between sulfate reducing and methanogenic bacteria. The structure of the methanogenic and sulfidogenic aggregates was more loose. In the methanogenic aggregates, only a few cells of sulfate reducing bacteria, present in the outer layers, could be detected, whereas methanogens were spread over the core of these aggregates. Sulfate reducing bacteria were mainly present in the outer 100 µm of the sulfidogenic aggregates, but were also present more inward in these aggregates. The methanogens were distributed over the inner part of the sulfidogenic aggregates in clusters with syntrophic bacteria.

INTRODUCTION

Methanogenic and sulfidogenic granular sludge consists of rigid, well settling microbial aggregates that develop by the mutual attachment of bacterial cells in the absence of a carrier material (28). They contain a variety of bacterial species involved in the anaerobic degradation of organic matter, including hydrolytic, fermentative, acidogenic, acetogenic, homoacetogenic, sulfate reducing and methanogenic bacteria. These aggregates develop spontaneously in wastewater treatment systems of the Upflow Anaerobic Sludge Bed (UASB) reactor design under a variety of operation conditions (28).

The formation, composition and functioning of UASB granules, has been investigated by means of a variety of analytical techniques (59). To characterize the bacterial species present, various types of activity tests, in combination with molecular, microbial and physiological assays, have been applied on granular sludge samples (containing many aggregates) as well as on individual granules (59). The spatial distribution of the bacterial species present within UASB aggregates has been studied using light, electron and laser scanning microscopy on either intact or sectioned individual aggregates (31). Based on these observations, conceptual models have been postulated to describe the distribution of acidogens, syntrophic and methanogenic bacteria within UASB aggregates (12, 14, 31). These models proposed a multi-layered structure with hydrogen consuming bacteria located at the outside of the aggregate, methanogens in the inner part, and hydrogen producing bacteria between the two layers.

Using the same analytical techniques, however, a homogeneous distribution of the different populations present in UASB granules has been reported as well (13). The use of molecular techniques has been particularly useful for the identification and localization of the different microbial populations present in methanogenic granular sludge. Slot/dot blot hybridization of the 16S rRNA extracted from granules allow to both identify and quantify the methanogenic, syntrophic and sulfate reducing populations (40, 42, 46). The application of fluorescent *in situ* hybridization (FISH) with specific probes for a bacterial species or population further allows their detection and localization within granular sludge (16, 52). Using the FISH technique, different layered population structures have been described in different UASB aggregates cultivated on different substrates (15, 16, 52).

Although these investigations considerably improved our understanding of the granular sludge composition and anatomy, there is still a lack of knowledge about the distribution of microbial activities within granular sludge. Population distributions determined by molecular probes do not necessarily correspond to microbial activity distributions, as bacterial populations can be dormant or express different activities. Activity distributions in anaerobic granular sludge are poorly documented, since *in situ* activity measurements require specific analytical tools, e.g. microsensors. The activity distribution of fermentative and methanogenic populations in UASB aggregates has been studied using miniaturized sensors for pH and glucose (10, 26, 27). Measurements of the local pH and glucose concentration with a μm resolution indicated an inhomogenic activity distribution, with acetogenic and methanogenic activity being predominantly located in, respectively, the outer layer (150-200 μm) and the center of the aggregates investigated (27).

The population dynamics between sulfate reducing (SRB) and methanogenic (MB) bacteria are another crucial factor governing the metabolic properties of granular sludge. Their dynamics have been studied in detail using molecular techniques (40, 42, 46), but their *in situ* activity distribution have, to the best of our knowledge, not yet been reported. Recently, two novel microsensors, i.e. a CH_4 biosensor (8) and a H_2S microsensor (19), have been developed to study the microbial ecology of sediments. In this paper, both microsensors were used to determine the *in situ* methanogenic and sulfate reducing activity, respectively, in UASB aggregates. These localized activity measurements were combined with molecular techniques to analyze on a microscale the structure, population (sulfate reducing, methanogenic and syntrophic bacteria) and activity distribution of three different types of UASB aggregates with a different degree of sulfate reducing activity.

MATERIALS AND METHODS

Aggregates. Aggregates were retrieved from three different UASB reactors. The methanogenic/sulfidogenic aggregates originate from a UASB reactor, treating wastewater from a potato processing plant (Leusden, Belgium). These aggregates were subcultured in the laboratory for several months at 30°C by batch-wise feeding twice a week. The feed (pH 6-7) contained a volatile fatty acids (VFA) mixture (13.8 mM acetate, 4.7 mM propionate and 2.3 mM butyrate), supplemented with 20 mM $NaSO_4$, 4 mM NH_4Cl, 0.32 mM $NaHPO_4$, 0.2 mM $MgCl_2$ and trace elements. Methanogenic aggregates were obtained from a UASB reactor in the Netherlands, treating paper mill wastewater (Eerbeek, the Netherlands). These aggregates were subcultured in the laboratory for three months at 30°C by batch-wise feeding three times a week. The feed (pH 7) contained a VFA mixture (6.25 mM acetate, 7.15 mM propionate and 5.00 mM butyrate), supplemented with 5.2 mM $(NH_4)Cl$, 10.2 mM NaH_2PO_4, 6.8 mM K_2HPO_4, 0.45 mM $MgSO_4.7H_2O$, 0.04 mM $CaCl_2$ and trace elements. Sulfidogenic aggregates were sampled directly from a full scale UASB reactor treating ethanol (12 mM) and sulfate (7 mM) containing wastewater (pH 7-7.5, 30-35°C) at Emmen (the Netherlands).

All types of aggregates had a typical diameter between 1 and 2 mm. The methanogenic and methanogenic/sulfidogenic aggregates had a regular spherical shape, whereas the sulfidogenic aggregates had a more loose, irregular shape.

Microsensor measurements. For microsensor measurements, aggregates were attached to insect needles in a flow cell at 30°C. The medium in the cell was kept anaerobic through continuous bubbling with N_2 or argon, which resulted in circulation and mixing of the medium. Anaerobicity was checked with an oxygen microsensor (47). Before measurements, the aggregates were pre-incubated one day in the measurement medium. The latter consisted of 5.2 mM $(NH_4)Cl$, 10.2 mM NaH_2PO_4, 6.8 mM K_2HPO_4, 0.45 mM $MgCl_2$, 0.04 mM $CaCl_2$ plus micronutrients at pH 7.0 for the methanogenic/sulfidogenic and methanogenic aggregates. The measurement medium for the sulfidogenic aggregates contained 0.19 mM $(NH_4)Cl$ and 10 mM KH_2PO_4 at pH 7.2. During the microsensor measurements the media were supplemented with different concentrations of sodium-acetate, sodium-propionate, ethanol, hydrogen and sulfate. The pH of the media and also in the aggregates was constant due to the phosphate buffer present in the measurement media. This was checked by recording pH microprofiles in the aggregates with pH microelectrodes (48).

Microsensors, mounted on micromanipulators, were positioned at the aggregate surface by means of a dissection microscope. Profiles were recorded by penetrating the aggregate with the microsensor using the micromanipulator in steps of 50 or 100 µm.

Hydrogen sulfide microsensors. The sulfide concentration profiles within the aggregates were measured with H_2S microsensors (19, 25) with a tip diameter of ca. 10 µm and a 90% response time of < 0.5 seconds. The microsensors were calibrated at 30°C by measuring the signal in dilution series of a standard solution, consisting of sulfide dissolved in strongly buffered medium with constant pH and flushed with nitrogen to avoid sulfide oxidation (24). The concentration of total dissolved sulfide ($H_2S+HS^-+S^{2-}$) in the dilution series was determined by a spectrophotometric method (6). The total

dissolved sulfide measured in the aggregate could then be calculated using the slope and intercept of the calibration curves. Since the sensor was calibrated in medium of the same pH as the measuring medium and the aggregate, no pH correction was necessary. The sulfide electrode had a linear response to H_2S concentrations up to 1000 µM. The detection limit of the microsensors varied between 1 - 3 µM total sulfide.

Methane microsensors. Methane microsensors were constructed and inoculated with the methane oxidizing bacterium *Methylosinus trichosporium* (8). Microsensor tip diameters were 25 - 30 µm and 90% response times were 30 to 100 seconds. As all measurements were performed under anoxic conditions, an oxygen scavenging guard capillary (9) was not applied. Calibrations were performed at 30°C by recording the microsensor signal when exposing the sensor tip to a range of N_2 and CH_4 gas mixing ratios (9). Calibrations were performed before and after measurements and any baseline drift was corrected for in the data processing. Interference from H_2S, CO_2, and H_2 were investigated by exposing the sensor tip to known concentrations or mixing ratios of these compounds. The response to sulfide was 25% of the response to an equal concentration of methane. Therefore, corrections of the methane profile were made by subtracting 25% of the corresponding sulfide concentration, as measured with the sulfide microsensor. There was no significant CO_2 response of the sensor. Occasionally, methane biosensors exhibit a response to H_2 in the same order as the methane response due to culture contamination, but as H_2 microsensor measurements showed H_2 concentrations below 5 µM in the aggregates, the H_2 interference was insignificant. Methane profiles could only be measured in the methanogenic/sulfidogenic and the methanogenic aggregates as no methane biosensor was available at the time of the measurements with the sulfidogenic aggregates.

Diffusivity microsensors. Microscale diffusivity sensors with a diameter of approximately 70 µm were constructed (49). Acetylene was used as the tracer substance instead of hydrogen (7) as H_2 metabolism inside the aggregates would interfere with the diffusivity measurements. A two-point calibration in agar and glass beads (49) was performed before the diffusivity sensor was motor-propagated in steps of 100 µm into the aggregate. The spatial resolution of a diffusivity sensor depends on the sensor diameter and was approximately a few hundred microns with this sensor. Thus, the measurements could not provide a detailed spatial distribution of diffusivity within the aggregate. Therefore, the stable readings in the center of the aggregate were taken to represent the entire aggregate.

Flux and activity calculations. Diffusive fluxes were calculated using Fick's first law:

$$J_n = -D\frac{\mathrm{d}C_n}{\mathrm{d}r_n} = -D\frac{C_{n+1} - C_{n-1}}{r_{n+1} - r_{n-1}}$$

with: J_n = flux at point n (mmol m^{-2} s^{-1}), D = molecular diffusion coefficient (m^2 s^{-1}), $\frac{\mathrm{d}C_n}{\mathrm{d}r_n}$ = concentration gradient at point n (mmol m^{-3} m^{-1}), C = substrate concentration (mmol m^{-3}), and r = distance from the aggregate center. The molecular diffusion coefficient for oxygen in water at 30°C is

2.75 x 10^{-9} m^2 s^{-1} (4). The molecular diffusion coefficients for methane and sulfide can be determined by multiplying this value for oxygen with 0.8495 and 0.7573, respectively (4), yielding a molecular diffusion coefficient of 2.34 x 10^{-9} m^2 s^{-1} for methane and 2.08 x 10^{-9} m^2 s^{-1} for total sulfide. The effective diffusion coefficient of these compounds within the aggregates can be calculated by correcting these values with the ratio of the diffusivity in aggregates and in water, as determined by diffusivity microsensor measurements (see above). The rate (R) of methanogenesis and sulfate reduction (mmol m^{-3} s^{-1}) inside the aggregate at point n was calculated with the following formula:

$$R_n = \frac{4\pi r_{n+1}^{\ 2} * J_{n+1} - 4\pi r_{n-1}^{2} * J_{n-1}}{\frac{4}{3}\pi r_{n+1}^{\ 3} - \frac{4}{3}\pi r_{n-1}^{3}} = 3 * \left(\frac{r_{n+1}^{\ 2} * J_{n+1} - r_{n-1}^{2} * J_{n-1}}{r_{n+1}^{\ 3} - r_{n-1}^{3}} \right)$$

Aggregate fixation and slicing. Aggregate samples for *in situ* hybridization analysis were fixed by over night incubation in paraformaldehyde (4% [w/v] in phosphate-buffered saline [PBS]) at 4°C and subsequently washed in PBS. After fixation, aggregates were embedded for ca. 12 hours in embedding medium (OCT compound; Sakura Finetek USA, Torrance, California) and frozen at -20°C. Thin sectioning of the aggregates was performed with a cryomicrotome (Microm HM 505 E) at -18°C. The vertical slices of about 10 µm thickness were collected on gelatin-coated microscopic slides. The slides were air dried and dehydrated in a series of increasing ethanol concentration (50, 80 and 96% [v/v]).

Nucleic acid extraction and PCR amplification. DNA and RNA was extracted from the aggregates by a combined bead beating (2 min at maximum speed with 0.75-1.0 mm glass beads), lysis (10 mg/ml lysosyme for 1 h at 37°C, 1% [w/v] sodium dodecyl sulfate and 0.25 mg/ml protinase K for 30 min at 55°C) and hot phenol-chloroform-isoamyl alcohol treatment (57). The ribosomal DNA was enzymatically amplified as described by Muyzer (35), using the eubacterial primer GM5F with GC-clamp and the universal primer 907R (Table 1). The ribosomal RNA was amplified according to Teske (57). A hot-start, touch-down PCR program was used for all amplifications to minimize non-specific amplification (35).

DGGE analysis of 16S rDNA fragments. DGGE was performed using the D-Gene system (BioRad) and the following specifications: 1x TAE (40 mM Tris, 20 mM acetic acid and 1 mM EDTA at pH 8.3), 1 mm thick gels, a denaturant gradient from 35% to 65% urea/formamide, a temperature of 60°C, and a constant voltage of 100V for 17 hours (35, 36). DGGE gels were photographed on a UV transillumination table (302 nm) with a Polaroid camera. Photos were scanned and inversed.

Blotting and hybridization analysis of DGGE gels. DGGE gels were blotted and hybridized with group specific probes for sulfate reducing bacteria as described previously (50). The probes used (Table 1) were probe 660 (specific for *Desulfobulbus* species), 687 (targeting *Desulfovibrio* species as well as some members of the *Geobacter*, *Desulfomonas*, *Desulfuromonas*, *Desulfomicrobium*, *Bilophila* and *Pelobacter* genus), and probe 804 (targeting *Desulfobacter*, *Desulfobacterium*, *Desulfosarcina*, *Desulfococcus* and *Desulfobotulus* species) developed by Devereux et al. (11).

TABLE 1. Oligonucleotide probes used for PCR amplification and (in situ) hybridization analyses.

Probe	Position[a]	Sequence, 5' → 3'	Target	Formamide (%)[b]	NaCl (mM)[c]
GM5F[d]	341-357	CCTACGGGAGGCAGCAG	Bacteria (36)	-[e]	-[e]
907R	907-928	CCGTCAATTCCTTTGAGTTT	All organisms (universal probe) (36)	-	-
ARC915	915-934	GTGCTCCCCCGCCAATTCCT	*Archaea* (55)	40	
EUB338	338-355	GCTGCCTCCCGTAGGAGT	Bacteria (1)	20	225[f]
SRB385	338-355	CGGCGTCGCTGCGTCAGG	SRB of the delta proteobacteria (2) plus several Gram-positive bacteria (e.g. Clostridium) (45)	35	80[f]
DSV698	698-717	GTTCCTCCAGATATCTACGG	*Desulfovibrio* (33)	35	88
DSD131	131-148	CCCGATCGTCTGGGCAGG	*Desulfovibrio* (33)	20	250
DSV407	407-424	CCGAAGGCCTTCTTCCCT	*Desulfovibrio* (33)	50	31.2
DSV1292	1292-1309	CAATCCGGACTGGGACGC	*Desulfovibrio* (33)	35	88
DSV214	214-230	CATCCTCGGACGAATGC	*Desulfomicrobium* (33)	10	500
DSS658	658-678	TCCACTTCCCTCTCCCAT	*Desulfosarcina* (33)	60	15.6
DSB985	985-1004	CACAGGATGTCAAACCCAG	*Desulfobacter* (33)	20	250
DSBO224	224-242	GGGACGCGGACTCATCCTC	*Desulfobotulus* (33)	60	15.6
DSMA488	488-507	GCCGGTGCTTCCTTTGGCGG	*Desulfomonile* (33)	60	15.6
DSR651	651-668	CCCCCTCCAGTACTCAAG	*Desulforhopalus* (33)	35	88
221	221-240	TGCGCGGACTCATCTTCAAA	*Desulfobacterium* (11)	35	88
660	660-679	GAATTCCACTTTCCCCTCTG	*Desulfobulbus* (11)	60	15.6
687	687-702	TACGGATTTCACTCCT	*Desulfovibrio* (11) plus members of the genera *Geobacter*, *Desulfomonas*, *Desulfuromonas*, *Desulfomicrobium*, *Bilophila*, and *Pelobacter*	-	-
804	804-821	CAACGTTTACTGCGTGGA	*Desulfobacterium*, *Desulfobacter*, *Desulfococcus*, *Desulfosarcina*, *Desulfobotulus* (11)	-	-
MPOB	222-240	ACGCAGGCCCATCCCCGAA	syntrophic propionate-oxidizing strains MPOB (*Syntrophobacter fumaroxidans*) and KOPROP1 and *Desulforhabdus amnigenus* (although these last two strains have one mismatch with the probe) (16, 17)	20	900
NON338	338-355	ACTCCTACGGGAGGCAGC	none (negative control) (32)	0	900

[a] Position in the 16S rRNA of *Escherichia coli* (5).

[b] Formamide concentration in hybridization buffer.

[c] Sodium chloride concentration in washing buffer.

[d] This primer has the following GC-clamp at the 5' end 5'- CGCCCGCCGCGCCCCGCGCCCGTCCCGCCGCCCCCGCCCG-3'.

[e] Probe not used for FISH.

[f] Plus 5 mM EDTA in washing buffer.

Excision and amplification of DGGE bands. DGGE bands were carefully excised on a UV transillumination table with a scalpel and transferred to a 1.5 ml tube with 500 µl water and approximately 500 ml glass beads of 0.75-1.0 mm diameter. The acrylamide bands were disrupted by bead beating at maximum speed twice for 1 min. The samples were left overnight at 4°C and the DNA was subsequently amplified by adding 1-10 µl of the samples' supernatant to the PCR mixture. The PCR was then performed as described above. A second DGGE was run to confirm that the amplified bands had the same position in the gel as the excised bands. Prior to sequencing, the PCR products were purified using the QIAquick PCR purification kit (Qiagen Inc.).

Sequencing and phylogenetic analysis. Amplified DGGE bands were sequenced using the Applied Biosystems PRISM Dye Terminator Cycle Sequencing Ready reaction kit supplied with Ampli*Taq* DNA polymerase. The sequencing products were analyzed with the Applied Biosystems 377 DNA sequencer. The partial sequences were added to the 16S rRNA parsimony tree of the Technical University of Munich using the program package ARB (56).

In situ hybridization. The protocol described by Manz et al. (32) was used for fluorescence *in situ* hybridization (FISH) of the aggregate slices with probe ARC915 for *Archaea* bacteria (55), probe SRB385 for the detection of general sulfate reducers of the delta subdivision, probes 221 and 660 for group specific SRB (Devereux et al. (11)), the probes DSV698, DSD131, DSV407, DSV1292, DSV214, DSS658, DSB985, DSBO224, DSMA488, DSR651 developed by Manz et al. (33) and probe NON338 as a negative control (Table 1). The probe MPOB described by Harmsen et al. (16) was used for detection of syntrophic bacteria (Table 1).

The probes were synthesized and labeled with a hydrophilic sulfoindocyanine dye CY3 or CY5 by Interactiva GmbH (Ulm, Germany). The hybridization buffer contained 0.9 M NaCl, a percentage (v/v) of formamide shown in Table 1, 20 mM Tris-HCl (pH 7.4) and 0.01% (w/v) SDS. The probe concentrations were 5 ng/µl. Hybridization was performed for 1 - 2 hours at 46°C. The aggregate slices were washed at 48°C for 15 min in a washing buffer containing 20 mM Tris-HCl (pH 7.4), 0.01% (w/v) SDS and a concentration of NaCl as mentioned in Table 1. The specimens were microscopically examined with a Zeiss LSM 510 confocal laser scanning microscope (Carl Zeiss, Jena, Germany), equipped with two HeNe lasers (543 nm, 633 nm). The hybridizations shown in the figures are representative for several independent hybridizations on several aggregates.

Sulfur analysis. For sulfur (elemental sulfur and polysulfide) determination 3 to 5 aggregates with a diameter of about 1.5 mm were put into a reaction tube and immediately fixed with 20 µl $ZnCl_2$ (2%). During this treatment, the polysulfide is converted to elemental sulfur. Elemental sulfur was extracted by shaking the samples with pure methanol (HPLC grade) for 6 hours. Identification and quantification of zerovalent sulfur was performed by high performance liquid chromatography (HPLC) using a Sykam S1100 pump (Gilching, Germany), a Zorbax ODS-column (125x4 mm, 5 µm; Knauer, Germany) and an Sykam S3000 UV-detector (265 nm). A mixture of 0.25% acetic acid (pH 4) and 100% methanol (10/90 v/v) was used as eluent, the flow rate was 1.2 ml/min. Under these conditions elemental sulfur eluted as cyclo-octasulfur (S_8) at 5.4 min. The precision for repeated injection of a 100 µM S^0-standard was 0.5% s.d. (n=8), the detection limit was about 1 µM. A second method was applied to confirm the identity of elemental sulfur in the aggregate, based on the reaction of S^0 with SO_3^{2-} according to the following simplified equation: $S^0 + SO_3^{2-} \Rightarrow S_2O_3^{2-}$ (22). A few aggregates were incubated with 1 ml 5% Na_2SO_3-solution for 2 hours at 90°C after fixation with $ZnCl_2$, followed by methanol extraction and HPLC analysis as described above. As an extra control, the presence or absence (after the sulfite treatment) of elemental sulfur in the methanol extracts was also confirmed by UV-spectroscopy.

RESULTS

Diffusivity measurements. Diffusivity microsensor measurements in the methanogenic-sulfidogenic aggregates showed that the diffusivity decreased by 50% when shifting from the water phase into the aggregate. Inside the aggregate, the diffusivity remained approximately constant at the resolution of the diffusivity microsensor. For the flux and activity calculations, this 50% ratio was used to calculate the apparent diffusion coefficients of methane and sulfide. Thus, the following diffusivity values were used in the calculations: 1.17×10^{-9} m^2 s^{-1} for methane and 1.04×10^{-9} m^2 s^{-1} for total sulfide.

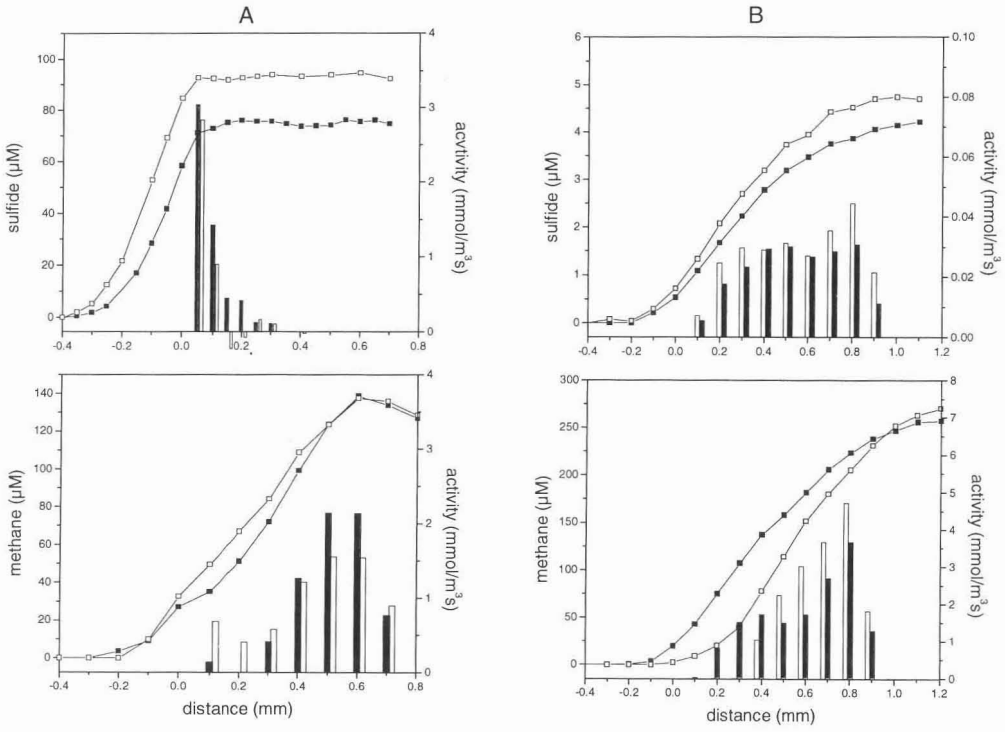

Fig. 1. Sulfide and methane microsensor profiles (lines) and activity values (bars) in methanogenic/sulfidogenic (A) and methanogenic (B) aggregates in the presence (□, open bars) and the absence (■, closed bars) of sulfate. No external electron donor was supplied during the measurements. The aggregates surface is at distance = 0 mm, the center of the aggregates is approximately at distance = 0.9 mm.

Endogeneous sulfide and methane microprofiles. In all methanogenic/sulfidogenic (Fig. 1A), methanogenic (Fig. 1B) and sulfidogenic (Fig. 2A) aggregates, endogenous sulfide production was measured in the absence of sulfate, even after one night's incubation in a sulfate- and electron donor-free medium. In addition, also endogeneous methane production was observed in the methanogenic-

sulfidogenic and methanogenic aggregates (Fig. 1). The addition of up to 10 mM sulfate significantly increased the sulfide production, without affecting the methane production in the methanogenic/sulfidogenic aggregates (Fig. 1A). In the methanogenic aggregates, only a negligible amount of sulfide (< 6 μM) was measured which, like the methanogenic activity, was not affected by the presence or absence of sulfate (Fig. 1B). Analysis of the sulfur content of all three types of aggregates revealed the presence of high amounts of elemental sulfur and/or polysulfide (up to 59 nmol mm^{-3}) inside the aggregates (Table 2).

TABLE 2. Characteristics and activities of the different aggregates used in this study.

	Sulfidogenic	**Methanogenic/sulfidogenic**	**Methanogenic**
Growth conditions			
Original substrate	Ethanol	Potato starch wastewater	Paper mill wastewater
Subculture medium	Not applicable	VFA mixture	VFA mixture
Sulfate conc. during subculturing (mM)	7	20	0.45
Average activity values[a] ($mmol\ m^{-3}s^{-1}$)			
Methane production	not determined	1 - 2	2 – 4
Sulfide production	1 – 6	2 - 3	0.02 - 0.06
Sulfur[b] concentration inside aggregates ($nmol/mm^3$)	ca. 28	ca. 21	ca. 59

[a] Calculated from the microprofile measurements
[b] Elemental sulfur and polysulfide

Microprofiles after addition of substrates. The production of methane and sulfide were stimulated when volatile fatty acids (acetate, propionate and/or butyrate), ethanol or hydrogen were added to the medium (Fig. 2). The sulfidogenic sludge, fed ethanol for more than one year, was also able to metabolize both hydrogen and acetate (Fig. 2A). The sulfide microprofiles in the sulfidogenic aggregates developed almost instantaneous upon switching from argon to H_2 gas. Although the sulfide production rates in the presence of hydrogen were comparable to that in the presence of ethanol, Fig. 2A shows that both substrates were consumed in a distinctly different zone within the aggregate. The predominant sulfidogenic activities with the substrates hydrogen and ethanol were located in the outer 200 μm and a layer located between 200-400 μm from the aggregate surface, respectively. Also sulfidogenesis with acetate as the substrate was mainly located in the outer 200 μm of the aggregate. Acetate was metabolized with a specific sulfidogenic activity half of that with ethanol as the substrate (Fig. 2A).

The addition of acetate as well as propionate resulted in sulfidogenic activity in the outer 100-150 μm of the methanogenic/sulfidogenic aggregates. These substrates also caused methanogenic activity, which only started from 300 μm onwards inside the aggregate. Interestingly, the addition of propionate resulted in a significant methane production in the core of the methanogenic/sulfidogenic aggregates (Fig. 2B). Sulfate reduction was not affected when methanogenic/sulfidogenic aggregates were supplied with 1 mM nitrate (data not shown).

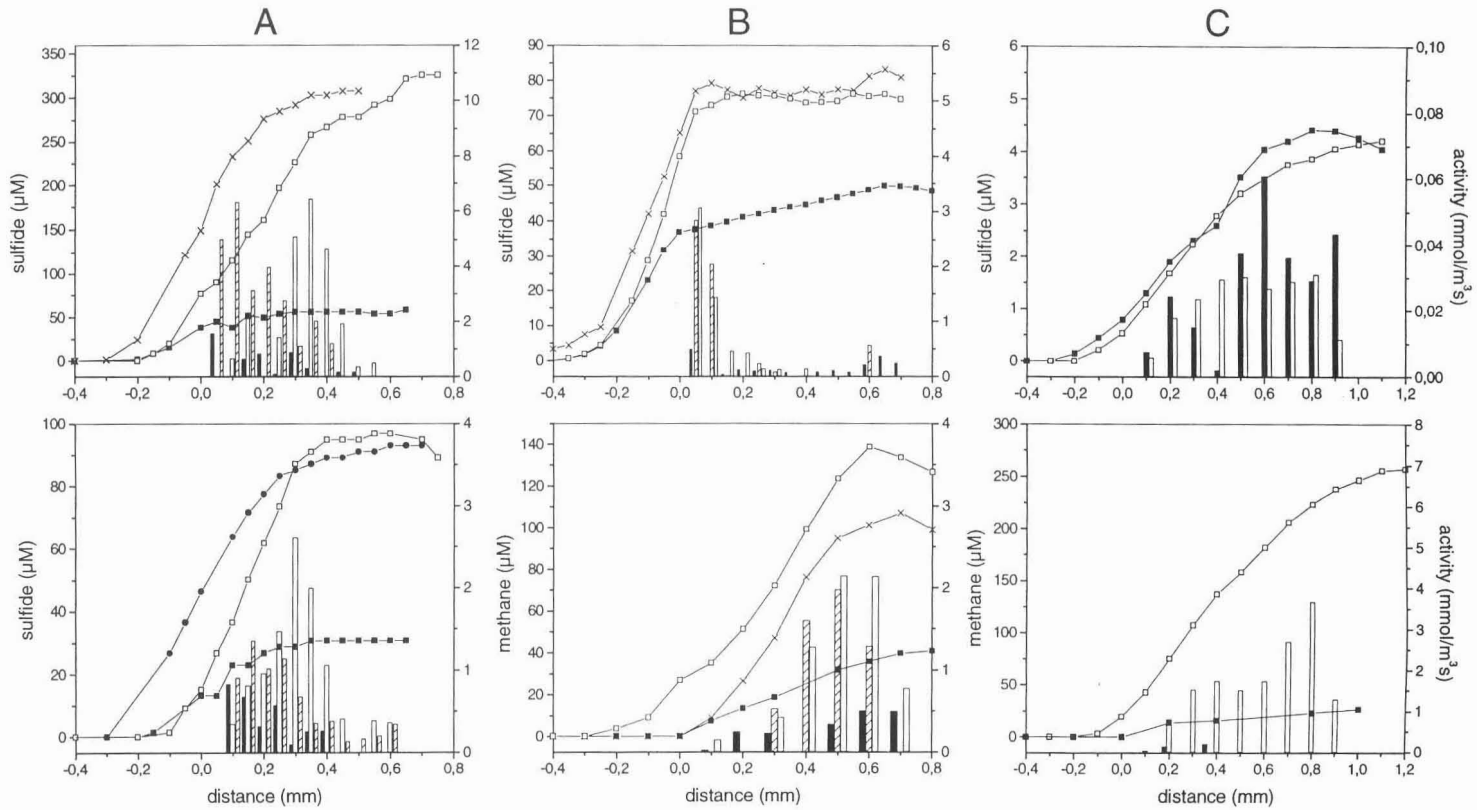

Fig. 2. Steady state microsensor profiles (lines) and activity values (bars) of sulfide and methane in aggregates in the presence of 10mM SO_4^{2-}. (A) Sulfidogenic aggregate after one night without electron donor (■, closed bars), with addition of 7 mM ethanol (□, open bars), saturation with hydrogen (x, crossed bars) and with addition of 7 mM acetate (●, shaded bars). (B) Methanogenic/sulfidogenic aggregate after one night without electron donor (■, closed bars), with addition of 1 mM acetate (x, shaded bars), and 1 mM propionate (□, open bars). (C) Methanogenic aggregate after one night incubation without electron donor (■, closed bars), with addition of a VFA mixture (6 mM acetate, 7 mM propionate, and 5 mM butyrate; □, open bars). The aggregates surface is at distance = 0 mm, the center of the aggregate is approximately at a distance = 0.6 mm for the sulfidogenic aggregates (A) and at a distance = 0.9 mm for both the methanogenic/sulfidogenic (B) and methanogenic (C) aggregates. The profiles in the upper and lower part of graph A are obtained from two different sulfidogenic aggregates and were measured at different times.

The addition of the VFA mixture to the methanogenic aggregates did not affect the sulfide microprofile, but gave rise to a substantial methane production (Fig. 2C). The highest methanogenic activity was observed in the core of the aggregates. The addition of 50 mM BES completely inhibited the methane production in the methanogenic aggregates after 3.5 hours incubation (Fig. 3).

Activity profiles. Table 2 compares the average activity values for the three types of aggregates, derived from the profiles presented in Fig. 1-3. Fig. 2 shows the distribution of this activity within the aggregates. In the sulfidogenic aggregates, sulfide production occurs in a much larger zone compared to the methanogenic/sulfidogenic aggregates, but it is still restricted to the outer 200 - 300 μm of the granules (Fig. 2A). In the methanogenic/sulfidogenic aggregates, sulfide production was localized in the outer 50 - 100 μm, and no methane producing activity was detected within that outer 100 μm shell. Methane is produced deeper in the methanogenic aggregates, beyond 100 μm (Fig. 2B). Also in the methanogenic aggregates, methane is produced mainly in the core of the aggregate, starting at 200 μm from the surface (Fig. 2C).

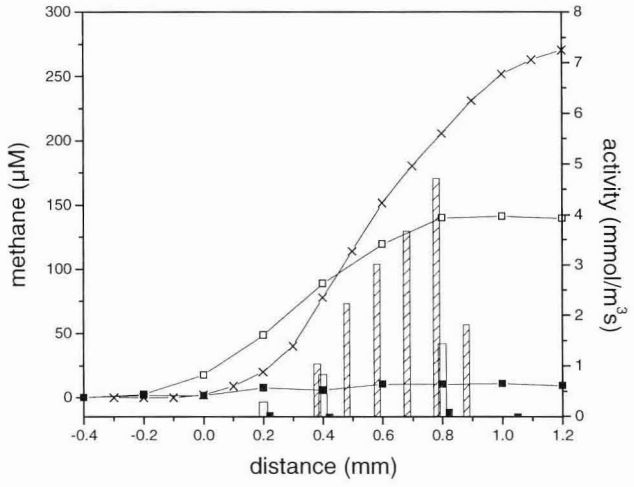

Fig. 3 Microsensor profiles (lines) and activity values (bars) in methanogenic aggregates of methane after addition of 50 mM BES at time = 0 (x, crossed bars), after 1 h 15 min (□, open bars), and after 3.5 h (■, closed bars). The aggregates surface is at distance = 0 mm, the center of the aggregate is approximately at distance = 0.9 mm from the surface.

Population analysis by DGGE. Denaturing gradient gel electrophoresis (DGGE) revealed that the three aggregates contained a different community composition on DNA level as well as on RNA level (Fig. 4). In all aggregates less cDNA bands (RT-PCR amplified 16S rRNA fragments) were seen than rDNA bands (PCR amplified 16S rDNA fragments). Blotting of DGGE gels and hybridization of these blots with group specific probes of SRB (660, 687, and 804) resulted for all samples in a positive hybridization signal with probe 687 (2-3 bands) and probe 660 (2-4 bands), but no hybridization was

obtained with probe 804 (data not shown), indicating the possible presence of *Desulfovibrio* and *Desulfobulbus* species.

11 bands were excised from the DGGE gel, from which 8 were successfully re-amplified and sequenced (numbers indicated in Fig. 4). The sequences were phylogenetically analyzed and depicted in a phylogenetic tree (Fig. 5). It was found that three of the DNA fragments resembled sequences of *Desulfovibrio* species (DGGE bands 2, 6 and 7), and one partial sequence (DGGE band 4) showed resemblance with the syntrophic bacteria *Syntrophobacter wolinii* and *Syntrophomonas wolfei*. The other 4 DNA fragments (DGGE bands 1, 3, 5, and 8) were found in diverse clusters, resembling sequences of *Holophaga*, *Clostridium*, *Eubacterium* and *Halobacteroides* species (Fig. 5).

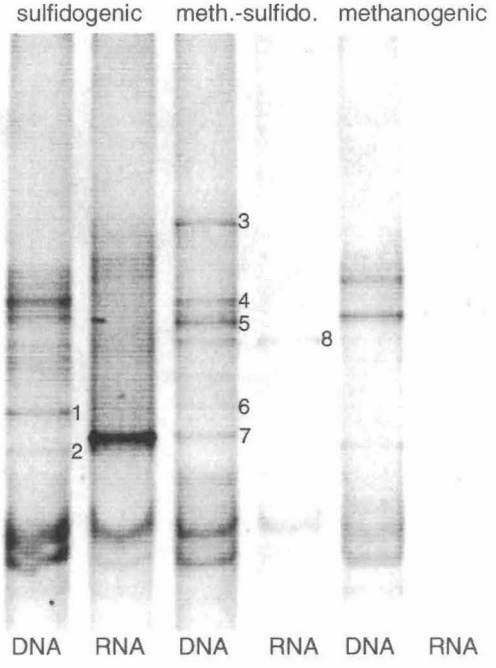

Fig. 4. DGGE of 16S rDNA and 16S rRNA PCR fragments from the sulfidogenic, methanogenic/sulfidogenic and methanogenic aggregates. The numbers refer to the numbers of the excised and sequenced bands. The curved bands in the lower part of the DGGE gel are single-stranded DNA and should be disregarded.

Population analysis by FISH. Phase-contrast light microscopy of the aggregate sections showed dense bacterial clusters, some void space and a regular surface of the aggregates. If excited with blue light (488 nm), cells and extracellular material exhibited strong green autofluorescence. Therefore, we exclusively applied CY3- or CY5-labelled probes for fluorescence in situ hybridization (FISH) analysis.

FISH analysis showed that the three aggregates have a different structure and population distribution. The methanogenic/sulfidogenic aggregates contain an inner core of *Archaea*, at ca. 100 µm from the surface of the aggregate (Figs. 6B and 6D). Blue autofluorescence in the center of unfixed aggregates confirms that the positive signal with probe ARC915 originates from methanogenic *Archaea*. The outer shell of the methanogenic/sulfidogenic aggregates (30 - 50 µm in thickness) contains dense

populations of SRB (Fig. 6D). Between these two zones only a low number of *Eubacteria* could be found (Fig. 6B), of which some hybridized with probe MPOB (clusters with big coccoid cells, Figs. 6F and 6H).

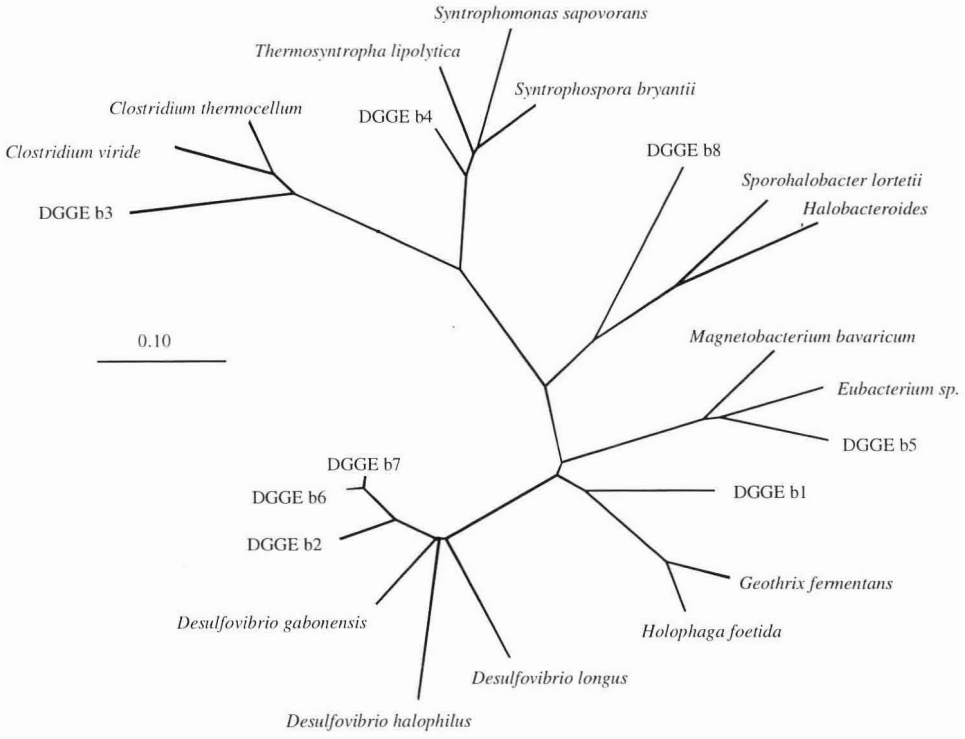

Fig. 5. Phylogenetic analysis of the partial sequences derived from excised DGGE bands depicted in figure 4. The phylogenetic parsimony tree was calculated with the ARB program. The bar indicates 0.1 estimated change per nucleotide.

The different populations in the sulfidogenic and methanogenic aggregates are more dispersed over the granules. Fig. 6A illustrates the irregular shape of the sulfidogenic aggregates, clearly showing eubacterial buddings at several locations on the aggregate surface. The SRB in the sulfidogenic aggregates are again situated at the outer layer of the aggregate, ca. 200 -300 μm in thickness (Fig. 6C), but do not form a close compact shell as was observed with methanogenic/sulfidogenic aggregates (Fig. 6D). Some SRB are also present deeper in the sulfidogenic aggregate. Cells hybridizing with probe MPOB are scattered over the interior part of the sulfidogenic aggregates (Figs. 6E and 6G). The methanogens in the sulfidogenic and also the methanogenic aggregates are present in clusters in the inner part of the aggregate and often a very compact core of MB can be found there (Figs. 6A, 6C, 6E and 7A). The methanogenic aggregates contained hardly any SRB (Fig. 7A) and no cells hybridizing with the MPOB probe could be detected.

FISH analysis with group specific probes for SRB resulted in hybridizations with probe DSV698 and 660 of cells in the outer layer of the methanogenic/sulfidogenic aggregates (Figs. 7B and 7D). No

distinct hybridization could be observed with the other group specific SRB probes applied (Table 1) in the methanogenic/sulfidogenic aggregates. In the sulfidogenic aggregates, a strong hybridization with the probe DSS658 was obtained, clearly showing clusters of coccoid cells at the surface and more inward (Fig. 7C). This was the only specific SRB probe that hybridized with the sulfidogenic aggregates during FISH analysis. Strong autofluorescence in the aggregates, especially with higher formamide concentrations, hampered quantitative analysis of the FISH results.

DISCUSSION

Architecture of UASB aggregates. This study clearly showed that different spatial arrangements of the SRB and MB populations can develop in UASB aggregates. SRB and MB were distributed in a layered structure in the methanogenic/sulfidogenic and sulfidogenic aggregates (Figs. 6-7), which resulted in a zonation where their activity is predominant (Figs. 1-3). A similar microzonation of predominant activities of the fermentative and methanogenic populations has been reported for glucose fed UASB aggregates (27). The differences in structure of the different types of UASB granules studied can be attributed to differences in wastewater composition on which the granules were cultivated, which was quite different in both sulfate concentrations and organic substrates (Table 2). The development of different types of aggregates depending on the type of substrate has indeed been reported previously (12, 13).

The core of all three types of aggregates was composed of MB, whereas SRB were mainly present in an outer shell around this MB core. This was also found by Sekiguchi et al. (52). The low SRB population density in the center of the aggregates contrasts the fact that SRB can outcompete methanogens because of their lower K_s values and more favorable thermodynamics for acetate and H_2 (23, 51, 61). Diffusional limitation of sulfate in the core of UASB aggregates has been suggested as a reason for the presence of MB in UASB aggregates treating sulfate rich wastewaters (43). From the *in situ* activity measurements performed in this study, we calculated that this is not the case in the aggregates investigated during reactor operation. This suggests that the MB core of the primary inoculum is conserved and that SRB colonize this core after feeding the granules a sulfate rich wastewater. A similar outgrowth of SRB after feeding methanogenic granular sludge a mixture of propionate and sulfate for 12 weeks was observed by Harmsen et al. (16). Besides the population dynamics upon exposure of the primary inoculum to a different substrate, also new granules are formed during reactor operation. The observed structures suggest that the initial aggregation is mediated by methanogenic bacteria, which indeed have better attachment characteristics compared to SRB (18, 38). SRB attach later on during aggregate growth on the sulfate rich wastewater.

The inner core of the methanogenic/sulfidogenic aggregates was one big center of MB (Figs. 6B, 6D and 6E). In contrast, the core of the methanogenic and sulfidogenic aggregates contained several smaller clusters of MB (Figs. 6A, 6C and 7A). It could be that substrates for the methanogenic and/or syntrophic bacteria in the sulfidogenic and methanogenic aggregates are diffusion limited, so no layered structure can

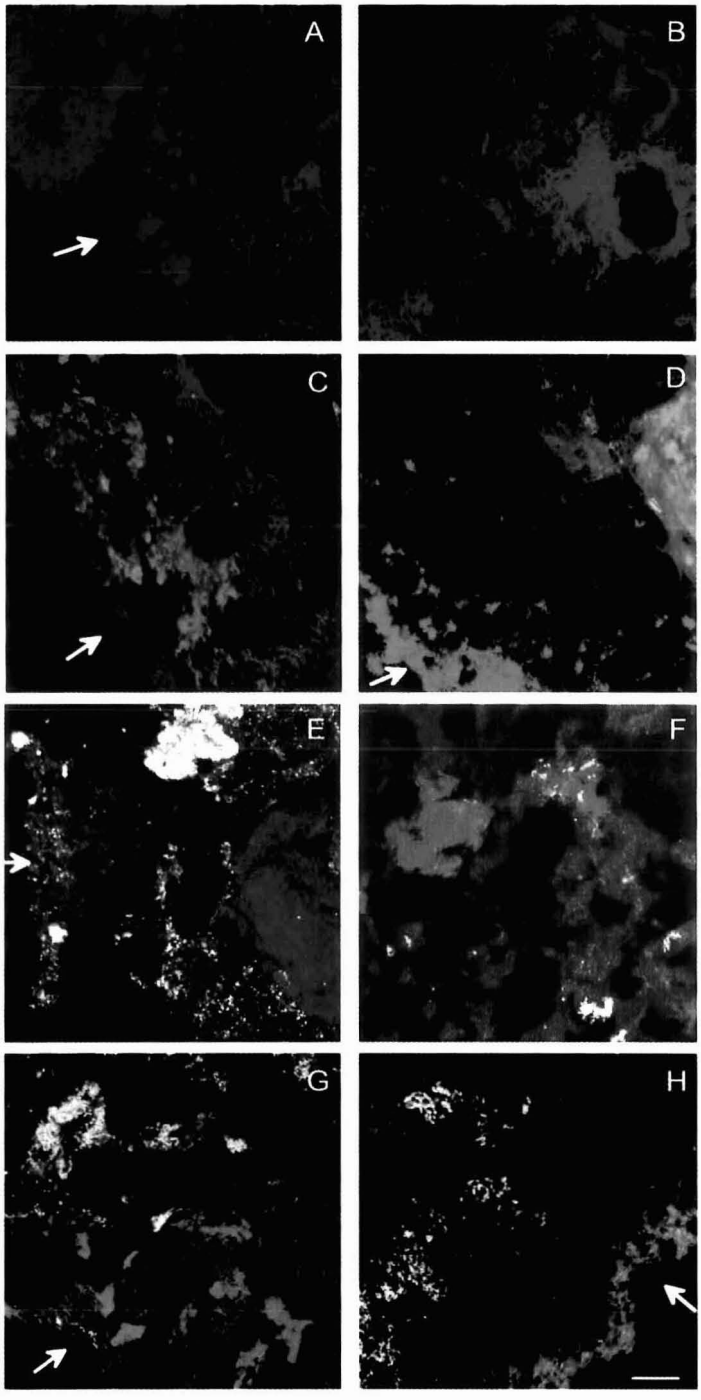
A
B
C
D
E
F
G
H

← Fig. 6. FISH analysis to study the population distribution within sulfidogenic and methanogenic/sulfidogenic aggregates using various probes labeled with CY3 and CY5. The photographs are overlays of two confocal microscopic images. EUB338 (artificial color blue) and ARC915 (artificial color red) hybridizations of sulfidogenic (A) and methanogenic-sulfidogenic (B) aggregates. SRB385 (artificial color green) and ARC915 (artificial color red) hybridization of sulfidogenic (C) and methanogenic/sulfidogenic (D) aggregates. ARC915 (artificial color red) and MPOB (artificial color white) hybridization of sulfidogenic (E) and methanogenic/sulfidogenic (F) aggregates. SRB385 (artificial color green) and MPOB (artificial color white) hybridization of sulfidogenic (G) and methanogenic/sulfidogenic (H) aggregates. The scale bar is 20 μm and the arrows indicate the aggregate surface.

develop with one big center of MB, surrounded by a layer of syntrophic bacteria. Indeed, the formation of clusters of methanogens in juxtaposition with syntrophic bacteria offers both groups of bacteria a nutritional advantage.

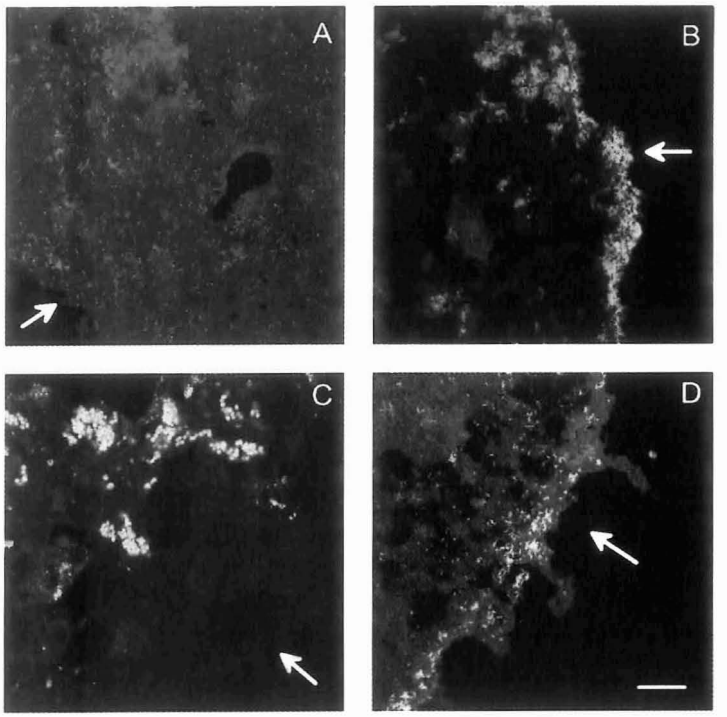

Fig. 7. FISH analysis to localize specific SRB populations within the aggregates. (A) probe SRB385 (artificial color green) and ARC915 (artificial color red) hybridization of methanogenic aggregates. This photograph is an overlay of two confocal microscopic images. (B) Hybridization with probe 660 (artificial color purple) and (D) probe 698 (artificial color purple) in a methanogenic/sulfidogenic aggregate. (C) Hybridization with probe 658 (artificial color purple) in a sulfidogenic aggregate. The scale bar is 20 μm and the arrows indicate the aggregate surface.

Endogenous microprofiles. Microsensor measurement of H_2S and CH_4 profiles indicated that both the SRB and MB populations were also active in the absence of externally supplied electron donor for at least 24 h (Fig. 1). This indicates that both SRB and MB metabolize storage material present in the aggregates, which was also found by de Beer et al. (10). This could be intracellular storage polymers, cell lysates, but also a third population could provide them with electron donor. Reducing compounds are, however, limited within the aggregates and the activity of both the SRB and MB increases considerably in the presence of externally supplied electron donor (Fig. 2).

The presence of elemental sulfur and/or polysulfides in all three aggregates explains the measured sulfide profiles in sulfate-free medium (Fig. 1), since sulfide could have been produced out of sulfur by sulfate or sulfur reducing bacteria. It is, however, unclear how the elemental sulfur and/or polysulfide is formed. Under anaerobic conditions and in the absence of nitrate, no sulfide could be (partially) oxidized. Also no sulfur disproportionation could occur and a reverse reaction of this last phenomenon has not yet been demonstrated. Some elemental sulfur and/or polysulfide might be formed through the presence of small amounts of oxygen during replacement of medium and/or transfer of the aggregates to the flow cell. It is, however, unlikely that this can support the formation of the high elemental sulfur and/or polysulfide concentrations observed (Table 2).

Characteristics of the SRB population. The measured sulfate reducing rates in the UASB aggregates are up to 1000 times higher than the rates reported for sediments, i.e. 0.0009 mmol S^{2-} m^{-3} s^{-1} (25) and 0.002-0.01 mmol S^{2-} m^{-3} s^{-1} (3). This is, however, not surprising as the SRB population density in sediments is significantly lower than in UASB aggregates. The latter resemble aerobic biofilms, where comparable activities have been measured in the deeper, anaerobic layers, i.e. 0.2 mmol S^{2-} m^{-3} s^{-1} (24) or 8 mmol S^{2-} m^{-3} s^{-1} (37). From the H_2S fluxes and the number of SRB (determined by FISH) in the methanogenic/sulfidogenic aggregates, the specific sulfate reduction rate was calculated to be 25 fmol SO_4^{2-} $cell^{-1}$ day^{-1}. This value is in the range of the specific sulfate reduction rates reported (21). The variations in the calculated activities of the SRB, and also of the MB, in the different aggregates (Fig. 2; Table 2) can be explained by the different types of aggregates and different times of measurement. The aggregates measured directly after retrieval from the UASB reactor were more active than those pre-incubated in the laboratory for one day or more before measurements.

The hybridization analysis (DGGE blot hybridizations and FISH) with group specific SRB probes revealed the presence of *Desulfovibrio*, *Desulfobulbus*, *Desulfosarcina* and/or *Desulfococcus* species. The methanogenic/sulfidogenic aggregates contained *Desulfovibrio* spp., as well as *Desulfobulbus* spp. These bacteria were located in the outer layer of the aggregates (Figs. 7B and 7D), where they metabolized VFA (Fig. 2B), and possibly H_2. These two SRB species were absent in the sulfidogenic granules, which contained predominantly the nutritional versatile *Desulfosarcina* and/or *Desulfococcus* species. The H_2S microprofiles measured in the sulfidogenic aggregates suggest that different metabolic SRB populations are present in the outer 400 µm (Fig. 2A). These different populations could, however, not be differentiated by the FISH technique with the probes applied. Actually, only a few of the specific SRB probes (Table 1) yielded a positive FISH hybridization in the aggregates (Figs. 7B, 7C and 7D). This suggests that UASB granules may contain specific SRB populations, for which specific probes need to be developed.

The H_2S microprofiles measured in the presence of acetate clearly localized the acetate oxidizing SRB activity (Fig. 2). Several acetate utilizing SRB species are known, like for instance *Desulfobacter*, *Desulfobacterium*, *Desulfococcus*, *Desulfosarcina* or *Desulfotomaculum* species. *Desulfobacter* species were not detected by the DGGE and FISH analysis. This is in agreement with other studies, which indicated that *Desulfobacter* plays an unimportant role in acetate degradation in methanogenic aggregates (40, 46). These studies suggested that acetate degradation is mediated by *Desulfotomaculum*-like species (40). However, we were not able to detect the Gram positive *Desulfotomaculum* species with the probes used for the FISH analysis. But also *Desulfosarcina* or *Desulfococcus* species, which were found to be present in the sulfidogenic aggregates by FISH analysis, are likely to be responsible for the degradation of acetate.

Besides the known SRB species reported above, the presence of other acetotrophic SRB species can not be excluded. Recently, two acetate utilizing SRB, i.e. *Desulforhabdus amnigenus* (41) and *Desulfobacca acetoxidans* (39) have been isolated from granular sludge. It should be noted that probe MPOB also hybridizes with *D. amnigenus* (Table 1), although it has one mismatch with the 16S rRNA sequence of *D. amnigenus* (15). It is, however, unlikely that *D. amnigenus* was present in the aggregate types investigated, as MPOB-like cells are coccoid (Figs. 6E-H (17)) as opposed to the rod-shaped *D. amnigenus* (41). Moreover, MPOB-like cells were found in juxtaposition with MB (Figs. 6G and 6H), which is a rather unlikely arrangement for an acetotrophic SRB, who does not depend on a partner to remove excess of reducing equivalents (41, 61). However, more research using specific 16S rRNA probes for these newly described organisms is needed to unequivocally determine their presence in the UASB aggregates investigated.

The low SRB population density in the methanogenic aggregates (Figs. 2C and 7A) is somewhat surprising. SRB are generally assumed to be more robust than MB (61). Moreover, SRB have the ability to use other metabolic pathways than sulfate reduction, like fermentation of lactate, ethanol or pyruvate (61), or syntrophic growth with methanogens (63). This enables them to remain present and active in sulfate-free media for days up to months. Actually the medium on which the methanogenic aggregates were subcultured did contain a minor amount of sulfate (0.45 mM), which could have supported the growth of SRB. Apparently, this small amount of sulfate could not support the development of a substantial SRB population.

Characteristics of the MB population. The calculated methanogenic rates in the aggregates are 10 times higher than methanogenic activities measured in sediments, 0.1 - 0.6 mmol of CH_4 m^{-3} s^{-1} (34), and during sewage sludge digestion, 0.6 mmol CH_4 m^{-3} s^{-1} (54). The morphology of the methanogens present in the center of the three types of UASB aggregates investigated resemble that of *Methanosaeta* (formerly *Methanotrix*) species, which are bamboo-shaped rods (63). This obligate aceticlastic methanogenic species was also found to be present in the core of other layered granules (14, 27, 31, 52). *Methanosaeta* species are the least sensitive among the methanogens for acetate diffusional limitations because of their lower K_s value for acetate compared to other methanogens (13, 14, 20). This, together with their ability to form close frameworks/mats (44), might be the reason for their presence in the center of the aggregates.

The presence of MB in the sulfidogenic granules (Figs. 6A, 6C and 6E) contrasts methanogenic activity tests with this sludge, which indicated the absence of any methanogenic activity (data not shown).

It has been reported that MB can maintain their ribosomal content for a longer period of time than is necessary to match their metabolic activity level (46). The long term survival of methanogens in granular sludge is well known (28) , a feature which enables rapid reactor start-up of methanogenic reactors. The persistence of MB can also cause unwanted substrate consumption by the MB in reactor applications where only sulfate reduction is wanted, i.e. sulfur and heavy metal removal (28).

The CH_4 microprofiles showed that methanogenesis was not affected by the addition of sulfate (Figs. 1 and 2). The data in literature concerning this phenomenon are somewhat contradictory. Methanogenesis was found to be inhibited upon sulfate addition in sediments (30, 62) or anaerobic digestors (29, 46). Others reported no effect at all on methanogenesis under sulfate rich conditions in the same environments, i.e. sediments (53) or anaerobic reactors (58, 63). The differences between these observations might be explained by substrate availability. SRB and MB compete for available hydrogen and/or acetate (61, 62). If these substrates are not limiting, as was the case during the microprofile measurements, no inhibition of methanogenesis will occur in the presence of high sulfate concentrations.

Characteristics of the syntrophic population. As methanogens can not use propionate as electron donor, the increase in methanogenic activity upon the addition of propionate (Fig. 2B) illustrates the dependency of methanogens on propionate-oxidizing syntrophic bacteria. The DGGE analysis suggested the presence of a relative of *Syntrophobacter wolinii* and *Syntrophomonas wolfei* (Fig. 5), whereas the FISH analysis using probe MPOB (Fig. 6G and 6H) suggests the presence of strain MPOB, recently classified as *Syntrophobacter fumaroxidans* (17). Recent studies revealed that syntrophic propionate-oxidizing bacteria such as *Syntrophobacter* spp. are themselves capable of oxidizing propionate by sulfate reduction (15, 60). The *Desulfobulbus* layer at the surface of the methanogenic/sulfidogenic aggregates (Fig. 7B) indicates that the syntrophic bacteria, although they may be capable of growing on propionate by sulfate reduction, cannot outcompete *Desulfobulbus* spp. in this granular sludge developed under sulfate rich conditions.

The MPOB-like cells did not grow on the surface of the granule, but rather grow more inwards. Methanogens can grow syntrophically with the acetate and H_2 producing syntrophic bacteria either in juxtaposition in the core or as adjacent layers within the aggregate (16, 52, 63). The latter type of syntrophic relationship was found in methanogenic/sulfidogenic aggregates (Fig. 6F). Actually, syntrophic bacteria were found between a layer of SRB and MB, providing both groups with H_2 and acetate, as postulated in the conceptual model of MacLeod et al. (31). In the sulfidogenic granules (Fig. 6E), MPOB-like cells were surrounded by MB cells, indicating that the MPOB-like cells grow indeed syntrophically and depended on the MB to remove the reducing equivalents.

Concluding remarks. Combining microsensors and molecular techniques provided direct information about sulfate reduction and methanogenesis in UASB aggregates. Data on the community structure could be related to the metabolic functions of the respective populations. SRB were mainly found in the outer layer (< 200 μm) and MB predominantly in the core of UASB aggregates. For further detailed investigation, microsensors for the substrate hydrogen and additional oligonucleotide probes for newly isolated syntrophic and SRB populations are under development.

ACKNOWLEDGMENTS

This work was financially supported by the Körber Foundation (Hamburg, Germany), the Max Planck Society (München, Germany), and the European Union (project MICROMARE contract MASCT 950029). We thank Helle Ploug for fruitful discussions, Bo Barker Jørgensen and Rudi Amann for their support, Gaby Eickert, Anja Eggers, Vera Hübner and Lars B. Pedersen for technical assistance with the microsensors, and Ramón Rosselló-Mora for his help with the phylogenetic analysis.

REFERENCES

1. **Amann, R., I. Krumholz, and D. A. Stahl.** 1990. Fluorescent-oligonucleotide probing of whole cells for determinative, phylogenetic, and environmental studies in microbiology. J. Bacteriol. **172:**762-770.
2. **Amann, R., J. Stromley, R. Devereux, R. Key, and D. A. Stahl.** 1992. Molecular and microscopic identification of sulfate-reducing bacteria in multispecies biofilms. Appl. Environ. Microbiol. **58:**614-623.
3. **Blaabjerg, V., K. N. Mouritsen, and K. Finster.** 1998. Diel cycles of sulphate reduction rates in sediments of a *Zostera marina* bed (Denmark). Aquat. Microb. Ecol. **15:**97-102.
4. **Broecker, W. S., and T.-H. Peng.** 1974. Gas exchange rates between air and sea. Tellus. **26:**21-35.
5. **Brosius, J., T. J. Dull, D. D. Sleeter, and H. F. Noller.** 1981. Gene organization and primary structure of a ribosomal RNA operon from *Escherichia coli*. J. Mol. Biol. **148:**107-127.
6. **Cline, J. D.** 1969. Spectrophotometric determination of hydrogen sulfide in natural waters. Limnol. Oceanogr. **14:**454-458.
7. **Damgaard, L. R., and N. P. Revsbech.** 1999. An acetylene-based microscale diffusivity sensor. In prep.
8. **Damgaard, L. R., and N. P. Revsbech.** 1997. A microscale biosensor for methane containing methanotrophic bacteria and an internal oxygen reservoir. Anal. Chem. **69:**2262-2267.
9. **Damgaard, L. R., N. P. Revsbech, and W. Reichard.** 1998. Use of an oxygen-insensitive microscale biosensor for methane to measure methane concentration profiles in a rice paddy. Appl. Environ. Microbiol. **64:**864-870.
10. **De Beer, D., J. W. Huisman, J. C. van den Heuvel, and S. P. P. Ottengraf.** 1992. The effect of pH profiles in methanogenic aggregates on the kinetics of acetate conversion. Water Res. **26:**1329-1336.
11. **Devereux, R., M. D. Kane, J. Wilfrey, and D. A. Stahl.** 1992. Genus- and group-specific hybridization probes for determinative and environmental studies of sulfate-reducing bacteria. System. Appl. Microbiol. **15:**601-609.
12. **Fang, H. H. P., H. K. Chui, and Y. Y. Li.** 1994. Microbial structure and activity of UASB granules treating different wastewaters. Water Sci. Technol. **30:**87-96.
13. **Grotenhuis, J. T. C., M. Smit, C. M. Plugge, X. Yuansheng, A. A. M. van Lammeren, A. J. M. Stams, and A. J. B. Zehnder.** 1991. Bacteriological composition and structure of granular sludge adapted to different substrates. Appl. Environ. Microbiol. **57:**1942-1949.
14. **Guiot, S. R., A. Pauss, and J. W. Costerton.** 1992. A structured model of the anaerobic granule consortium. Water Sci. Technol. **25:**1-10.
15. **Harmsen, H. J. M., A. D. L. Akkermans, A. J. M. Stams, and W. M. de Vos.** 1996. Population dynamics of propionate-oxidizing bacteria under methanogenic and sulfidogenic conditions in anaerobic granular sludge. Appl. Environ. Microbiol. **62:**2163-2168.
16. **Harmsen, H. J. M., H. M. P. Kengen, A. D. L. Akkermans, A. J. M. Stams, and W. M. De Vos.** 1996. Detection and localization of syntrophic propionate-oxidizing bacteria in granular sludge by in situ hybridization using 16S rRNA-based oligonucleotide probes. Appl. Environ. Microbiol. **62:**1656-1663.

17. **Harmsen, H. J. M., B. L. M. van Kuijk, C. M. Plugge, A. D. L. Akkermans, W. M. de Vos, and A. J. M. Stams.** 1998. Description of *Syntrophobacter fumaroxidans* sp. nov., a syntrophic propionate-degrading sulfate-reducing bacterium. Int. J. Syst. Bacteriol. **48:**1383-1387.

18. **Isa, Z., S. Grusenmeyer, and W. Verstraete.** 1986. Sulfate reduction relative to methane production in high-rate anaerobic digestion: microbial aspects. Appl. Environ. Microbiol. **51:**580-587.

19. **Jeroschewski, P., C. Steuckart, and M. Kühl.** 1996. An amperometric microsensor for the determination of H_2S in aquatic environments. Anal. Chem. **68:**4351-4357.

20. **Jetten, M. S. M., A. J. M. Stams, and A. J. B. Zehnder.** 1990. Acetate threshold values and acetate activating enzymes in methanogenic bacteria. FEMS Microbiol. Ecol. **73:**339-344.

21. **Jørgensen, B. B.** 1978. A comparison of methods for the quantification of bacterial sulfate reduction in coastal marine sediments. Geomicrobiol. **1:**49-64.

22. **Karchmer, J. H.** 1979. The analytical chemistry of sulfur and its compounds. Wiley-Interscience.

23. **Kristjansson, J. K., P. Schönheit, and R. K. Thauer.** 1982. Different K_s values for hydrogen of methanogenic bacteria and sulfate reducing bacteria: an explanation for the apparent inhibition of methanogenesis by sulfate. Arch. Microbiol. **131:**278-282.

24. **Kühl, M., and B. B. Jørgensen.** 1992. Microsensor measurements of sulfate reduction and sulfide oxidation in compact microbial communities of aerobic biofilms. Appl. Environ. Microbiol. **58:**1164-1174.

25. **Kühl, M., C. Steuckart, G. Eickert, and P. Jeroschewski.** 1998. A H_2S microsensor for profiling biofilms and sediments: application in an acidic lake sediment. Aquat. Microb. Ecol. **15:**201-209.

26. **Lens, P., D. de Beer, C. Cronenberg, S. Ottengraf, and W. Verstraete.** 1995. The use of microsensors to determine population distribution in UASB aggregates. Water Sci. Technol. **31:**273-280.

27. **Lens, P. N. L., D. de Beer, C. C. H. Cronenberg, F. P. Houwen, S. P. P. Ottengraf, and W. H. Verstraete.** 1993. Heterogeneous distribution of microbial activity in methanogenic aggregates: pH and glucose microprofiles. Appl. Environ. Microbiol. **59:**3803-3815.

28. **Lettinga, G.** 1995. Anaerobic digestion and wastewater treatment systems. Antonie van Leeuwenhoek. **67:**3-28.

29. **Li, Y.-Y., S. Lam, and H. H. P. Fang.** 1996. Interactions between methanogenic, sulfate-reducing and syntrophic acetogenic bacteria in the anaerobic degradation of benzoate. Water Res. **30:**1555-1562.

30. **Lovley, D. R., D. F. Dwyer, and M. J. Klug.** 1982. Kinetic analysis of competition between sulfate reducers and methanogens for hydrogen in sediments. Appl. Environ. Microbiol. **43:**1373-1379.

31. **MacLeod, F. A., S. R. Guiot, and J. W. Costerton.** 1990. Layered structure of bacterial aggregates produced in an upflow anaerobic sludge bed and filter reactor. Appl. Environ. Microbiol. **56:**1598-1607.

32. **Manz, W., R. Amann, W. Ludwig, M. Wagner, and K.-H. Schleifer.** 1992. Phylogenetic oligodeoxynucleotide probes for the major subclasses of proteobacteria: problems and solutions. Syst. Appl. Microbiol. **15:**593-600.

33. **Manz, W., M. Eisenbrecher, T. R. Neu, and U. Szewzyk.** 1998. Abundance and spatial organization of Gram-negative sulfate-reducing bacteria in activated sludge investigated by in situ probing with specific 16S rRNA targeted oligonucleotides. FEMS Microbiol. Ecol. **25:**43-61.

34. **Mountfort, D. O., and R. A. Asher.** 1981. Role of sulfate reduction versus methanogenesis in terminal carbon flow in polluted intertidal sediment of Waimea Inlet, Nelson, New Zealand. Appl. Environ. Microbiol. **42:**252-258.

35. **Muyzer, G., T. Brinkhoff, U. Nübel, C. Santegoeds, H. Schäfer, and C. Wawer.** 1998. Denaturing gradient gel electrophoresis (DGGE) in microbial ecology, p. 1-27. *In* A. D. L. Akkermans, J. D. van Elsas, and F. J. de Bruijn (eds.), Molecular Microbial Ecology Manual, vol. 3.4.4. Kluwer, Dordrecht, The Netherlands.

36. **Muyzer, G., E. C. de Waal, and A. G. Uitterlinden.** 1993. Profiling of complex microbial populations by denaturing gradient gel electrophoresis analysis of polymerase chain reaction-amplified genes encoding for 16S rRNA. Appl. Environ. Microbiol. **59:**695-700.

37. **Okabe, S., T. Matsuda, H. Satoh, T. Itoh, and Y. Watanabe.** 1998. Sulfate reduction and sulfide oxidation in aerobic mixed population biofilms. Water Sci. Technol. **37:**131-138.

38. **Omil, F., S. J. W. H. Oude Elferink, P. Lens, L. Hulshoff-Pol, and G. Lettinga.** 1997. Effect of the inoculation with *Desulforhabdus amnigenus* and pH or O_2 shocks on the competition between sulfate reducing and methanogenic bacteria in an acetate fed UASB reactor. Biores. Technol. **60:**113-122.

39. **Oude Elferink, S. J. W. H., W. M. Akkermans-van Vliet, J. J. Bogte, and A. J. M. Stams.** 1999. *Desulfobacca acetooxidans* gen. nov. sp. nov., a novel acetate-degrading sulfate reducer isolated from sulfidogenic granular sludge. Int. J. Syst. Bacteriol. In Press.

40. **Oude Elferink, S. J. W. H., H. T. S. Boschker, and A. J. M. Stams.** 1998. Identification of sulfate reducers and *Syntrophobacter* sp. in anaerobic granular sludge by fatty-acid biomarkers and 16S rRNA probing. Geomicrobiol. **15:**3-17.

41. **Oude Elferink, S. J. W. H., R. N. Maas, H. J. M. Harmsen, and A. J. M. Stams.** 1995. *Desulforhabdus amnigenus* gen. nov. sp. nov., a sulfate reducer isolated from anaerobic granular sludge. Arch. Microbiol. **164:**119-124.

42. **Oude Elferink, S. J. W. H., W. J. C. Vorstman, A. Sopjes, and A. J. M. Stams.** 1998. Characterization of the sulfate-reducing and syntrophic population in granular sludge from a full-scale anaerobic reactor treating papermill wastewater. FEMS Microbiol. Ecol. **27:**185-194.

43. **Overmeire, A., P. Lens, and W. Verstraete.** 1994. Mass transfer limitation of sulfate in methanogenic aggregates. Biotechnol. Bioeng. **44:**387-391.

44. **Patel, G. B.** 1984. Characterization and nutritional properties of *Methanotrix concilii* sp. nov., a mesophilic, aceticlastic methanogen. Can. J. Microbiol. **30:**1383-1396.

45. **Ramsing, N. B., H. Fossing, T. G. Ferdelman, F. Andersen, and B. Thamdrup.** 1996. Distribution of bacterial populations in a stratified fjord (Mariager Fjord, Danmark) quantified by in situ hybridization and related to chemical gradients in the water column. Appl. Environ. Microbiol. **62:**1391-1404.

46. **Raskin, L., B. E. Rittmann, and D. A. Stahl.** 1996. Competition and coexistance of sulfate-reducing and methanogenic populations in anaerobic biofilms. Appl. Environ. Microbiol. **62:**3847-3857.

47. **Revsbech, N. P.** 1989. An oxygen microelectrode with a guard cathode. Limnol. Oceanogr. **55:**1907-1910.

48. **Revsbech, N. P., and B. B. Jørgensen.** 1986. Microelectrodes: their use in microbial ecology. Adv. Microb. Ecol. **9:**293-352.

49. **Revsbech, N. P., L. P. Nielsen, and N. B. Ramsing.** 1998. A novel microsensor for determination of apparent diffusivity in sediments. Limnol. Oceanography. **43:**986-992.

50. **Santegoeds, C. M., T. G. Ferdelman, G. Muyzer, and D. de Beer.** 1998. Structural and functional dynamics of sulfate-reducing populations in bacterial biofilms. Appl. Environ. Microbiol. **64:**3731-3739.

51. **Schönheit, P., J. K. Kristjansson, and R. K. Thauer.** 1982. Kinetic mechanism for the ability of sulfate reducers to outcompete methanogens for acetate. Arch. Microbiol. **132:**285-288.

52. **Sekiguchi, Y., Y. Kamagata, K. Nakamura, A. Ohashi, and H. Harada.** 1999. Fluorescence in situ hybridization using 16S rRN-targeted oligonucleotides reveals localization of methanogens and selected uncultured bacteria in mesophilic and thermophilic sludge granules. Appl. Environ. Microbiol. **65:**1280-1288.

53. **Senior, E., E. B. Lindström, I. M. Banat, and D. B. Nedwell.** 1982. Sulfate reduction and methanogenesis in the sediment of saltmarsh on the East Coast of the United Kingdom. Appl. Environ. Microbiol. **43:**987-996.

54. **Smith, P. H., and D. T. Mah.** 1966. Kinetics of acetate metabolism during sludge digestion. Appl. Microbiol. **14:**368-371.

55. **Stahl, D. A., and R. Amann.** 1991. Development and application of nucleic acid probes, p. 207-248. *In* E. Stackebrandt and M. Goodfellow (eds.), Nucleic Acid Techniques in Bacterial Systematics, vol. 8. John Wiley & Sons Ltd.

56. **Strunk, O., O. Gross, B. Reichel, M. May, S. Hermann, N. Stuckmann, B. Nonhoff, M. Lenke, T. Ginhart, A. Vilbig, T. Ludwig, A. Bode, K.-H. Schleifer, and W. Ludwig.** 1998. ARB: a software environment for sequence data. http://www.mikro.biologie.tu-muenchen.de/pub/ARB. Department of Miocrobiology, Technische Universität München, Munich, Germany.

57. **Teske, A., C. Wawer, G. Muyzer, and N. B. Ramsing.** 1996. Distribution of sulfate-reducing bacteria in a stratified fjord (Mariager Fjord, Denmark) as evaluated by most-probable-number counts and denaturing gradient gel electrophoresis of PCR-amplified ribosomal DNA fragments. Appl. Environ. Microbiol. **62:**1405-1415.

58. **Ueki, K., A. Ueki, K. Takahashi, and M. Iwatsu.** 1992. The role of sulfate reduction in methanogenic digestion of municipal sewage sludge. J. Gen. Appl. Microbiol. **38:**195-207.

59. **Verstraete, W., D. de Beer, M. Pena, G. Lettinga, and P. Lens.** 1996. Anaerobic bioprocessing of waste. World J. Microbiol. Biotechnol. **12:**221-238.

60. **Wallrabenstein, C., E. Hauschild, and B. Schink.** 1995. *Syntrophobacter pfenningii* sp.nov., new syntrophically propionate-oxidising anaerobe growing in pure culture with propionate and sulfate. Arch. Microbiol. **164:**346-352.

61. **Widdel, F.** 1988. Microbiology and ecology of sulfate- and sulfur-reducing bacteria, p. 469-585. *In* A. D. J. Zehnder (ed.), Biology of anaerobic microorganisms. John Wiley & Sons, New York.

62. **Winfrey, M. R., and J. G. Zeikus.** 1977. Effect of sulfate on carbon and electron flow during microbial methanogenesis in freshwater sediments. Appl. Environ. Microbiol. **33:**275-281.

63. **Wu, W.-M., M. K. Jain, E. C. De Macario, J. H. Thiele, and J. G. Zeikus.** 1992. Microbial composition and characterization of prevalent methanogens and acetogens isolated from syntrophic methanogenic granules. Appl. Microbiol. Biotechnol. **38:**282-290.

Summary

Biofilms, aggregates and flocs are complex microbial systems, with diverse microbial populations and metabolic reactions. They are of great importance in wastewater treatment systems (e.g. activated sludge basins and bioreactors), where they handle the degradation of organic waste and removal of nutrients (NH_3, NO_3^-, PO_4^{2-}). Biofilm systems can also be found in many different natural environments. Our knowledge of these microbial agglomerates is limited, because the conventional techniques like isolation of microorganisms and the 'black box' approach for these systems were insufficient to understand the behavior of the entire microbial community. The microbial processes within biofilms, aggregates and flocs are closely coupled leading to internal cycles. As mass transfer is hindered within these biofilm systems, various microenvironments arise and a stratified structure is formed. The thickness of active layers is in the order of microns to millimeters. Therefore techniques with a high spatial resolution are needed to understand and better relate the bacterial populations within these complex systems with their microenvironment and microbial activity. The combination of molecular techniques (e.g. fluorescence *in situ* hybridization (FISH), denaturing gradient gel electrophoresis (DGGE) and specific PCR for functional genes), with microsensors for different chemical compounds, enables us to study these systems on a microscale and to determine the population distribution and activity (chapter 1 gives a short introduction of these techniques). With these advanced techniques, anaerobic-aerobic interactions were studied in several microbial systems with emphasis on sulfate reduction.

A model reactor (a flow cell with recirculated artificial wastewater, inoculated with activated sludge) was used to study the development of a biofilm and the effects of liquid flow velocity and substrate concentrations on the oxygen distribution in such a biofilm (chapter 2). The oxygen concentration profiles from the surface to the substratum was measured with oxygen microsensors and the two-dimensional oxygen distribution at the substratum of the biofilm with a planar optode. It was found that the biofilm had a heterogeneous structure with patches of aerobic and anaerobic zones at the bottom of the biofilm, that became more anaerobic in the course of the biofilm development. A lower flow velocity or the addition of for instance glucose decreased the oxygen concentration within the biofilm. Before sulfate reduction could be measured the entire biofilm sloughed off. A different approach was used to study the development of sulfate reducing bacteria (SRB), their distribution and activity in a developing biofilm.

The activated sludge basin of a municipal wastewater treatment plant was chosen for continuation of the biofilm development study (chapter 3 and 4). Oxygen impermeable plastic foil was submerged in the activated sludge basin and samples were taken weekly for microsensor and molecular analysis in the laboratory. The oxygen microsensor measurements showed that the growing biofilm contained anaerobic zones from the first week on, which increased in thickness during the following weeks. Although the conditions were favorable for SRB from the first week on, sulfide production was first detected with microsensors for sulfide on the 6th week of biofilm development. All sulfide produced in the anoxic zone was oxidized in the aerobic zone, thus a closed sulfur cycle was established. From the oxygen and sulfide flux calculations it was derived that 50-70% of the

oxygen diffusing in the biofilm was used for re-oxidation of the sulfide. Thus the sulfate reduction was as important as the aerobic mineralization in this biofilm.

Contrary to the microsensor measurements, FISH analysis revealed the presence of SRB from the first week on, with only a slight increase over the weeks (from 2.7 x 10^8 SRB/ml in the 2nd week of biofilm growth to 3.1 x 10^9 SRB/ml in the 11th week). As no suitable electron acceptor like nitrate or iron was present in the anaerobic zones, and thus sulfide could not be re-oxidized, we must conclude that these SRB were not sulfidogenically active in the first 6 week. Analysis of the gene for dissimilatory sulfite reductase, a key enzyme for sulfate reduction, showed an increase of this gene from the 6th week on, coinciding with the first sulfide production. It is speculated that a different group of SRB, not detected by FISH, is responsible for the sulfide production and the increase of the dissimilatory sulfide reductase gene. As the main biomass in an activated sludge basin is present in the form of activated sludge flocs, these flocs were investigated for their anaerobic processes (chapter 5). With oxygen microsensors it was found that 5 out of 7 investigated sludges did not contain anaerobic zones in the flocs. This could be explained by the loose structure of these flocs, allowing oxygen transport through convection, instead of diffusional transport which probably occurred in the denser 2 flocs. Although SRB were present in the activated sludge flocs on basis of FISH analysis and dissimilatory sulfite reductase gene content, no sulfate reduction could be measured either with microsensor measurements nor with the $^{35}SO_4^{2-}$ radiotracer method even under anoxic incubation conditions. Thus, also here we must conclude that the sulfate reducing bacteria are not sulfidogenically active and that there is a serious discrepancy between population analysis and functional analysis.

In the last study (chapter 6), dense aggregates from three different upflow anaerobic sludge blanket (UASB) reactors (a sulfidogenic, a methanogenic-sulfidogenic and a methanogenic digestor), were investigated. These aggregates were completely anaerobic and sulfide and methane production could be measured. As predicted by models, a layer structure was found with molecular analysis as well as with microsensor measurements. Methanogenic bacteria formed the core of the aggregate, SRB were present in the outer layer and syntrophic bacteria were detected between the SRB and methanogens, providing both populations with acetate and hydrogen. Whereas the methanogenic-sulfidogenic aggregates had a distinct layered structure, the populations within the methanogenic and sulfidogenic aggregates were more spread out. Thus, in these anaerobic aggregates the measured microbial activity agreed with the detected population structure.

This work shows the importance and strength of combining methods, like microsensor and molecular analysis, for the study of function and structure of complex microbial systems.

Samenvatting

Biofilmen, aggregaten en vlokken zijn complexe microbiële systemen met vele, diverse microbiële populaties en metabolische reacties. Zij zijn van groot belang in de waterzuivering, zoals in actief-slib basins en bioreactoren, waar ze het organisch afval afbreken en nutriënten (NH_3, NO_3^-, PO_4^{2-}) verwijderen. Biofilm systemen komen ook veelvuldig voor in natuurlijke omgevingen. Onze kennis van deze microbiële agglomeraten is echter beperkt, aangezien conventionele technieken zoals isolering van microorganismen en de 'black box' benadering voor deze systemen ontoereikend zijn om het gedrag van de gehele microbiële gemeenschap te beschrijven. Microbiële processen in biofilmen, aggregaten, en vlokken zijn nauw gekoppeld, wat tot interne element-cyclussen kan leiden. Daar massatransport in de biofilm systemen geremd is, ontstaan verscheidene micro-omgevingen en ontwikkelt zich een gestratificeerde structuur. De dikte van de actieve lagen varieert van enkele micrometers tot enkele millimeters. Dientengevolge zijn technieken nodig met een hoog oplossend vermogen om de micro-omgeving en de activiteit van bakteriële populaties goed te kunnen bestuderen. Molekulaire technieken, zoals fluorescerende *in situ* hybridisatie (FISH), denaturerende gradiënt gel electroforese (DGGE) en speciefieke PCR, gekombineerd met microsensormetingen ter detectie van chemische gradiënten, maken het mogelijk om deze complexe microbiële systemen op micro-schaal te onderzoeken (hoofdstuk 1 geeft een korte introductie van de methoden). Anaerobe en aerobe interacties in verschillende microbiële biofilm systemen werden met deze geavanceerde technieken bestudeerd, waarbij de nadruk op de sulfaat reductie werd gelegd.

Een model reactor, een flow cel met re-circulerend kunstmatig afvalwater, beënt met actief slib, werd gebruikt om de ontwikkeling van een biofilm te bestuderen, en tevens om de invloed van doorstroomsnelheid en substraat concentraties op de zuurstof-verdeling in een dergelijke biofilm te bepalen (hoofdstuk 2). De zuurstof-concentratieprofielen werden met microsensoren van het oppervlak tot de substratum van de biofilm gemeten. Twee-dimensionale beelden van de zuurstof-concentratie aan het substratum van de biofilm werden verkregen met een 'planar optode'. Het bleek dat de biofilm een heterogene struktuur had met anaerobe en aerobe plekken, die naarmate de ontwikkeling vorderde steeds meer anaerobe werd. Het verlagen van de doorstroomsnelheid en toevoeging van bijvoorbeeld glucose had tot gevolg dat de zuurstof-concentratie in de biofilm afnam. Echter, voordat sulfaat reductie gedetecteerd kon worden liet de gehele biofilm los. Een ander systeem moest gezocht worden om de onwikkeling van sulfaat reducerende bakteriën (SRB), hun verdeling en hun activiteit in een groeiende biofilm te onderzoeken.

Het actief-slib basin van een waterzuiveringsinstallatie werd gekozen om de biofilm-ontwikkelings-studie voort te zetten (hoofdstuk 3 en 4). Plastikfolie, ondoordringbaar voor zuurstof, werd in het basin gehangen en monsters van deze folie werden wekelijks naar het laboratorium gebracht voor microsensormetingen en molekulaire analyse. De zuurstof-microsensormetingen lieten zien dat vanaf de eerste week anaerobe zones in de biofilm aanwezig waren, en dat deze in omvang toenamen gedurende de volgende weken. Ondanks de gunstige condities voor SRB vanaf de eerste week, kon sulfaat reduktie pas vanaf de 6e week gedetekteerd worden. Al het geproduceerde sulfide werd in de aerobe zones van de biofilm gereoxideerd, waardoor een gesloten cyclus ontstond. Uit de zuurstof- en sulfide-fluxen werd berekend dat 50 tot 70% van de in de biofilm diffunderende zuurstof

werd gebruikt voor reoxidatie van de sulfide. Het bleek dus dat de sulfaat reductie in deze biofilm even belangrijk was als de aerobe mineralisatie.

In tegenstelling tot de microsensormetingen, toonde de FISH analyse aan dat SRB in de eersten weken van de biofilmontwikkeling aanwezig waren en slechts weinig toenamen in aantal in de weken daarop (van 2.7 x 10^8 SRB/ml in de 2e week tot 3.1 x 10^9 SRB/ml in de 11e week van de biofilmontwikkeling). Omdat geen sulfide productie gemeten kon worden en in de anoxische zones geen elektronenacceptor aanwezig was voor reoxidatie van sulfide, moet aangenomen worden dat de SRB in de eerste 6 weken niet sulfidogeen actief waren. De analyse van het gen voor het dissimilatorische sulfiet reductase, een sleutel enzym bij de sulfaat reductie, wees uit dat het gen vanaf de 6e week toenam, tegelijk met de gemeten sulfide productie. Het is denkbaar dat een andere groep SRB, die niet met de FISH analyse gedetecteerd wordt, voor de toename van het sulfiet reductase gen verantwoordelijk is.

Aangezien de meeste biomassa in actief-slib basins in de vorm van vlokken aanwezig is, werden verschillende aktief-slib vlokken op anaerobe processen onderzocht (hoofdstuk 5). Uit zuurstof-microsensormetingen bleek dat 5 van 7 onderzochte vlok-typen geen anaerobe zones bezaten. Dit kan verklaard worden door de losse struktuur van de 5 vlokken, waardoor het zuurstof-transport zowel door middel van diffusie als door middel van convectie plaats kon vinden. De andere twee vlokken hadden een dichtere stuktuur waardoor het zuurstof-transport waarschijnlijk alleen door diffusie plaats vond. Alhoewel de FISH analyse aantoonde dat SRB aanwezig waren en ook het dissimilatorische sulfiet reductase gen gedetecteerd werd, kon noch met microsensormetingen noch met de $^{35}SO_4^{2-}$ radiotracer methode sulfaatreductie gemeten worden, zelfs niet onder volledig anaerobe condities. Daarom moet aangenomen worden dat ook in dit systeem de sulfaat reducerende bakteriën niet sulfidogeen actief waren en dat er een discrepantie tussen de populatie analyse en de functionele analyse bestaat.

In de laatste studie (hoodstuk 6) werden kompakte aggregaten uit drie verschillende anaerobe bioreactoren (zogenoemde upflow anaerobic sludge blanket (UASB) reactors) onderzocht. De anaerobe aggregaten uit een methanogene, een sulfidogene en een methano-sulfidogene reaktor produceerden methaan en sulfide. Mathematische modellen voorspelden dat de aggregaten een gestratificeerde struktuur bezitten, wat met de microsensormetingen en ook met de molekulaire methoden bewezen kon worden. Methanogene bakteriën werden in de kern van de aggregaten gevonden en SRB in de buitenste laag. Syntrofe bakteriën bevonden zich tussen de methanogene en sulfaat reducerende bakteriën in, en konden zo beide populaties van acetaat en waterstof voorzien. De methano-sulfidogene aggregaten toonden een exact gestratificeerde struktuur, terwijl de methanogene en sulfidogene aggregaten uit meer diffuse lagen bestonden. In deze studie werd zodoende een overeenstemming gevonden tussen struktuur en functie analyse.

Dit promotie onderzoek laat het belang en de mogelijkheden zien van de kombinatie van microsensoren en molekulaire technieken. Daar detectie van populaties met molekulaire technieken meestal geen uitspraak over de activiteit van de organismen geeft, is het belangrijk om deze gegevens te kombineren met functie analyses, zoals met microsensormetingen.

Zusammenfassung

Biofilme, Aggregate und Flocken sind komplexe mikrobielle Systeme, mit verschiedenen mikrobiellen Populationen und metabolischen Prozessen. Sie sind von großer Bedeutung in der Abwasserreinigung (z.B. in Belebtschlammbecken und Bioreaktoren), wo sie die organischen Abfallstoffe zersetzen und die Nährstoffe (NH_3, NO_3^-, PO_4^{2-}) entfernen. Biofilm-Systeme kommen auch in verschiedenen natürlichen Umgebungen vor. Unsere Kenntnisse über mikrobielle Agglomerate sind jedoch begrenzt, da die konventionellen Techniken wie die Isolierung von Mikroorganismen und die 'black box' Betrachtung für diese Systeme unzureichend sind um das Verhalten der gesamten mikrobiellen Gemeinschaft zu verstehen. Mikrobielle Prozesse in den Biofilmen, Aggregaten und Flocken sind eng aneinander gekoppelt, was zu internen Stoff-Zyklen führt. Da der Stofftransport in diesen Biofilmsystemen eingeschränkt ist, entstehen unterschiedliche Mikro-Umgebungen, was oft zu einer stratifizierten Struktur führt. Die Dicke der aktiven Schichten liegt zwischen einigen Mikrometern bis einigen Millimetern. Daher werden Methoden mit einer hohen Auflösung benötigt, um die bakteriellen Populationen und ihre Aktivität in bezug zur Mikro-Umgebung besser zu verstehen. Zur Detektion verschiedener Populationen kamen im molekularmethodischen Ansatz Fluoreszenz-*in situ*-Hybridisierung (FISH), denaturierende Gradienten-Gel-Elektrophorese (DGGE) und spezifische Polymerase-Kettenreaktion (PCR) für funktionelle Gene zur Anwendung. Die chemischen Gradienten innerhalb der Systeme wurden mittels Mikrosensoren untersucht. Die Kombination dieser Methoden ermöglichte die Untersuchung der Anordnung von Populationen und ihrer Aktivität mit einer Auflösung von wenigen Mikrometern (Kapitel 1 gibt eine kurze Übersicht dieser Methoden). Mit diesen Techniken wurden die aeroben und anaeroben Interaktionen in verschiedenen Systemen mit dem Schwerpunkt Sulfatreduktion untersucht.

Ein mit Belebtschlamm beimpfter Modell-Reaktor (eine Durchflußzelle mit rezirkulierendem künstlichem Wasser) wurde verwendet um die Entwicklung eines Biofilmes und um den Einfluß von Flußgeschwindigkeit und Substratkonzentration auf die Sauerstoffverteilung in solch einen Biofilm zu untersuchen (Kapitel 2). Die Sauerstoff-Konzentrationsprofile wurden von der Oberfläche bis zum Substratum mit Sauerstoff-Mikrosensoren gemessen. Die zweidimensionale Sauerstoffverteilung am Substratum des Biofilmes wurde mit einer 'Planar Optode' aufgezeichnet. Es zeigte sich, daß der Biofilm eine heterogene Struktur mit Bereichen aerober und anaerober Zonen an der Unterseite entwickelte, die im Laufe des Biofilmwachstums zunehmend anaerober wurden. Die Verminderung der Durchflußgeschwindigkeit oder die Zugabe von z.B. Glucose hatte eine Abnahme des Sauerstoffgehaltes im Biofilm zur Folge. Bevor jedoch Sulfatreduktion detektiert werden konnte, hatte sich der gesamte Biofilm abgelöst. Ein anderes System mußte somit gesucht werden, um die Entwicklung der sulfatreduzierenden Bakterien (SRB), ihre Anordnung und Aktivität in einem wachsenden Biofilm zu verfolgen.

Das Belebtschlammbecken einer Kläranlage wurde für die Fortsetzung der Biofilm-Entwicklungsstudie ausgewählt (Kapitel 3 und 4). Sauerstoffundurchlässige Kunstoffolie wurde in das Belebtschlammbecken eingebracht und Proben dieser Folie wurden wöchentlich ins Labor für die Analyse mit Mikrosensoren und molekularbiologischen Methoden überführt. Die Sauerstoff-Mikrosensormessungen zeigten, daß anaerobe Zonen ab der ersten Woche der Biofilmentwicklung

vorhanden waren, welche in den nächsten Wochen an Ausdehnung zunahmen. Obwohl die Bedingungen für SRB günstig waren, konnte die Sulfidproduktion erst nach der 5. Woche der Biofilmentwicklung mit Sulfid-Mikrosensoren gemessen werden. Das in den anaeroben Schichten erzeugte Sulfid wurde in den sauerstoffhaltigen Zonen komplett oxidiert, womit ein geschlossener Schwefelzyklus vorliegt. Aus den Sauerstoff- und Sulfid-Flüssen konnte berechnet werden, daß 50-70% des in den Biofilm eindringenden Sauerstoffes für die Reoxidation des Sulfids benötigt wird. Somit ist die Sulfatreduktion in diesem Biofilm ebenso bedeutend wie die aerobe Mineralisierung.

Im Gegensatz zu den Mikrosensormessungen zeigte die FISH-Analyse, daß SRB im Biofilm ab der ersten Woche anwesend waren, und während der nächsten Wochen geringfügig zunahmen, von 2.7 x 10^8 SRB/ml in der 2. Woche auf 3.1 x 10^9 SRB/ml in der 11. Woche der Biofilmentwicklung. Da keine Sulfidproduktion detektiert werden konnte und in den anoxischen Schichten kein Elektronenakzeptor für eine dynamische Sulfidoxidation vorhanden war, ist anzunehmen, daß die SRB in den ersten 6 Wochen nicht sulfidogen aktiv waren. Die Analyse des Gens für die dissimilatorische Sulfitreduktase, ein Schlüssel-Enzym bei der Sulfatreduktion, zeigte eine Zunahme des Gens ab der 6. Woche, welche mit der ersten detektierbaren Sulfidproduktion überlappte. Anzunehmen ist, daß eine weitere Gruppe der SRB, die nicht mit der FISH Analyse erfaßt wurde, für die Sulfidproduktion und die Zunahme des dissimilatorischen Sulfitreduktase-Gens verantwortlich war.

Da die Biomasse in den Belebtschlammbecken überwiegend in Form von Belebtschlammflocken vorliegt, wurden diese Flocken auf anaerobe Prozesse untersucht (Kapitel 5). Die Sauerstoff-Mikrosensormessungen ergaben, daß in 5 von 7 untersuchten Belebtschlammflocken keine anaeroben Zonen vorhanden waren. Dies könnte erklärt werden durch die lockere Struktur der Flocken, die ein Eindringen von Sauerstoff in die Flocke mittels Konvektion zusätzlich zum diffusiven Sauerstoff-Transport ermöglicht. In den kompakteren Flocken bestimmt möglicherweise hauptsächlich Diffusion den Sauerstoff-Transport. Obwohl mittels FISH-Analyse und Bestimmung des dissmililatorischen Sulfitreduktase-Gens SRB in den Belebtschlammflocken nachgewiesen werden konnten, wurde weder mit Mikrosensormessungen noch mit der $^{35}SO_4^{2-}$-Radiotracer-Methode, selbst unter anaeroben Inkubations-Bedingungen, keine Sulfatreduktion detektiert. Somit konnten auch in diesem System inaktive sulfatreduzierende Bakterien nachgewiesen werden, und es zeigte sich wiederum eine Diskrepanz zwischen Struktur- und Funktionsanalyse.

In der letzten Studie (Kapitel 6) wurden kompakte Aggregate von drei verschiedenen anaeroben Flüssigbett-Reaktoren, sogenannte upflow anaerobic sludge blanket (UASB) reactors, untersucht. Die anaeroben Aggregate aus einem methanogenen, einem sulfidogenen und einem methano-sulfidogenen Reaktor produzierten Sulfid und Methan. Hypothetische Modelle nehmen eine stratifizierte Struktur der Aggregate an, die sowohl mit molekularen Methoden als auch mit Mikrosensormessungen bestätigt werden konnte. Methanogene Bakterien wurden im Zentrum der Aggregate gefunden, SRB in der äußeren Schicht. Zwischen diesen beiden Populationen wurden syntrophe Bakterien nachgewiesen, welche Substrate wie Acetat und Wasserstoff für methanogene und sulfatreduzierende Bakterien produzieren. Die methano-sulfidogenen Aggregate zeigten eine exakt geschichtete Struktur, während die sulfidogenen und methanogenen Aggregate eine mehr

diffuse Schichtstruktur hatten. Insgesamt wurde in den anaeroben Aggregaten eine Übereinstimmung zwischen Struktur- und Funktionsanalyse gefunden.

Diese Arbeit zeigt, wie wichtig es ist molekulare Methoden mit Mikrosensormessungen zu kombinieren, da von der molekularen Detektion bestimmter Populationen nichts über ihre Aktivität aussagt werden kann.

Appendix

List of Publications

I. Manuscripts presented in this thesis and contributions of (co-)authors

- **Microsensor as a tool to determine chemical microgradients and bacterial activity in wastewater biofilms and flocs.** Published in Biodegradation (1998) **9**: 159-167, by Cecilia M. Santegoeds, Andreas Schramm, and Dirk de Beer.

- **Oxygen dynamics at the base of a biofilm studied with planar optodes.** Published in Aquatic Microbial Ecology (1998) **14**: 223-233, by Ronnie N. Glud, Cecilia M. Santegoeds, Dirk de Beer, Oliver Kohls, and Niels B. Ramsing.

- **Structural and functional dynamics of sulfate-reducing populations in bacterial biofilms.** Published in Applied and Environmental Microbiology (1998) **64**: 3731-3739, by Cecilia M. Santegoeds, Timothy G. Ferdelman, Gerard Muyzer, and Dirk de Beer.

- **Diversity and distribution of sulfate reducing bacteria in a developing biofilm.** In preparation (FEMS Microbial Ecology), 1999, by Cecilia M. Santegoeds, Dror Minz, Werner Manz, Michael Wagner, Dirk de Beer and Gerard Muyzer.

- **An interdisciplinary approach to the occurrence of anoxic microniches, denitrification, and sulfate reduction in aerated activated sludge.** Submitted to Applied and Environmental Microbiology (1999), by Andreas Schramm, Cecilia M. Santegoeds, Helle K. Nielsen, Helle Ploug, Michael Wagner, Milan Pribyl, Jiri Wanner, Rudolf Amann, Dirk de Beer.

- **Distribution of sulfate reducing and methanogenic bacteria in UASB aggregates determined by microsensor and molecular analysis.** In preparation (Applied and Environmental Microbiology), 1999, by Cecilia M. Santegoeds, Lars R. Damgaard, Jakob Zopfi, Gijs Hesselink, Piet Lens, Gerard Muyzer and Dirk de Beer.

II. Further publications

- Denaturing gradient gel electrophoresis used to monitor the enrichment culture of aerobic chemoorganothrophic bacteria from a hot spring cyanobacterial mat. Published in Applied and Environmental Microbiology (1996) **62**: 3922-3928, by Cecilia M. Santegoeds, Stephen C. Nold, and David. M. Ward.

- Biodiversity within hot spring microbial mat communities: molecular monitoring of enrichment cultures. Published in Antonie van Leeuwenhoek (1997) **71**: 143-150, by David M. Ward, Cecilia M. Santegoeds, Stephen C. Nold, Niels B. Ramsing, Michael J. Ferris, Mary M. Bateson.

- A nitrite microsensor for profiling environmental biofilms. Published in Applied and Environmental Microbiology (1997) **63**: 973-977, by Dirk de Beer, Andreas Schramm, Cecilia M. Santegoeds, and Michael Kühl.

- Denaturing gradient gel electrophoresis (DGGE) in microbial ecology. Published in Molecular Microbial Ecology Manual (1998) **3.4.4**: 1-27, by Gerard Muyzer, Thorsten Brinkhoff, Ulrich Nübel, Cecilia M. Santegoeds, Hendrik Schäfer, and Cathrin Wawer.

- Biofilm dynamics studied with microsensors and molecular techniques. Published in Water Science and Technology (1998) **37**: 125-129, by Cecilia M. Santegoeds, Gerard Muyzer, and Dirk de Beer.

- Anaerobic processes in activated sludge. Published in Water Science and Technology (1998) **37**: 605-608, by Dirk de Beer, Andreas Schramm, Cecilia M. Santegoeds, and Helle Nielsen.

- A polyphasic approach to study the diversity and vertical distribution of sulfur-oxidizing *Thiomicrospira* species in coastal sediments of the german Wadden sea. Published in Applied and Environmental Microbiology (1998) **64**: 4650-4657, by Thorsten Brinkhoff, Cecilia M. Santegoeds, Kerstin Sahm, Jan Kuever, and Gerard Muyzer.